Torben Wilhelm Kuehnast, BSc

Establishment of biofilm assays in *Propionibacterium acnes*

MASTER THESIS

to be awarded the degree of
Master of Science (MSc) in Molecular Microbiology
at the University of Graz, Austria

supervised by
Assoz.Prof. Dipl.-Biol. Dr.rer.nat. Stefan Schild
Institute of Molecular Biosciences

Graz, 2016

AFFIDAVIT

I declare that I have authored this thesis independently, that I have not used other than the declared sources/resources, and that I have explicitly indicated all material which has been quoted either literally or by content from the source used. The text document uploaded to UNIGRAZonline is identical to the present master's thesis dissertation.

_____ _____

Date Signature

Danksagung

Mein allererster Dank geht an Prof. Dr. Stefan Schild, der mich während der Arbeit vorbildlich begleitet und unterstützt, und unter hohem Aufwand meine Wünsche und Ziele stets mit einbezogen hat.

Weiters möchte ich mich bei Prof. Dr. Joachim Reidl bedanken, der in mir das Interesse für Bakteriologie und Infektionsbiologie geweckt, und mich bei meinen ersten eigenen wissenschaftlichen Gehversuchen im Labor betreut hat. Auch an die Firma ORIGIMM und Dr. Andreas Pilz ergeht mein Dank, für das Vertrauen und die exzellente Zusammenarbeit. Bedanken möchte ich mich auch bei Prof. Dr. Kai-Uwe Fröhlich, der mir bei meiner Bachelorarbeit über molekulare Exobiologie eine wissenschaftliche Freiheit gewährte, die mich sehr inspiriert hat. Ich möchte mich natürlich bei meinen Kollegen im Labor bedanken, durch dessen positives Klima die Arbeit umso angenehmer war. Im besonderen Maße gilt dies bei Dina und Katharina, die mir unter Aufopferung ihrer Zeit immer alles geduldig gezeigt haben.

Ohne die ständige, bedingungslose Unterstützung meiner Mutter wäre all das nicht möglich gewesen. Auch bei meinem Stiefvater Erich möchte ich mich bedanken, der hoffentlich stolz auf das wäre, was ich auch dank seines Fundaments leisten durfte. Robin und Pia, vielen Dank für die Hilfe und das Teamwork der letzten Jahre. Dasselbe gilt für Rosi und Benji und die ganze Familie.

Es gab noch viele andere, die mich die letzten Jahre begleitet haben. Auch an sie geht mein ganz herzlichster Dank.

Table of Contents

Zusammenfassung

Propionibacterium acnes ist ein Gram-positives Bakterium, das als Kommensaler hauptsächlich auf der Haut des Menschen vorkommt. Es wird angenommen, dass es bei Störungen des Immunsystems für die Hautkrankheit *Acne vulgaris* verantwortlich ist. Zusätzlich ist es häufig für chronische Entzündungen von Implantaten verantwortlich. Ein gewichtiger Faktor dieser Erkrankungen ist auf dessen Fähigkeit zurückzuführen Biofilme zu produzieren. Im Zuge dieser Arbeit wurden drei Assays entwickelt, die *in vitro* Biofilme genauer analysieren. Diese verschiedenen phänotypischen Charakterisierungsmöglichkeiten bestanden aus der Quantifizierung des statistischen Biofilms über einen dynamischen Zeitraum, der makroskopischen Evaluierung der Aggregationen, sowie der mikroskopischen Analyse der Biofilm-Morphologie. Die Protokolle wurden bei 51 *P. acnes* Stämmen angewandt und deren Charakteristika mit dem Ort der Isolierung und dem Serotyp verglichen. Außerdem wurden die Grundlagen geschaffen zukünftige genetische Deletionen durchzuführen, die dann mittels der etablierten Assays ausgewertet werden sollen.

Abstract

Propionibacterium acnes is a Gram-positive bacterium which usually lives on the human skin as commensal. In case of a dysfunction of the immune system it is assumed to be responsible for the skin disorder *acne vulgaris*. Additionally, it frequently leads to chronic infections of implants. A substantial factor of this virulence is said to be its ability to form biofilms. In the course of this study three assays were established, which analysed *in vitro* produced biofilm. These phenotypic characterizations included the quantification of a static biofilm over a dynamic time scale, the macroscopic evaluation of aggregation and the microscopic analysis of biofilm morphology. These protocols were applied for 51 *P. acnes* strains, while comparing the point of isolation, as well as the respective serotypes. Additionally, in order to characterize future mutants with the established biofilm assays, a genetic knockout construction was initialized.

1 Introduction

P. acnes and *acne vulgaris*

One of the most famous and inconvenient accompaniment of modern mankind, especially of the youth, has ever since been a skin disorder called acne. In a superficial society where the face is perceived as the main factor of human interaction, a permanent inflammation and scarring of it burdens affected patients enormously. Insufficient self-confidence, chronical stress and depression are possible consequences. At the same time effective cures are scarce and accompanied by substantial side effects. This is not surprising, as basic knowledge of acne development from a molecular biology point of view is still lacking.

In the early course of research a prominent protagonist came to the fore – the bacterium *Propionibacterium acnes*, which was found predominantly, as its name indicates, in *acne vulgaris* infections. Additionally to acne, *P. acnes* had been identified as resistant pathogen involved in the infection of implants. In further consequence implants have to be replaced. Considering both diseases, the lack of efficient therapies and the lack of detailed molecular biological knowledge, it became clear that successful *P. acnes* combating required more micro- and moleculobiological effort.

The main environment of *P. acnes* is the human skin, where it lives as a harmless commensal. It is a rod shaped, non-motile, non-spore-forming Gram positive bacteria and part of the *Actinobacteria* phylum featuring a high guanine and cytosine content. It grows anaerobically but tolerates oxygen. First sequenced in 2004, the circular genome features a size of 2.65 Mb [1].

Under special circumstances the strain becomes virulent (*acne vulgaris*), which is why it is described as opportunistic pathogen and requiring biosafety level 2. According to newest insights these circumstances at first demand a host inflammatory dysregulation [2]. People without this particular precondition stay healthy. The second key aspect, however, suggests a factor which is directly produced by *P. acnes*, the virulence factor biofilm.

Bacterial Biofilms

Some bacteria, including *P. acnes*, are able to surround themselves in a matrix of extracellular polymers which can be made of polysaccharides, DNA, amyloid fibrils, biofilm-associated proteins and lipids (figure 1) [4; 6; 5; 3]. The matrix serves as

physical protection from hostile cells (immune system) and dehydration. It is usually regulated by quorum sensing systems, but also by changes of the environment [7]. The structure can be three dimensional where aggregates of cells are alternated by water filled channels. These channels are responsible for supplying the cells of the biofilm with nutrients. The reduced flow through the matrix (while sometimes relying solely on diffusion) forces the bacteria to slow down metabolism. Unfortunately, it also results less interaction with antimicrobial substances, which cause less damage due to the lack of proliferation and active metabolism. Biofilm synergizes with bacterial persistence. In clinics biofilm establishment is one of the major virulence factors against the effective use of antibiotics. The biofilm characteristic includes the ability to adsorb to numerous surfaces while resisting the environmental flow. This way they open up new ecological niches like the surface of ships, oil and water pipes, but also implants in the body or on the skin surface. The dynamic process usually consists of bacterial attachment on the surface, proliferation with biofilm production, stagnation and detachment [6].

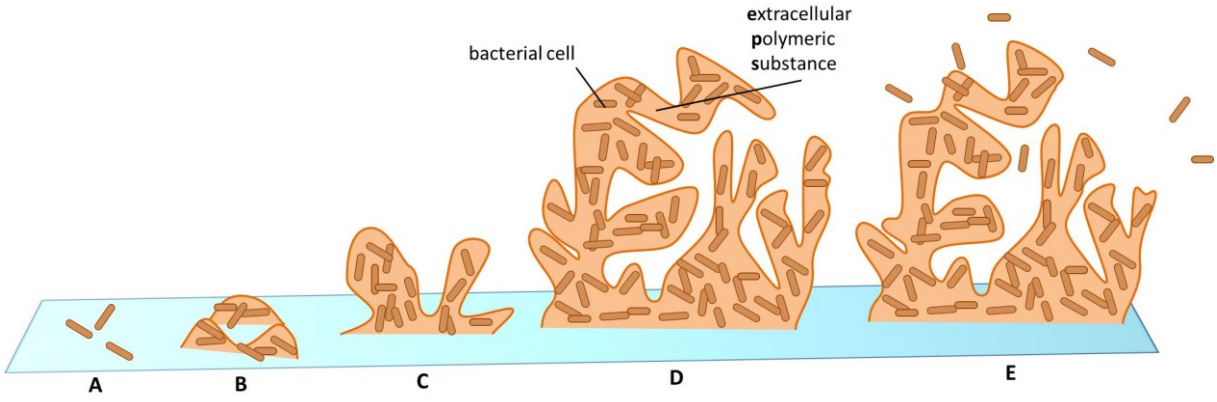

Figure 1: Biofilm dynamics. The establishment of the biofilm begins with attachment to a surface of a few planktonic cells (A), followed by proliferation and eps secretion (extracellular polymeric substance) seen in (B). The biofilm structure grows (C) into a matrix of sessile cells, alternated by caverns and channels of water (D). At one point cells within the matrix go over into the planktonic phase and leave the biofilm again.

Biofilm in *P. acnes*

P. acnes biofilms were described for the first time in 2003 [8]. *In vivo* it was demonstrated that biofilm establishment was directly responsible for enhanced antimicrobial and antibiotics resistance on all kind of implants [9; 8]. The second pathogenicity of *P. acnes*, *acne vulgaris*, is also assumed to be influenced by biofilm. Generally, *P. acnes* forms epidermal biofilms on the skin (stratum corneum) and in

the hair follicles close to the sebaceous gland, both visualized in 2012 [10; 11]. When inflammatory dysregulation occurs, accompanied by enhanced sebum production and other chemical changes (shift in hormonal balance in the teenage years), *P. acnes* proliferates in the follicles, closes the opening, creates an enlarged anaerobic environment, mediates a strong inflammatory reaction and survives immunogenic responses [12]. Such biofilm aggregates have been found in 47% of the follicles of acne patients, compared to only 21% in control groups without acne [11].

The first visualization of an *in vitro* biofilm has been shown by SEM (scanning electron microscopy) [13], followed by fluorescence microscopy [9]. Differences between planktonic and biofilm cells were seen by SEM, as well as putative biofilm matrix structures by TEM (transmission electron microscopy) [14].

Biofilm *in vitro* Phenotypes

The molecular biological foundation to work with a microorganism and to manipulate it genetically is to establish a reproducible phenotype. Manipulations have to become visible when comparing wildtype to mutant. The most straight forward approach was to quantify strain specific, *in vitro* created biofilms. Coenye et al modified a biofilm microtiterplate test of *Staphylococcus* for *P. acnes* [9; 15]. They managed to quantify biofilm mass by crystal violet staining and absorbance measurement, which grew on the surface of plastic wells. The biofilm adsorbs to most surfaces (like titanium, polymethylmethacrylate bone cement, steel or silicone) equally [13; 8]. Although it seems biofilm is associated to the follicle epithelium *in vivo* [11], coating plastic surfaces with plasma proteins did not improve biofilm attachment [13]. Two years later, Holmberg et al created another modified version, comparing (surface swabbed) skin isolates to implant isolates [14]. These published protocols served as foundation for creating a phenotypic analysis of biofilm quantity.

To tighten these results, two other characteristics were to be investigated. The second phenotype, the macroscopic aggregation of *P. acnes*, should be analysed by recording characteristic strain appearances. The third phenotype consisted of visualizing the 3D morphology of the biofilm by fluorescence microscopy. As the broad expertise of the laboratory was focused on Gram negative pathogens, such as *Vibrio cholerae* and *Haemophilus influenzae*, protocols on the Gram positive *P. acnes* had to be newly researched and modified. Establishing these three phenotypic characterizations were the main aims of this work.

Establishing the biofilm assay on quantity required the examination and reproduction of existing published protocols, adapting and replacing components and in particular investigating certain aspects like the optimal growth medium for biofilm production, i.e. BHI (Brain Heart Infusion), modified BHI, as well as TG (thioglycolate).

Another aspect was to identify the optimal time points for biofilm analysis. Dynamic progresses of its construction and degradation were to be analysed on a broad diversity of different *P. acnes* subgroups. Older protocols used different (and partially contradicting) time points to describe the biofilm dynamic, ranging from 24h to 96h for the maximum quantity.

Once the biofilm assays were established, they were to be applied on possible candidates varying in their phenotype. For this, 32 skin isolates (coming from acne patients and healthy people) and 19 implant isolates (both provided by ORIGIMM) were to be analysed on their individual biofilm quantity, macroscopic structure and on their microscopic morphology.

Serotype specific biofilms

Sequencing revealed variations in the genome of *P. acnes.* Between 2005 and 2012 six main serotype groups were identified, mainly by McDowell et al: IA1, IA2, IB, IC, II and III [16–19]. The most detailed version (eMLST) from 2012 was based on six housekeeping genes (*aroE*, *atpD*, *gmk*, *guaA*, *lepA* and *soda)* and two putative virulence factor genes *tly* and *camp2* [16]. In 2015 Barnard et al simplified the identification process, based on six sequences for "*the 16S rRNA gene (all isolates), ATPase (types IA1, IA2, and IC), sodA (types IA2 and IB), atpD (type II), and recA (type III) housekeeping genes, as well as a Fic family toxin gene (type IC)*" [20]. The strains from ORIGIMM were identified according to this method (by Ingenetix). Literature suggests different associations of pathogenicity from the different serotypes. After obtaining the phenotypic results from each strain, they were to be analysed and compared according to their serogroup, as well as their location of isolation (skin vs implant associated strains). These comparative analyses should reveal correlations in biofilm quantity and morphology between serotypes or isolation areas.

Knockout Strategy by Double Homologous Recombination

Aside from exploring the characteristic diversity of existing strains of different serotypes and points of isolation, the long-ranging idea behind the establishment of the assays was to offer a foundation for chemical, biochemical and moleculobiological manipulation. There are many possible ways to manipulate the biofilm with: chemicals, antibiotics, antibodies or even other interacting cells. With these biofilm assays to avail, all of them could be screened whether there's an influence on *in vitro* biofilm formation.

The focus of the last chapter of this work, however, is the moleculobiological research of the genes involved in biofilm establishment. The direct and sharp approach to this is the surgical knockout of single genes, followed by comparison of the wildtype to the knockout mutant phenotype. If the mutant shows alterations in the triple phenotypic analysis, an involved in biofilm establishment is probable.

To this point, there has been just one publication showing a successful knockout in *P. acnes* by Sörensen et al 2010. This knockout involved the deletion of a putative virulence factor, the *camp2* gene [21]. The method was based on creating a knockout vector carrying the up- and downstream sequence of the target gene and a selection marker, which was to replace the target gene by double homologous recombination.

Generally, the process of a double homologous recombination means that two homologous dsDNA sequences meet within the cell and due to homology the strands are exchanged. When taking a chromosomal dsDNA strand and a circular plasmid, this feature can be used to have the plasmid being incorporated into the chromosome within the first recombination event. The knockout plasmid has to be constructed in a way that it contains homologous sequences of the up- and downstream regions of the target gene in the chromosome (see figure 2/A). When the plasmid gets into contact with the homologous region on the chromosome, either the up-, or the downstream region will recombine, which (in the case the plasmid is still circular) leads to an integration of the plasmid into the chromosome. This means that either up- or downstream of the target gene the complete vector has been integrated. At the same time the up- and downstream sequences are now present on the chromosome twice: one surrounding the target gene, and directly before or after it surrounding a selection cassette (which initially has been placed between the vector up- and downstream sequences).

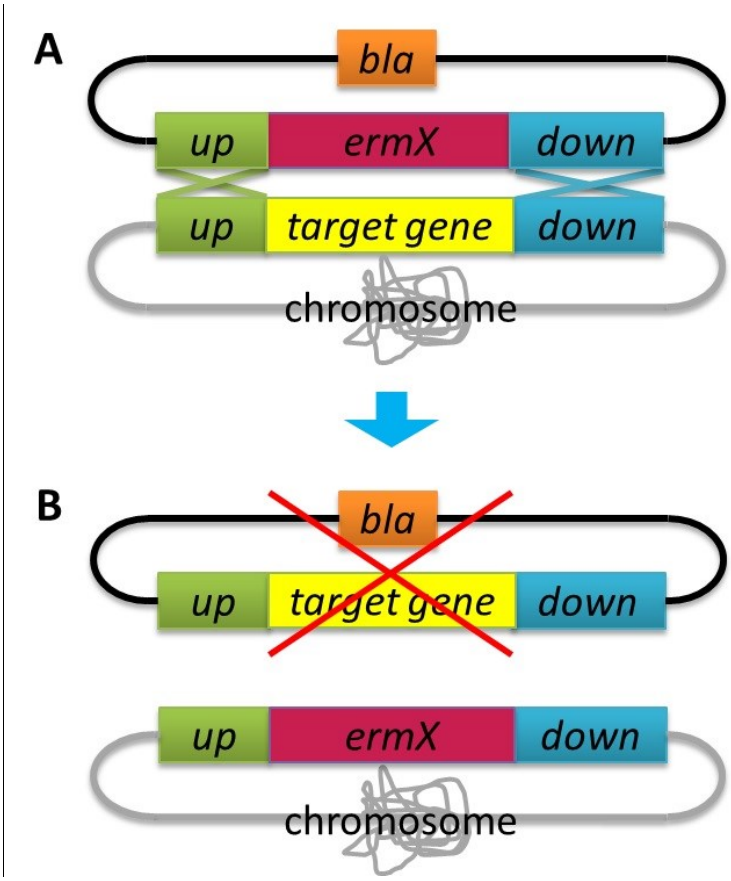

Figure 2: Double homologous recombination. Gene knockout by homologous recombination starts with a vector, containing a plasmid backbone selection marker (*bla*, ampicillin resistance), a second selection marker (*ermX*, erythromycin resistance) and homologous sequences of the up- and downstream regions of the target gene. Either up-, or downstream regions can recombine (panel A), which lead to full integration of circular plasmid into the chromosome up or downstream of the target gene. On the chromosome the second recombination event takes place. This leads to excision of the target gene from the chromosome and the achievement of a knockout mutant (panel B).

In the laboratory this is commonly achieved by inserting a large quantity of vectors into a large quantity of cells (by transformation or conjugation) and then applying a selection pressure like ampicillin. Only those with the vector (carrying the Amp^R) will survive. But additionally, they are not given the ability to replicate the plasmid. If the plasmid cannot be replicated itself, the cells carrying the vector will survive, but they cannot pass on the resistance to the daughter cells. The only way for a cell to successfully proliferate is by finding other measures of keeping this DNA in the cell: recombining it into the chromosome.

Now a second recombination event is required to create the full knockout. On the chromosome there are two sequences which are homologous: the upstream region of the target gene is homologous to the upstream region we inserted into the

chromosome by our plasmid. Same counts for the downstream region. These can recombine again while on the chromosome. This second recombination event leads to the excision of the sequences which are between the respective homologous fragments. The excised fragment will form a new plasmid with these parts, and leave the rest on the chromosome (figure 2/B). This excised plasmid will randomly either contain the initial selection cassette between its up- and downstream regions, or the wildtype target gene. The chromosome will lose the plasmid backbone, and keep either the up- and downstream regions containing the wildtype gene, or the second selection cassette. If it keeps the selection cassette, then the wildtype gene is now located on the plasmid. As the plasmid has no means to replicate, daughter cells will lose the plasmid (with the wildtype gene sitting in it) and henceforth proliferate as knockout mutant.

Knockout Strategy for *P. acnes*

The general direction of this strategy was to be adapted for *P. acnes*. Sörensen et al transformed a non-replicable plasmid into *P. acnes*, got transformants surviving the selection pressure (thus indicating recombination of the plasmid into the chromosome) and showed at least one mutant with a second recombination event deleting the wildtype gene [21].

Within the last chapter of this work seven possible genes were investigated bioinformatically, which could be involved in the establishment of the biofilm. These were based on published sequencing data [1; 22; 21], together with the *camp2* gene from Sörensen et al as control. The genes were cloned into an appropriate vector (according to the above mentioned recombination strategy) and transformed into *P. acnes*. Transformants, respectively recombinants should be screened for mutants with verified first recombination events. The result shall be anticipated at this point that the event only be partially achieved so far. Thus this work contains a detailed list of all applied variations within the study, so that it serves as a foundation of knowledge where future knockout research can be started from.

2 Materials

2.1 Media

BHI broth - Bacto™ Brain Heart Infusion (Becton Dickinson)	
BHI powder	37 g / l

BHI powder ingredients	
Calf brain	7.7 g / l
Beef heart	9.8 g / l
Proteose peptone	10 g / l
Dextrose	2 g / l
Sodium chloride	5 g / l
Disodium phosphate	2.5 g / l

BHI agar - Bacto™ Brain Heart Infusion (Becton Dickinson)	
BHI powder	37 g / l
Agar	16 g / l

BHG broth - Bacto™ Brain Heart Infusion (Becton Dickinson) plus glucose	
BHI powder	37 g / l
Glucose	0.2% (w/v)

TG broth - Thioglycollate [sic] medium (VWR chemicals)	
TG powder	29.75 g / l

TG powder ingredients	
Pancreatic digest of casein	15 g /l
Yeast extract	5 g /l
Dextrose	5.5 g /l
Sodium chloride	2.5 g /l
L-Cystine	0.5 g /l
Sodium thioglycolate	0.5 g /l
Resazurin sodium	0.001 g /l
Agar	0.75 g / l

TG agar - Thioglycollate medium (VWR chemicals)	
TG powder	29.75 g / l
Agar	15 g / l

LB - Lysogeny broth	
Tryptone	10 g / l
Yeast extract	5 g / l
Sodium chloride	10 g / l

LB agar - Lysogeny broth agar	
Tryptone	10 g / l
Yeast extract	5 g / l
Sodium chloride	10 g / l
Agar	16 g / l

2.2 Antibiotics

Ampicillin (Amp)	
Stock	100 mg / ml
Usage	50 µg / ml When in addition to second antibiotic 100 µg / ml When without other antibiotics.

Erythromycin (Em)	
Stock	100 mg / ml, in ethanol [absolute]
Usage *P. acnes* *E. coli*	10 µg / ml 500 µg / ml

2.3 Solutions and Buffers

Solution I	
Tris/HCl	50 mM, pH 8
EDTA	10 mM

Autoclaving.

Adding 100 µg RNase A / ml.

Stored at 4°C after addition of RNase A.

Solution II	
NaOH	0.2 M
SDS	1% (w/v)

Store at room temperature.

Solution III	
Potassium acetate	2.8 M

Adjusted to pH 5.1 using acetic acid.

TE buffer - Tris EDTA	
Tris/HCl	10 mM, pH 8
EDTA	10 mM

TNE buffer - Tris NaCl EDTA buffer	
Tris/HCl	10 mM, pH 8
Sodium chloride	10 mM
EDTA	10 mM

TNEX buffer - Tris NaCl EDTA triton-X buffer	
Tris/HCl	10 mM, pH 8
Sodium chloride	10 mM
EDTA	10 mM
Triton X-100	1% (v/v)

TAE buffer 50x **- Tris Acetate EDTA buffer**	
Tris/HCl	242 g / l, pH 8
Glacial acetic acid	5.71 %
EDTA	50 mM

EP buffer - Electroporation buffer	
Sodium phosphate	7 mM

Titrated to pH 7 with orthophosphoric acid (to avoid precipitation).

Autoclaved separately.

Magnesium chloride	1 mM

Autoclaved separately.

Sucrose	273 mM

Sterile filtrated.

All components pooled before usage. Molar concentrations stand for the final concentrations.

Lysozyme	
Lysozyme powder	5 mg / ml, in H_2O

Proteinase K	
Proteinase K powder	20 mg / ml, in H_2O

Ethidium bromide	
Ethidium bromide	0,025 % (v/v)

Crystal violet	
Crystal violet	0.1 % (w/v)

SYTO 9	
SYTO 9	5 µM, in BHI

Loading dye 6x	
Tris/HCl	10 mM, pH 7.6
EDTA	60 mM
Glycerol	60 %
Xylene cyanol FF	0.03 %
Bromophenol blue	0.03 %

2.4 Strains

***Propionibacterium acnes* – skin isolates**				
#	**Strain**	**Serotype**	**SC***	**Info**
60	NCTC737	IA1	S1560	Reference strain, acne
61	P.acn 25	IA1	S1561	
62	PV10	IA1	S1562	Acne
63	P.acn. 10	IA2	S1563	
64	P.acn 31	IA2	S1564	
65	P.acn 87	IB	S1565	
66	W1392	IB	S1566	
67	PV66	IC	S1567	Acne
68	ATCC11828	II	S1568	Subcutaneous abscess
69	20C large C	III	S1569	Skin
70	20C small C	III	S1570	Skin
71	Asn 12 large C	II	S1571	
72	Asn 12 small C	III	S1572	
73	A010 SK1	IA1	S1573	Acne
74	A010 SK2	IA1	S1574	Acne
75	A015 SK1	IA1	S1575	Acne
76	A015 SK2	IA1	S1576	Acne
77	A016P SK1	IA1	S1577	Acne
78	A016P SK2	IA1	S1578	Acne

79	A016H SK2	IA1	S1579	Acne
80	A016H SK3	IA1	S1580	Acne
81	TW SK3	IA1	S1581	Healthy
82	A002	IA1	S1582	Acne
83	A003	IA1	S1583	Acne
84	A011	IA1	S1584	Acne
85	H005 SK1	IA1	S1585	Healthy
86	H005 SK2	IA1	S1586	Healthy
87	H009 SK1	II	S1587	Healthy
88	H009 SK2	II	S1588	Healthy
89	AP SK1	IA1	S1589	Healthy
90	MBE SK1	IA1	S1590	Healthy
91	MBE Sk2	IA1	S1591	Healthy

Propionibacterium acnes – implant isolates

#	Strain	Serotype	SC*	Isolation location
10	IAI 001	n.d.	S1810	K-TEP
11	IAI 002	IB	S1811	H-TEP
12	IAI 004	IA1	S1812	Implant WS
13	IAI 005	IB	S1813	Aggregate
14	IAI 006	IA1	S1814	Plates & screws
15	IAI 007	IA1	S1815	Aggregate
16	IAI 008	IC	S1816	Loop-recorder
17	IAI 009	IB	S1817	Pacemaker
18	IAI 010	III	S1818	H-TEP
19	IAI 011	IA1	S1819	Osteosynthesis
20	IAI 012	II	S1820	Screws
21	IAI 013	IA1	S1821	Clavicula
22	IAI 014	IB	S1822	Screws
23	IAI 015	IA1	S1823	Osteosynthesis
24	IAI 016	IA1	S1824	K-TEP
25	IAI 017	IB	S1825	K-TEP
26	IAI 018	IA2	S1826	Shoulder
27	IAI 019	IB	S1827	Osteosynthesis
28	IAI 020	IA1	S1828	Screws WS

Other microorganisms		
Strain	**SC***	**Properties**
Escherichia coli DH5α λpir	S179	Transformation
Escherichia coli GM2163	A/E479	*dam*-negative
Escherichia coli ML1061 [pUC19]	A/E265	*pUC19*
Saccharopolyspora erythraea	S/1879	*ermE* cassette

* Strain collection (A=Achims/S=Stefans/E=*E.coli*)

2.5 Primer List

Primer	Site	Sequence (5' -> 3')
[A] PAZ_C18730.1	SphI	AAA gcatgc AAACTCGGCTATTGCGTCTT
[A] PAZ_C18730.2	XbaI	ATA tctaga GGATCTCCTCAGATGTATCT
[A] PAZ_C18730.3	PstI	AAActgcag TTCGCCGGCAAGACATTCGA
[A] PAZ_C18730.4	KpnI	TAA ggtacc TCCCACTGCTGCGCG
[A] PAZ_C18730.5		GCGTCATGGTCGATGTACGC
[B] PAZ_C21800.1	SphI	TTA gcatgc GGCGACCTCGTTGATC
[B] PAZ_C21800.2	XbaI	ATA tctaga CAGTGACTCCTCAGCGGAA
[B] PAZ_C21800.3	PstI	AAA ctgcag ACTGTGGCAGGTCAGG
[B] PAZ_C21800.4	KpnI	TAA ggtacc CCCGCGCTACGTCG
[B] PAZ_C21800.5		ACCGACGGCATCGGGGGCGT
[C] PAZ_C22060.1	SphI	AAA gcatgc GATGACCCCGGATACTCA
[C] PAZ_C22060.2	XbaI	ATA tctaga TGCTTCTCCTCTTATTTGGG
[C] PAZ_C22060.3	PstI	AAA ctgcag TCACCATCGGCGATAACC
[C] PAZ_C22060.4	KpnI	TAA ggtacc CTCACGCCCGCGTC
[C] PAZ_C22060.5		GGAACATCGGCATACTCAGC
[D] PPA0230_1.1	SphI	AAA gcatgc CCACGGTCGGGCAC
[D] PPA0230_1.2	XbaI	ATA tctaga GAGCCCATCACCTGATCAAC
[D] PPA0230_1.3	PstI	AAA ctgcag GCGACATCGATGTGACG
[D] PPA0230_1.4	KpnI	TAA ggtacc AACCGATGGCAGGCAG
[D] PPA0230_1.5		TGGGTCGGTGATGGCGTGGG
[E] PPA0146.1	SphI	AAA gcatgc TCGCGTCTTCGCTGAC
[E] PPA0146.2	XbaI	ATA tctaga CAACGACGATGACCTCGAC
[E] PPA0146.3	PstI	AAA ctgcag CGAGGTGACTGAATTCCA
[E] PPA0146.4	KpnI	AAT ggtacc GAGCCAAGACCTTGAGG
[E] PPA0146.5		AGGCAAAGACTTCCACCTCG

[F] PPA0148.1	SphI	AAA gcatgc TGGTGAACAAACCCATATCC
[F] PPA0148.2	XbaI	ATA tctaga GACGCAATCCTCTCGATGAG
[F] PPA0148.3	PstI	AAA ctgcag TGGCGAATTCTTCCCGC
[F] PPA0148.4	KpnI	TAA ggtacc CTGGCCAACACCTGC
[F] PPA0148.5		CTGGCCAACACCTGCGGCAC
[G] PPA0687.1	SphI	AAA gcatgc CCACGCCCACCACC
[G] PPA0687.2	XbaI	ATA tctaga AAAGGTTCTCCGTTTATTGG
[G] PPA0687.3	PstI	AAA ctgcag GTCAGAACGCACTCGCTA
[G] PPA0687.4	KpnI	TAA ggtacc AAGAGCTTCCATTTGGTGG
[G] PPA0687.5		ATTATACTGACACACCTGCC
[H] PPA1185.1	SphI	AAA gcatgc ACCTGGCACGAAGATTATC
[H] PPA1185.2	XbaI	ATA tctaga TTAGTCTCCAACCATGTCTCGA
[H] PPA1185.5		CGAACTCATCGCCCCTGACG
[I] PPA2181.1	SphI	AAA gcatgc ATCGATCACCAGTTTTACGT
[I] PPA2181.2	XbaI	ATA tctaga CCGTCCACGGTACAGGC
[I] PPA2181.3	PstI	AAA ctgcag GAGGCTGAGGTCACAAGT
[I] PPA2181.4	KpnI	TAA ggtacc TGGCGCCAAAGGCGTA
[I] PPA2181.5		ATGCTGGGGCTGTCGGTATG
ermC.fw_XbaI	XbaI	AAT tctaga CTCATGTTTGACAGCTTATC
ermC.rv_PstI	PstI	TAActgcagAAAAAATAGGTACACGAAAAACAA
ermE_XbaI.fw	XbaI	AAA tctaga AGCCCGACCCGAGCAC
ermE_PstI.rv	PstI	AAA ctgcag AGAAGGTCGAACTCGCAC

3 Methods

3.1 General Protocols

3.1.1 Gel DNA Extraction

DNA from agarose gels was extracted using the QIAquick Gel Extraction Kit according to the manufacturer protocol.

3.1.2 PCR Purification

DNA from PCR batches was purified using the QIAquick PCR Purification Kit according to the manufacturer protocol.

3.1.3 Plasmid Isolation

Plasmids were isolated using the QIAquick Plasmid Mini or Midi Kit according to the manufacturer protocol.

3.1.4 "Quick and Dirty" Plasmid Purification

4 ml of ONC were harvested by centrifugation of 2 x 2 ml (5 min, 6000 g), removing the supernatant and fully resuspending the cell pellet in 400 µl of solution I. 400 µl of solution II were added, carefully mixed by inverting the Eppendorf-tube and incubated for 5 min at room temperature. Afterwards 400 µl of ice-cold solution III were added, well mixed by inverting and incubated on ice for 15 min. The suspension was centrifuged 20 min at 4°C with maximum speed. 800 µl of supernatant was pipetted into a new Eppendorf-tube and mixed with 600 µl of isopropanol, inverted and centrifuged for 20 min (4°C, max rpm). The supernatant was removed and the DNA pellet washed with 800 µl of ice-cold ethanol [70%], once again followed by centrifugation for 20 min (4°C, max rpm). The supernatant was completely removed by pipette and the DNA pellet dried at 37°C. Afterwards 30 µl of H_2O were added, the pellet was resolved and frozen at -20°C.

3.1.5 Chromosomal DNA Isolation (*E. coli*)

2 ml of an ONC were centrifuged (5 min, RT, 5000 rpm), the supernatant was removed by pipetting, 1 ml of TNE was added and the pellet resuspended. After centrifugation (5 min, RT, 5000 rpm) the supernatant was once again removed, 270 µl of TNEX were added and the pellet resuspended. 30 µl of lysozyme was pipetted and the solution was incubated for 20 minutes at 37°C, degrading peptidoglycan. In

order to free the DNA from proteins 15 µl of proteinase K was added. After inverting the Eppendorf tube a few times it was incubated at 65°C for 2h. The cloudy solution should become clear. A (green – for chromosomal DNA) “Phase lock gel” tube was spun down as preparation and the complete volume of suspension was pipetted into it. After adding 400 µl of phenol and inverting the tube a few times the emulsion became milky. To separate the phases again the green “Phase lock gel” tube was centrifuged for 10 minutes at RT and 13000 rpm. The topmost (hydrophilic) phase containing dissolved chromosomal DNA (approximately 300 µl) was pipetted into a fresh Eppendorf tube and mixed with 30 µl NaCl [5 M] and 750 µl freezing ethanol [100 %] by inverting, leading to a white precipitate. Precipitation was enhanced by leaving the solution in -20°C for 15 minutes. In order to pelletize the precipitate the tube was centrifuged (30 minutes, 4°C, 13000 rpm). The supernatant was removed by pipetting and 1 ml freezing ethanol [70%] was filled into the tube without resuspending the pellet. A last centrifugation step followed (30 minutes, 4°C, 13000 rpm), the supernatant was removed as completely as possible (by pipette) and the remaining ethanol evaporated by incubating the open tube at 37°C for half an hour, until no smell of ethanol was sensible. The ethanol-free pellet was resolved in 75 µl H_2O by pipetting the water onto it and incubating it for at least 10 minutes.

3.1.6 Colony-PCR

Colony-PCR was performed as a fast way to screen for target DNA sequences using Taq Polymerase according to manufacturer protocol. Table 1 and 2 give a representative example for the used mixes and PCR programs.

Table 1: Colony-PCR components

Component	Volume [µl]
Template DNA	3
dNTPs (10 mM)	0.5
Forward primer (10 µM)	0.5
Reverse primer (10 µM)	0.5
ThermoPol Buffer (NEB) 10x	2.5
H_2O	17.75
Taq Polymerase (NEB)	0.25
Total	25

The C-PCR was performed by following the PCR program shown in table 2.

Table 2: Colony-PCR program

PCR step	Temperature	Duration	
Initial denaturation	95°C	3 minutes	
Cycle denaturation	95°C	30 seconds	32 Cycles
Cycle annealing	<50 °C – 70 °C>	45 seconds	
Cycle Extension	72°C	<1 kbp / minute>	
Final Extension	72°C	5 minutes	

3.1.7 Q5-PCR

The Q5 PCR protocol was used to create high quality DNA fragments for cloning and as screen method (Lysate-PCR) when the target DNA had a high GC content. Table 3 includes all the components which were prepared within a single PCR tube.

Table 3: Q5-PCR components

Component	Volume [µl]
Template DNA	2
dNTPs (10 mM)	0.5
Forward primer (10 µM)	1.25
Reverse primer (10 µM)	1.25
Q5 Reaction Buffer (NEB)	5
H_2O	9.75
Q5 Polymerase (NEB)	0.25
Q5 High GC Enhancer (NEB)	5
Total	25

The Q5-PCR was performed by following the PCR program shown in table 4.

Table 4: Q5-PCR program

PCR step	Temperature	Duration	
Initial denaturation	98°C	2 minutes	
Cycle denaturation	98°C	20 seconds	32 Cycles
Cycle annealing	<60 °C – 70 °C>	45 seconds	
Cycle Extension	72°C	< 2-3 kbp / minute>	
Final Extension	72°C	5 minutes	

3.1.8 Agarose Gel Electrophoresis

TAE buffer 50x was diluted to 1x using H_2O in order to reach the target volume of 50 – 250 ml per gel. Agarose was added (0.8 to 2 % [w/v]) and all was heated by microwave until the agarose was solved. Vaporized volume was refilled with H_2O. Ethidium bromide was added (to reach 0.025 % end concentration), followed by careful mixing and pouring into the gel chamber. The placeholders for the slots were put into the solution. The target DNA solution was prepared by adding loading dye 6x to a total concentration of 1x. After cooling and solidifying of the gel, the slots were filled with the target DNA solution (volume between 6 µl and 35 µl, depending on the size of the slot).The gel within the chamber was surrounded by TAE buffer 1x. The amount of volt depended on the size of the gel and varied between 80 V (50 ml gel) and 125 V (250 ml). When the electrophoresis finished, the gel was exposed to UV-light (316 – 343 nm) and an image was taken.

In case of a preparative agarose gel, the target DNA bands were cut out of the gel while keeping the UV exposition time as short as possible. The DNA in the gel pieces was purified using Qiagen Gel Extraction Kit and eluted in H_2O.

The standard used in all agarose gels was 2log (NEB). The intensities of the bands, the sequence sizes and the respectively mass are shown in figure 3. All gels were pipetted with 6 µl of 2log containing the masses written in the first column.

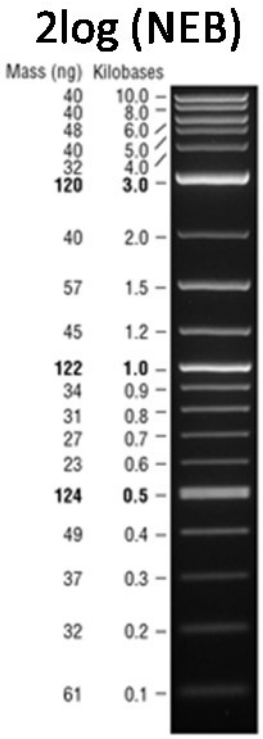

Figure 3: 2log (NEB) standard DNA ladder. 6 µl with total 1 µg of DNA were separated according to the image by agarose gel electrophoresis. The three dense bands (3000, 1000 and 500 bp) were marked in all images with agarose gels.

3.1.9 Restriction Digest

Restriction digest was performed with the appropriate enzymes (NEB) overnight at 37°C, using following recipe:

Table 5: Restriction components

Component	Volume [µl]
Target DNA fragment	15
Restriction enzyme 1 (NEB)	2
Restriction enzyme 2 (NEB)	2
Cutsmart Buffer (NEB)	10
H_2O	71
Total	100

3.1.10 Dephosphorylation

Dephosphorylation was performed by adding 1 µl of Antarctic Phosphatase (NEB) and 10 µl of 10x Antarctic Phosphatase Buffer (NEB) to 100 µl volume, incubated for 1h at 37°C, followed by heat inactivation for 10' at 65°C.

3.1.11 Ligation

Ligation was prepared using 1 µl of (digested & dephosphorylated) pUC19, 1 µl of T4 DNA ligase (NEB) and 1.5 µl of T4 DNA ligase buffer (NEB). The remaining 11.5 µl volume (to reach the maximum volume of 15 µl) was split into respective volume of the three inserts (UP, DN and *ermX* cassette), so that the final molar ratio was 1:1:1. Additionally it was tried to have a molar ratio between vector and insert of at least 1:3. Ligation was performed for 1h at 18°C, 1h at 24°C and another hour at 18°C. A heat inactivation for 10' at 65°C followed.

3.1.12 Electrocompetent *E. coli* and *Transformation*

100 ml LB were inoculated with a single colony and incubated overnight at 37°C and 180 rpm. Using the ONC, 2 x 400 ml of LB was brought to an OD_{600} of 0.1. This was incubated to an OD_{600} of 0.8 – 1 (37°C and 180 rpm) and left on ice for half an hour. Centrifugation at 5000 g for 10 minutes and 4°C followed. The supernatant was removed and the pellet resuspended in 2 x 200 ml ice-cold H_2O. After centrifugation (5000 g, 10', 4°C) another washing step followed, removing the supernatant and adding 2 x 100 ml ice-cold H_2O. The pellet was resuspended and centrifuged (5000 g, 10', 4°C). The supernatant was removed and the pellet resuspended in 2 x 35 ml ice-cold glycerol [15% in H_2O]. After a final centrifugation step (5000 g, 10', 4°C) the supernatant was (mostly) removed, leaving just a few drops of liquid together with the pellet. The remaining volume was used to resuspend the pellet into a thick, viscous bacterial solution. 80 µl of it was aliquoted into tubes and frozen at -80°C.7 µl of the ligation batch or 2 – 4 µl of plasmid ("Quick and Dirty" Plasmid Purification) were pipetted to 100 µl of electrocompetent *E. coli* cells, incubated for 10 minutes on ice, pipetted into pre-cooled 0.2 mm electroporation cuvettes and electroporated using 2400 V for 3 – 5 ms. The cells were resuspended in 1 ml pre-warmed LB, regenerated for 20 minutes at 37°C and another 40 minutes at 37°C/180 rpm.

100 µl and 400 µl of the electroporation batch were pipetted onto plates including the selection antibiotics.

3.2 Established Protocols for *P. acnes*

3.2.1 Static Biofilm Assay

The goal of the static biofilm assay was to quantify the amount of biofilm a *P. acnes* strain was producing. The measured mass contained cell material attached to plastic surface, and (yet unknown) extracellular matrix components creating the biofilm. After fixing the biofilm to the surface, it was stained with crystal violet. This was resolved in ethanol and its absorption recorded using a platereader at 595 nm. The absorption correlated with the amount of biofilm.

The static biofilm assay was established, based on published data [13; 9; 14] with modifications incorporating the new emerged insight on the special biofilm/aggregate definition of *P. acnes* biofilm and expertise of the lab.

The anaerobic atmosphere, which was mandatory for growth, was created by using AnaeroGen™ 2.5L (Thermo Scientific) packs. According to the manufacturer the AnaeroGen™ sachet would reduce the oxygen level in the jar to below 1% within 30 minutes. The resulting carbon dioxide level would be between 9% and 13%.

3.2.1.1 Preparation

The *P. acnes* strains were plated onto BHI or TG plates (from -80°C) and incubated anaerobically for 3 to 4 days. The cells on the respective plates were taken with a blue pipette tip as pellet, resuspended in respective broth and used for the inoculation of 150 µl volume per well in a density of OD_{600} = 0.1. BHI from the same batch of equal volume and media were added in order to serve as sterile control and blank for both the OD_{600}/growth or biofilm measurement.

As the used *P. acnes* strains had no known resistances to any sort of antibiotics, all laboratory work was performed under a sterile working bench while applying special sterility caution.

The microtiterplates were packed into oxygen-impermeable bags (GENbag, Biomérieux) together with an anaerobic sachet (creating an anaerobic atmosphere) and a piece of wet paper. It was then incubated for the respective time (like 72h, 120h and 168h) at 37°C.

3.2.1.2 Analyses

After the respective time passed, the microtiterplates were first photographed using ChemiDocs™ Image Lab™ program. The wells were analysed for characteristic macroscopic phenotypes.

Two wells of each strain were resuspended by pipetting up and down (including the biofilm material and used for OD_{600} measurement.

Regarding biofilm analysis of the remaining wells, the planktonic cells and broth were carefully removed by pipetting from the side of the wall of the well. The pull from the pipette would remove planktonic cells and most BHI, while leaving the biofilm attached to the ground. These were dried at 99°C for 30 minutes, incubated with 100 µl methanol for 10 minutes and once again freed from methanol using the same drying technique. The fixed biofilm was stained using 100 µl of crystal violet [0.1% (w/v) in H_2O] and an incubation time of 2 minutes. It was submerged in a basin of H_2O allowing the water to fill up all wells and turned around. This procedure was repeated once.

To receive a homogenous solution the wells were filled with 150 µl of ethanol. The crystal violet formerly staining the biofilm should be resolved. After surrounding the plate with Parafilm (so that each well is sealed individually) and incubation overnight at 4°C, any remaining visibly attached biofilm was resuspended. The microtiterplate was instantly measured in the platereader at 595 nm. Strong biofilms reached the maximum detection capacity of 3.5 relative absorption units, which received a 1:10 dilution and appropriate back-calculation.

The measurement resulted in the raw biofilm production in the microtiterplate, which comprised the photometric measurement of crystal violet at 595 nm (which initially stained the biofilm and was further resolved in ethanol). The sterile control/blank of the respective media was also treated the same as the biofilm. These showed the background signals which were only due to the media. The average of all available blanks was subtracted from all individual biofilm quantity values (“biofilm – blank”). The OD_{600}, which was measured before applying the fixing technique, was taken from at least two wells of each screened biofilm strain, as well as at least two sterile controls/blanks. The average of all available blanks (of one plate) was subtracted from each individual OD_{600} measured biofilm value. The median and interquartile [25]

range were shown in the figures of this work. Finally, as different strains could possibly produce equal amounts of biofilm, but grow with different speed, the ratio of "biofilm – blank" divided by the OD_{600} values were set up to standardize the biofilm quantity of all strains to OD_{600} = 1. These values were taken for most analysis (like the serotype comparison).

3.2.2 Chromosomal DNA Isolation of *P. acnes*

When clean DNA was required, for example as template for PCR construction of inserts, this chromosomal DNA Isolation protocol was used.

The target strain was densely plated onto a TG plate to get large amounts of cell material. This was incubated 3 days anaerobically at 37°C. Cells were resuspended in 1.5 ml TNE buffer. After centrifugation for 3 minutes and 5000 g the supernatant was removed and 400 µl of TNE was added. 100 µl of 0.1 mm sized beads and the 400 µl of bacteria suspension were added to a 2 ml screw-mountable cryo tube and cooled on ice for a few minutes. In order to open the cells mechanically by the beads, repeated steps of vigorous mixing was needed. This was done by the PowerLyser™ (an enhanced vortex), shaking the cryo tube for 1 minute with 3000 rpm, followed by 1 minute of cooling on ice. Mixing was repeated 3 times. After the beads sedimented to the bottom, the supernatant was pipetted into a fresh 2 ml tube. 70 µl of proteinase K [20 mg / ml] was added and incubated for 3h at 56°C. Phenol extraction was performed with phase lock gel (5-Prime) with half of the volume of phenol. DNA precipitation was achieved by the $^{EtOH}/_{NaCl}$ method. The DNA pellet was washed with ethanol [70%]. After removal of the ethanol by pipette and drying at 37°C until all alcoholic smell disappeared, the pellet was solved using 50 µl H_2O.

The protocol offered high yields of DNA and served as complication-free template for PCR. It should be noted however that the DNA was heavily fragmented with a smear of DNA (in agarose gel electrophoresis) ranging from 6 kb to 3 kb (main bulk) to 500 bp.

3.2.3 Lysate-PCR

When single *P. acnes* transformation colonies were to be screened rapidly for the presence or absence of a defined fragment, Lysate-PCR was used.

A large pellet was taken up from the grown cells (incubated 3 days anaerobically at 37°C) with the top of a blue pipette tip and resuspended in 400 µl TNE buffer. 100 µl of 0.1 mm sized beads and the 400 µl of bacteria suspension were added to a 2 ml screw-mountable cryo tube and cooled on ice for a few minutes. In order to open the cells mechanically by the beads, repeated steps of vigorous mixing was needed. This was done by the PowerLyser^{TM} (an enhanced vortex), shaking the cryo tube for 1 minute with 3000 rpm, followed by 1 minute of cooling on ice. Mixing was repeated 3 times. Finally the cryo tube was centrifuged for 1 minute at 13.000 rpm, whereas 2 µl of supernatant served as template for a standard Lysate PCR (see methods/Colony-PCR).

3.2.4 Fluorescence Microscopy

The target strains were taken from -80°C and incubated for 4 days on BHI media anaerobically at 37°C. The grown colonies were resuspended in liquid BHI, the OD_{600} was measured and an appropriate volume was taken to dilute 300 µl of BHI to an OD_{600} of 0.1. The 300 µl were loaded into a sterile syringe and carefully injected into one of the tubes of each chamber of the flowcell (Technical University of Denmark) with a glued (AquaSil, nontoxic silicone glue) cover glass on top. It should slowly fill the inner parts of the tube and the chamber completely. The flowcells were incubated anaerobically at 37°C for 5 days with the cover glass being on the floor. This way biofilm would grow on the cover glass.

In order to prepare microscopy one of the tubes was closed at the end and 300 µl of SYTO9 (5 mM, in BHI) were carefully and slowly injected into the tube. This way all bacteria suspension (planktonic *P. acnes* cells) leaked out of the flowcell through the open tube and only the biofilm attached to the cover glass would remain within the SYTO9 solution. After 30 minutes of incubation (SYTO9 permeates the cell wall and binds nucleic acids) the flowcells were microscoped, using a Nixon microscope (Eclipse Ti Series, 40 x objective). When exposed to blue light (absorption maximum at 485 nm), DNA bound SYTO9 emitted green light (emission maximum at 498 nm). Starting from the cover glass, images were taken every 2 µm of the Z layer. This way a 3D structure was recorded and further analysed using Comstat [25; 23; 24] to obtain parameters such as biomass, average and maximum thickness.

3.3 Gene Knockout in *P. acnes*

The strategy of the gene knockout in *P. acnes* is written down in detail in the following chapters. It contains the bioinformatical identification of potential biofilm related genes, the construction of a knockout-vector in *E. coli* containing these genes and the transformation into *P. acnes*.

3.3.1 Bioinformatical Screening

The genomes of several *P. acnes* strains were already sequenced and analysed bioinformatically for possible biofilm related genes in 2004 [1]. More detailed comparative genome and transcriptome analysis followed in 2011 [22]. Promising candidates mentioned in these publications were evaluated for their connections to biofilm formation. The sequences of six of those were taken as basis for primer design and vector cloning.

3.3.1.1 Genome list

All genomic and transcriptomic analysis based on two strains: “KPA” as serotype IB strain (first ever sequenced *P. acnes*), and “266” as IA1 strain. The sequenced strains, their KEGG entry and different serotyping are shown in table 6.

Table 6: ***Target knockout strains***

Shortform	“KPA”	“266”
Strain name	KPA171202	266
KEGG entry	T00188	T01971
Genbank entry	AE017283.1	CP002409.1
McDowell et al 2005 [19]	IB	IA
McDowell et al 2012 eMLST [16]	IB1 (ST10)	IA-CC6 (ST25)
Lomholt et al 2010 analysis [12]	I-2 (ST34)	I-1A (ST18)
Reference	[1]	[22]

3.3.1.2 Vector Backbone – pUC19

As backbone for the knockout-vector pUC19 was chosen, as it was comparably small (better transformation efficiency or larger recombination overhangs), had a high copy (better amplification yield) and mediated ampicillin resistance for easy selection.

3.3.1.3 Erythromycin Cassette

ermC

The first trials of vectors were constructed using *ermC* with pIDN2 serving as template [26]. It encoded for a 23S rRNA (adenine-N6)-dimethyltransferase (EC 2.1.1.184), mediating the erythromycin resistance.

The only published sequence of the pIDN family was pIDN4 with a difference in orientation of the *ermC*-cassette (compared to pIDN2). Exact switching points were unknown. Thus the smallest possible size of the surroundings of the gene was chosen to guarantee successful cloning, including the core transcription and translation parts (like -35/-10 region and terminator). See appendix for the exact *in silico* predicted sequence which already includes primer added restriction sites.

ermE

The last trials were performed with the *ermE* cassette from *Saccharopolyspora erythraea* (DSM No.: 40517). It encoded for an enzyme with the same function as *ermC* (KEGG database - SACE_0733, EC 2.1.1.184).

The sequence of *ermE* was available on KEGG database (SACE_0733). The primers for PCR amplification were chosen to produce a product equal in the size to published data [21]: 277 nucleotides upstream of the GTG start codon and 230 nucleotides downstream of the TAG stop codon. This led to a PCR product (including XbaI and PstI cutting palindromes) of 1672 bp. The exact sequence is shown in appendix.

3.3.2 Construction of the Vectors

3.3.2.1 Insert Description

The target genes (A – G + I) were supposed to be deleted by endogenous, double homologous recombination (introduction/figure 2) within the chromosome. To do so

upstream and downstream regions (see figure 4/A, “UP” and “DN”) of the target genes had to be subcloned into pUC19, with a size of ~ 800 bp (638 bp for [C] PAZ_c22060). These UP and DN segments surrounded an erythromycin cassette, which would replace the target gene and knock it out.

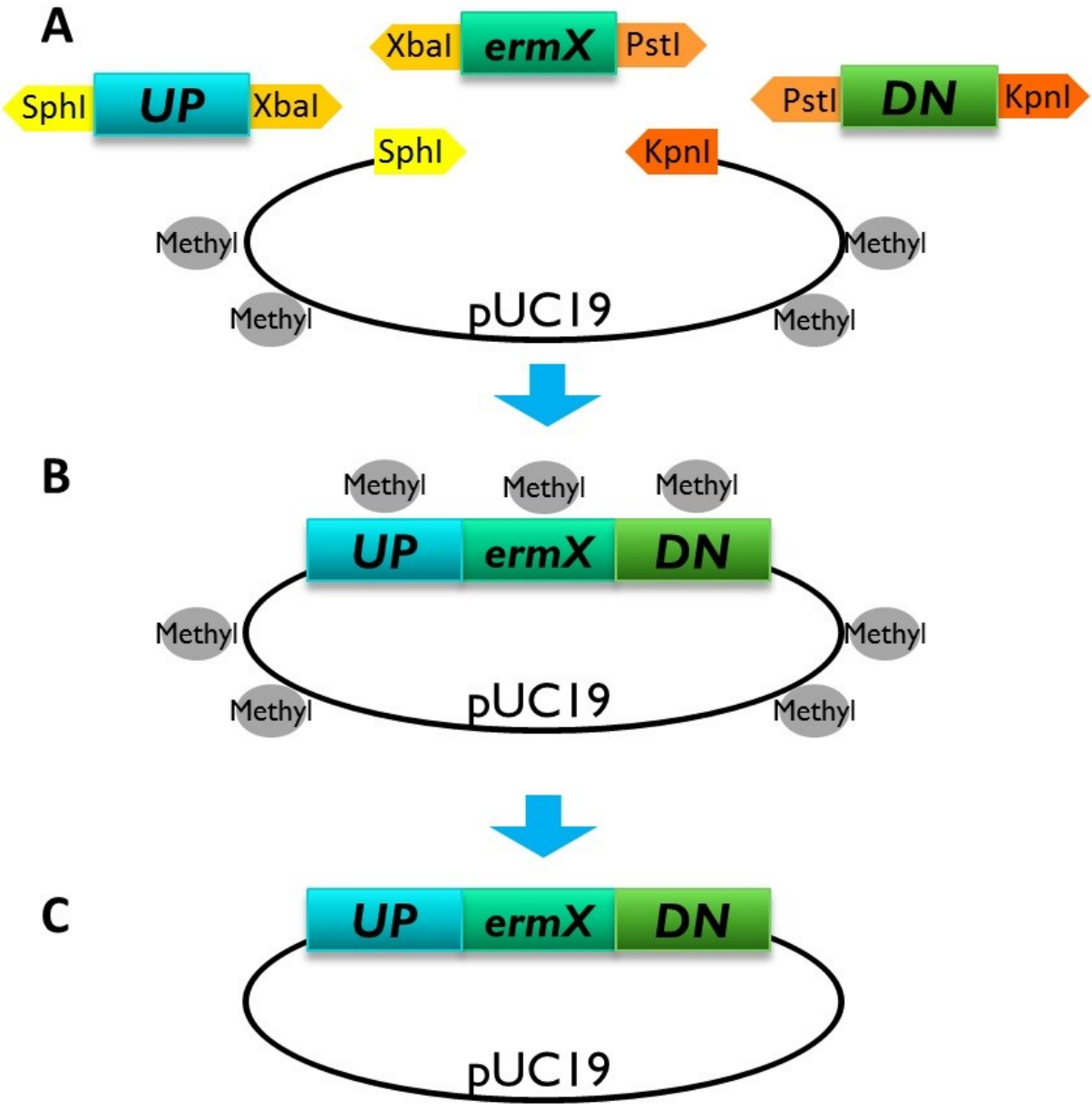

Figure 4: Creation of the knockout vector. The first step (panel A) was to prepare the inserts: up- and downstream (UP/DN) regions of the target genes, the resistance cassette (*ermC* or *ermE*) and the vector backbone pUC19, all with the respective restriction sites. These were ligated and transformed (B) into DH5α λpir. After plasmid isolation it was transformed into GM2163 (C) to get rid of the methylations.

Connecting the upstream part of the UP-insert to the left side of the pUC19 vector was done by a SphI restriction site (figure 4/A, connecting yellow ends). The SphI

sites were added to the upstream ends of the UP-inserts by using respective primers, which were named [X] gene_name.**1** (see materials/primer list). The UP sequence of each individual gene started 818 bp upstream (638 bp with gene [C]) of the start codon, and ended right before the start codon (see results/table 8 and 9 for exact size).

The downstream parts of the UP-regions were connected to the upstream part of *ermE/ermC* (either/or represented by *ermX*) cassette using the XbaI restriction site (figure 4/A/light orange). Downstream UP primers were given the number 2, upstream *ermE/C* primers the name *ermE/C* forward/fw, downstream ermE/C primers the name ermE/C reverse/rv, upstream DN received the number 3 and downstream DN the number 4. The DN inserts started immediately after the stop codon and were, if possible, of equal size as the respective UP insert.

A double recombination event would replace the target gene's raw open reading frame (from start to stop codon) with the erythromycin cassette. This would make sure that other independent regulations involving the upstream and downstream regions were left untouched.

3.3.2.2 Preparation of Inserts

Q5-PCRs (general protocols) were performed to create the above mentioned inserts. Chromosomal DNA from strain #60, isolated by the "Chromosomal DNA Isolation of *P. acnes*" protocol, was used as template for all UP and DN inserts. #60 as IA1 strain was supposed to have a genome close to the sequenced "266" strain (table 6). Later successful cloning confirmed sequence homology. The same protocol was used to isolate template DNA from *S. erythraea* for the *ermE* cassette. For the *ermC* cassette the vector pIDN2 served as template.

All PCR reaction batches were purified using agarose gel electrophoresis and gel DNA extraction kit.

The inserts were digested by the respective enzymes using the restriction digest protocol and cleaned by PCR purification kit.

3.3.2.3 Preparation of pUC19

The vector pUC19 was isolated from *Escherichia coli ML1061 [pUC19]* using the plasmid isolation midi kit protocol, followed by a restriction digest, dephosphorylation and cleaning by agarose gel electrophoresis and gel DNA extraction kit.

The complete uncut sequence is available in the appendix.

3.3.2.4 Vector Construction and Verification

The ligation product of inserts (UP/*ermX*/DN) with pUC19 was transformed into DH5α λpir (figure 4, A to B) and the constructs verified by Colony PCR. Vectors from positive transformants were isolated by “quick and dirty” plasmid purification.

To eliminate methylations of the DNA (figure 4, B to C) the vectors were transformed into the *dam*-negative strain GM2163, followed by plasmid midi isolation for high yields.

3.3.3 Transformation into *P. acnes*

The following protocols were a combination of published data and expertise from the lab [27; 21]. However, over time several parts were varied. For a list of all variations see results/figure 11.

3.3.3.1 Creating Electrocompetent *P. acnes* Cells

Strain #60, #86 and/or #66 were streaked densely onto TG plates from -80°C and incubated for 3 days (37°C, anaerobically). The film of bacteria was pelleted by a blue pipette tip and resuspended in 40 ml of BHI media (1 full TG plate resulted in an OD_{600} of ~2 – 4 per ml). This was used to inoculate 400 ml of BHI to an OD_{600} of ~ 0.1 and incubated anaerobically at 37°C for 3 days, leading to an OD_{600} of approximately 0.4 to 0.6 (strain #60). Alternatively, the inoculated media was incubated for 10 days at 25°C anaerobically, which would result in an OD_{600} of approximately 0.4 – 0.5 (#60: 0.5, #86: 0.4).

Cells of 400 ml were centrifuged at 4°C (10’, 4000 g), resuspended in 400 ml EPB, centrifuged again (10’, 4000 g, 4°C), resuspended in 100 ml EPB, centrifuged (10’, 4000 g, 4°C) and resuspended in ~ 1ml of the remaining liquid. Aliquots of 100 µl were created from this 1 ml, containing approximately 20 OD_{600} units each.

The aliquots were kept on ice until usage at the same day.

3.3.3.2 Electroporation in *P. acnes*

The constructed plasmid (pUC_UP_*ermX*_DN) of each respective gene was amplified in GM2163 (*dam* negative) by Qiagen midi kit to a concentration of 0.5 – 3.1 µg/µl. 10 µl of each plasmid were added to the 100 µl transformation batch within a 2 mm electroporation cuvette and electroporated using 1500 V. The 110 µl were resuspended in 1 ml BHI media, centrifuged and plated onto TG plates. These were incubated for 24h at 37°C/anaerobically.

The next day, 1 ml of BHI media was pipetted onto the plates to resuspend the bacterial growth on the surface with a sterilized spreader rod. The suspension was pipetted onto a fresh TG plate [10 µg erythromycin / ml] and incubated for 5 to 8 days at 37°C/anaerobically.

3.3.3.3 Lysate-PCR of Transformants

After 5 to 14 days a few colonies were growing on TG [Em10] plates. These colonies were streaked densely onto fresh TG [Em10] plates. A Lysate-PCR was performed with this cell material. The resulting PCR batch was analysed by agarose gel electrophoresis.

4 Results

Summary

The chapter results begins with the static biofilm assay on 32 skin isolates and shows the amount of biofilm produced first in TG, then in BHI and finally in BHG media over a period of one week. The media and time points representing *P. acnes* biofilm dynamics in the most significant way were picked for future assays. At the same time the biofilm production of the strains was assigned to respective serotype groups and compared to spot quantitative differences and correlations. The established assay was extended to 19 implant isolates, while comparing biofilm quantity of implant and skin isolates and the respective serotype group. Simultaneously, macroscopic images of the wells used in the static biofilm assay were taken and compared, regarding serotype and isolation location. The third phenotype characterization of *P. acnes* was about analysing the biofilm structure under the fluorescence microscope. Finally, the attempt to knock out genes in *P. acnes* is described and its results shown in the last part of this chapter.

4.1 Static Biofilm Assay – Skin Isolates

The biofilm assay was used for 32 strains (skin isolates of different serotypes) while varying the media BHI, BHG or TG and the incubating time of 3, 5 or 7 days. The goal was to find out the media giving the most significant biofilm results, as well as an analysis of the biofilm dynamics over time. The resulting 32 quantities of biofilm were evaluated for similarities and differences between the serotypes.

4.1.1 TG

4.1.1.1 72h incubation in TG

The static biofilm assay after three days of incubation in TG medium gave the results shown in figure 5.

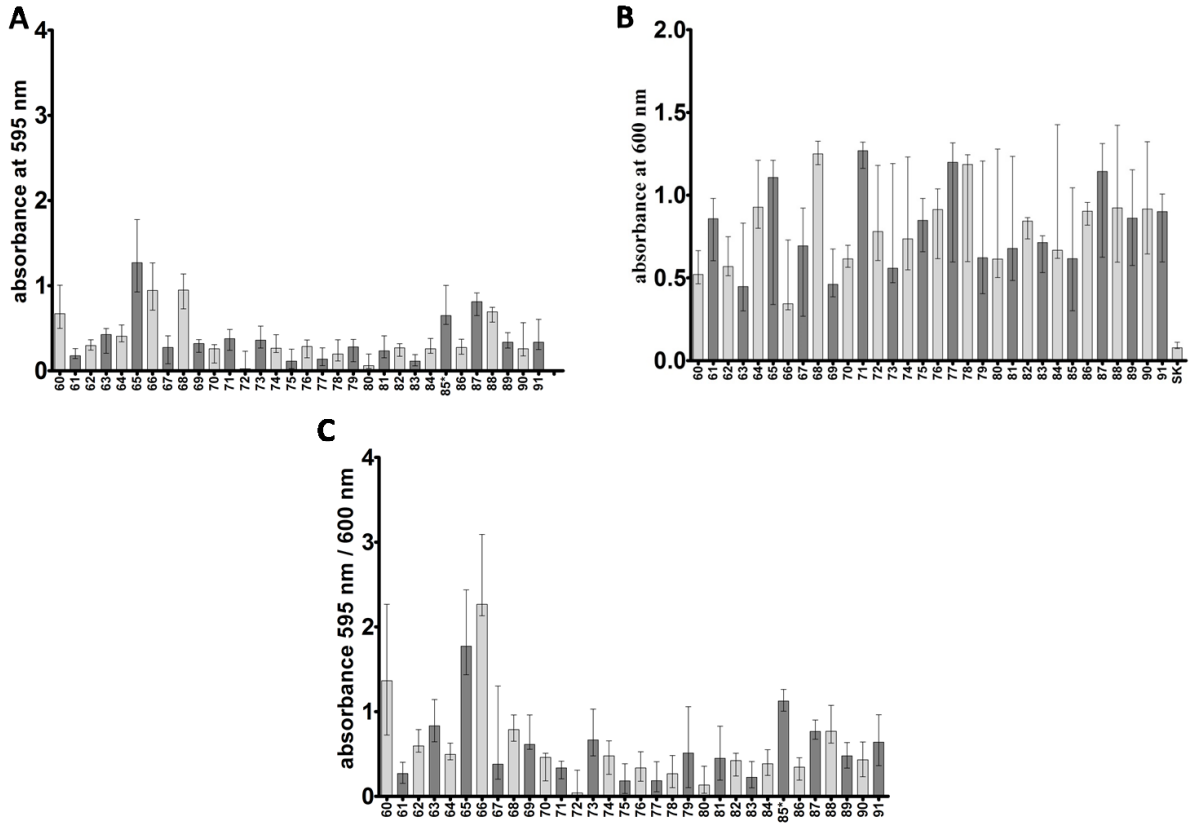

Figure 5: Static biofilm assay for TG, 72h, skin isolates. The results of the static biofilm assay for 32 skin isolates (in TG medium, 72h incubation) are summed up. Panel (A) shows biofilm quantity via absorbance of crystal violet at 595 nm. The blank was already subtracted. The bars peak at the median of at least 12 values with whiskers indicating the interquartile range of 25%. (B) depicts the growth (OD_{600}) of each strain at the respective time point. The ratio between the values of (A) and (B) led to the relative biofilm quantity standardized to OD_{600} = 1 (C). #*85 consists of 6 values.

Panel A displays the relative biofilm absorbance in a platereader at 595 nm, with the blank already being subtracted. Strain #65, #66, #68, #85 and #87 had values above 1. This meant that pronounced amounts of biofilm were attached to the surface of the microtiterplate, while at the same time withstanding the pull of the multipipette. However, the general differences between the other strains were insignificant. The growth of the strains is visible in panel B. Overall relative high values (compared to the other two media) of partially over OD_{600} = 1 within three days were reached. With such massive growth and relatively low biofilm production the ratio was at very low levels (panel C).

4.1.1.2 120h incubation in TG

Two days later (compared to 72h) the strains were analysed again (figure 6).

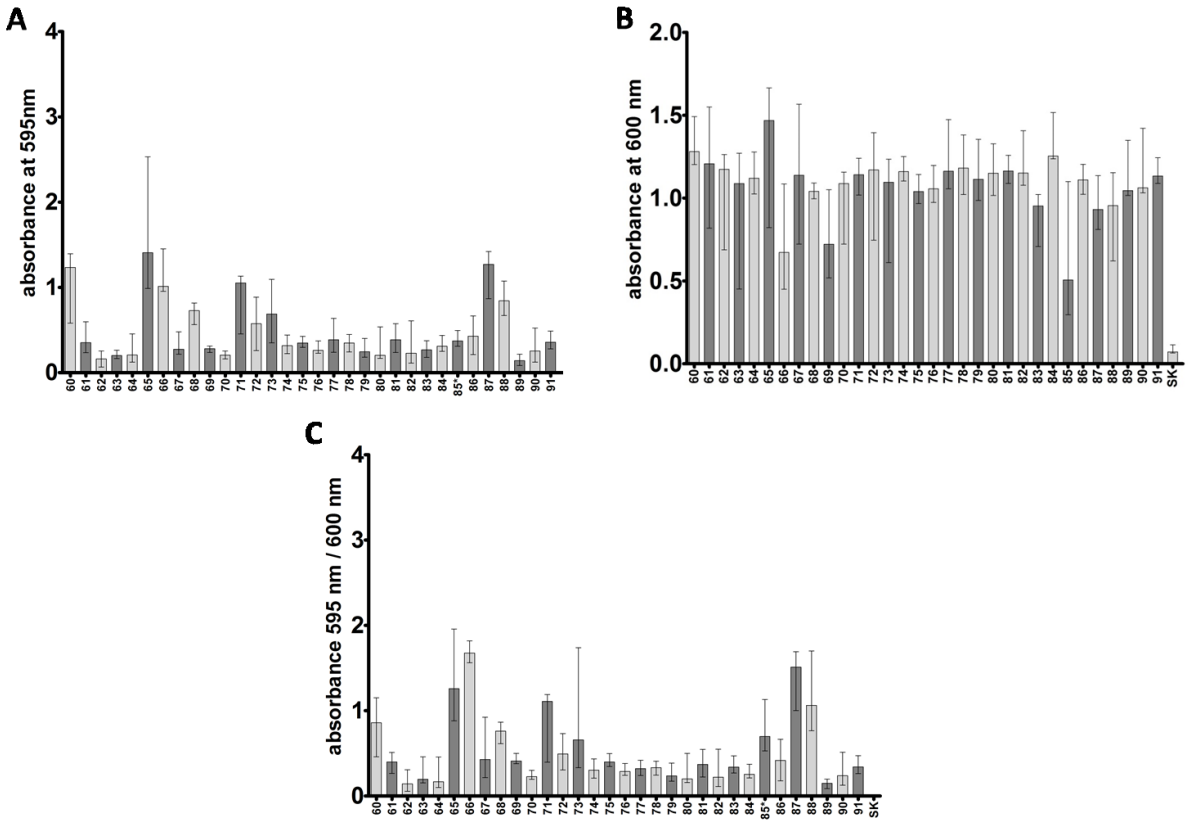

Figure 6: Static biofilm assay for TG, 120h, skin isolates. The results of the static biofilm assay for 32 skin isolates (in TG medium, 120h incubation) are summed up. Panel (A) shows biofilm quantity via absorbance of crystal violet at 595 nm. The blank was already subtracted. The bars peak at the median of at least 12 values with whiskers indicating the interquartile range of 25%. (B) depicts the growth (OD_{600}) of each strain at the respective time point. The ratio between the values of (A) and (B) led to the relative biofilm quantity standardized to OD_{600} = 1 (C). #*85 consists of 6 values.

The biofilm production raised slightly as seen in figure 6/A compared to figure 5/A (72h). The biofilms of #65, #66 and #68 remained elevated compared to 72h, with a slight increase of strain #65. The general range of values of each individual strain stayed the same, showing that the biofilm quantity was reproducible. The growth rate kept its trend with some of them hitting the 1.5 level. The ratio of biofilm / growth remained very low (figure 6/C).

4.1.1.3 168h incubation in TG

Figure 7 shows the biofilm quantity (panel A), growth rate (panel B) and ratio of biofilm / growth (panel C) after incubation for a week.

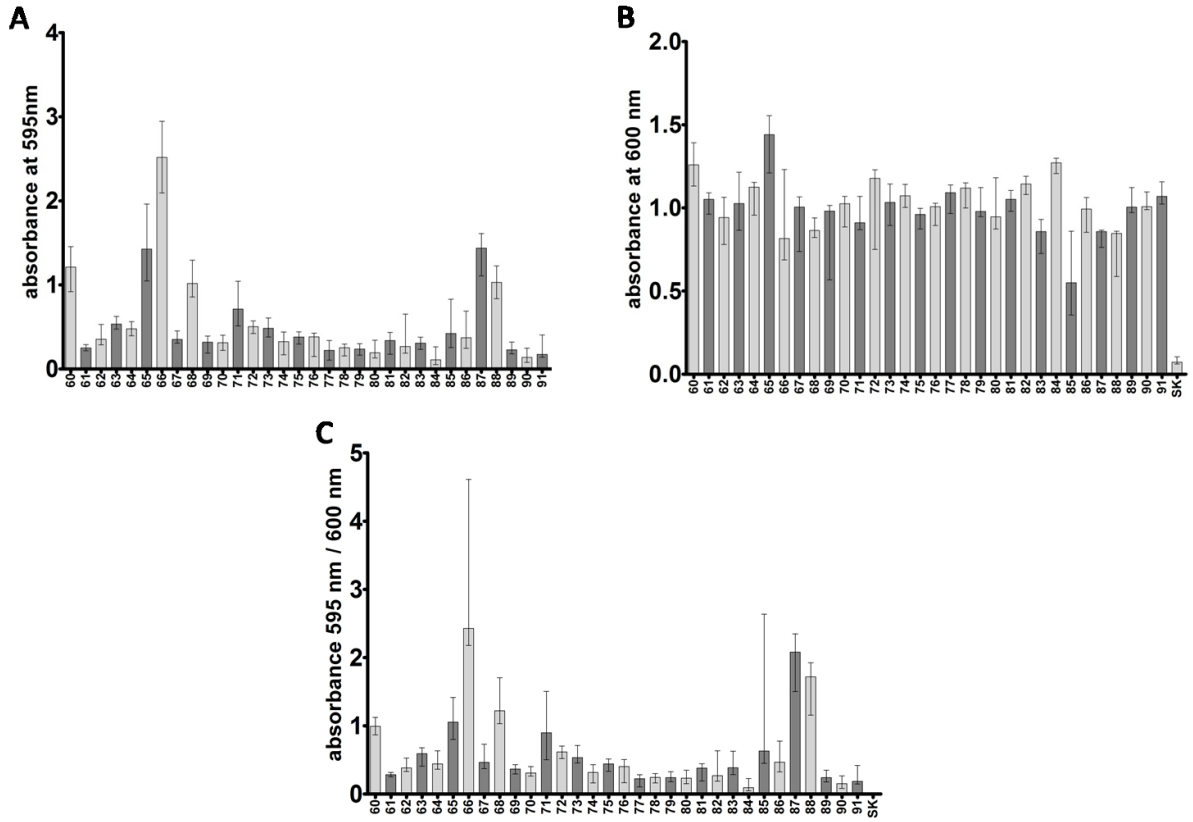

Figure 7: Static biofilm assay for TG, 168h, skin isolates. The results of the static biofilm assay for 32 skin isolates (in TG medium, 168h incubation) are summed up. Panel (A) shows biofilm quantity via absorbance of crystal violet at 595 nm. The blank was already subtracted. The bars peak at the median of at least 12 values with whiskers indicating the interquartile range of 25%. (B) depicts the growth (OD_{600}) of each strain at the respective time point. The ratio between the values of (A) and (B) led to the relative biofilm quantity standardized to OD_{600} = 1 (C).

The additional two days gave strain #65 and #66 another biofilm boost. The other strains didn't change noticeably in their biofilm dynamic (figure 7/A). Meanwhile, almost all strains reached a growth plateau between 1 and 1.5, indicating that nutriments dwindled (panel B). The biofilm / growth ratio remained at low levels, when comparing these results with the following ones (BHI and BHG). Thus, TG was considered to be a comparably unfavourable media for static biofilm assay and consequently discarded in following experiments. However, the growth in TG was exceptionally good. Thus TG was chosen whenever quick growth was needed.

4.1.2 BHI

Three days of incubation in BHI led to the results of figure 8.

4.1.2.1 72h incubation in BHI

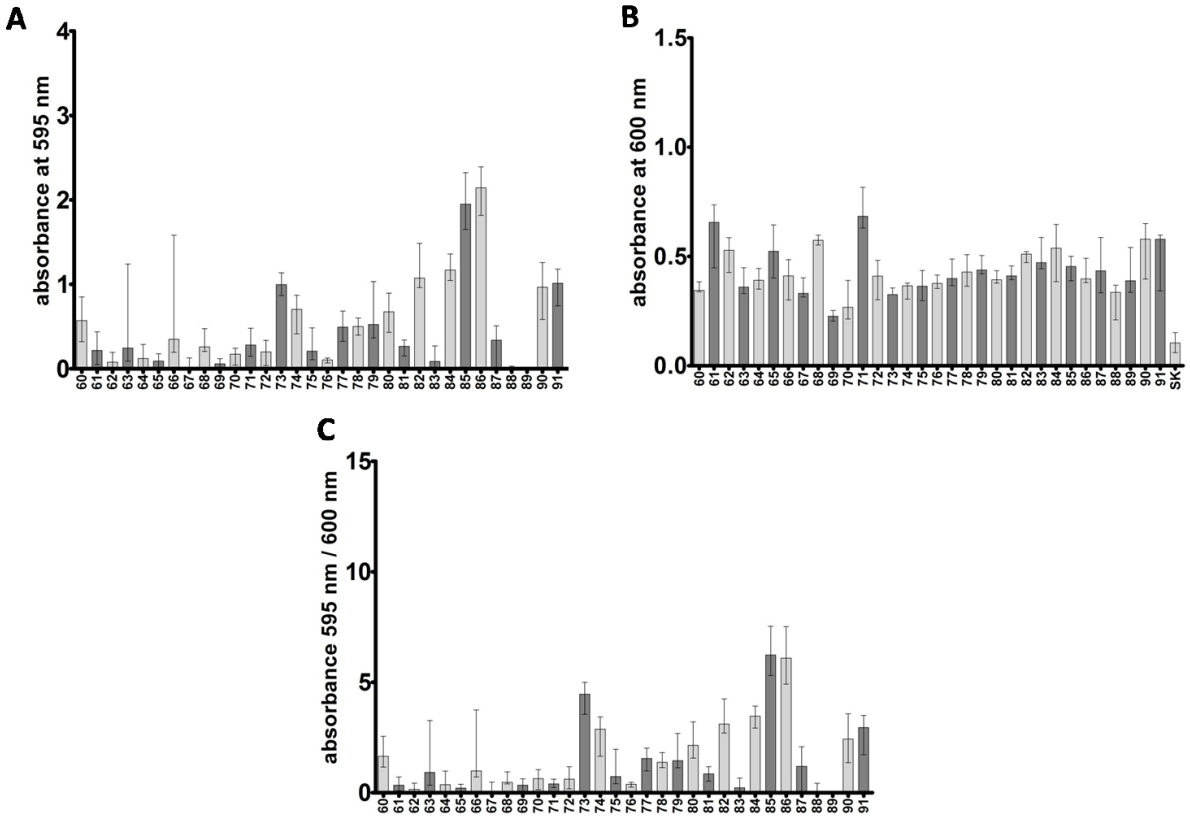

Figure 8: Static biofilm assay for BHI, 72h, skin isolates. The results of the static biofilm assay for 32 skin isolates (in BHI medium, 72h incubation) are summed up. Panel (A) shows biofilm quantity via absorbance of crystal violet at 595 nm. The blank was already subtracted. The bars peak at the median of at least 12 values with whiskers indicating the interquartile range of 25%. (B) depicts the growth (OD_{600}) of each strain at the respective time point. The ratio between the values of (A) and (B) led to the relative biofilm quantity standardized to OD_{600} = 1 (C).

Around 14 strains depicted increased biofilm production (figure 8/A). This assay appeared to deliver noticeably more robust values than in TG. Strain #85 and #86 reached values above 2 after 3 days of incubation only. The growth on the other side turned out to be lower compared to TG (panel B). The biofilm / growth rate kept the tendencies of the biofilm production, as strains with strong variation from growth average did not produce biofilm anyway (like strain #69, panel C).

4.1.2.2 120h incubation in BHI

5 days of incubation in BHI medium had the following results: (figure 9)

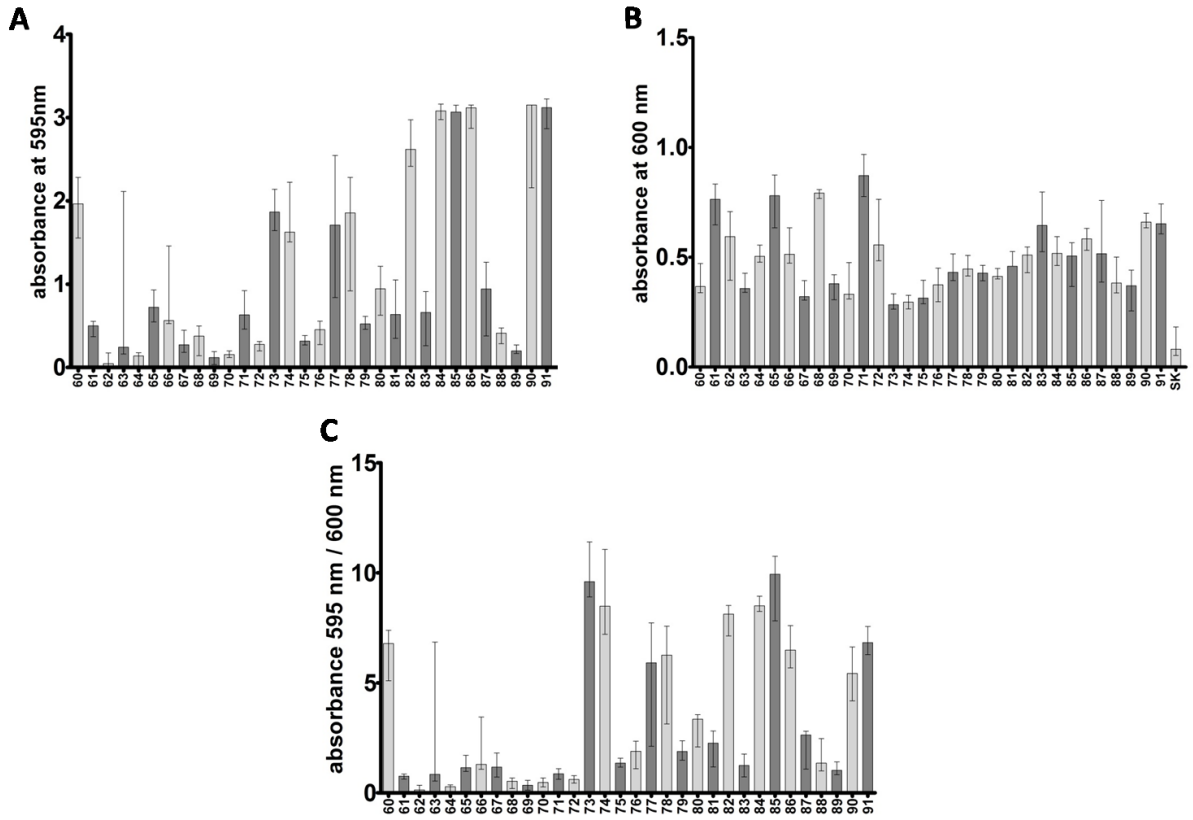

Figure 9: Static biofilm assay for BHI, 120h, skin isolates. The results of the static biofilm assay for 32 skin isolates (in BHI medium, 120h incubation) are summed up. Panel (A) shows biofilm quantity via absorbance of crystal violet at 595 nm. The blank was already subtracted. The bars peak at the median of at least 12 values with whiskers indicating the interquartile range of 25%. (B) depicts the growth (OD_{600}) of each strain at the respective time point. The ratio between the values of (A) and (B) led to the relative biofilm quantity standardized to OD_{600} = 1 (C).

One can see obvious differences in biofilm production between the strains (figure 9/A). The strains #60 (serotype IA1), #73 (IA1), #74 (IA1), #77 (IA1), #78 (IA1), #82 (IA1), #84 (IA1), #85 (IA1), #86 (IA1), #90 (IA1) and #91 (IA1) all varied significantly

and with low interquartile (25) range from the other ones. Some of them produced lower amounts of biofilm (like #87 or #71). But also these values, in this particular height, were reproducible and characteristic for the strain, also when compared to the other time points. When looking at the serotype groups of the strains with high biofilm production, it became obvious that all of them belong to the IA1 serotype. This correlation was significant and continued for all assays within the study.

The biofilm / growth ratio (figure 9/C) slightly shifted the biofilm values. #73 and #74 produced comparably lower amounts of biofilm than #84 and #86. At the same time #73 and #74 had lower growth in the same incubation time. The ratio biofilm per growth balanced this disparity and brought all 4 strains to a similar level.

4.1.2.3 168h incubation in BHI

The data after 7 days of incubation in BHI is pictured in figure 10.

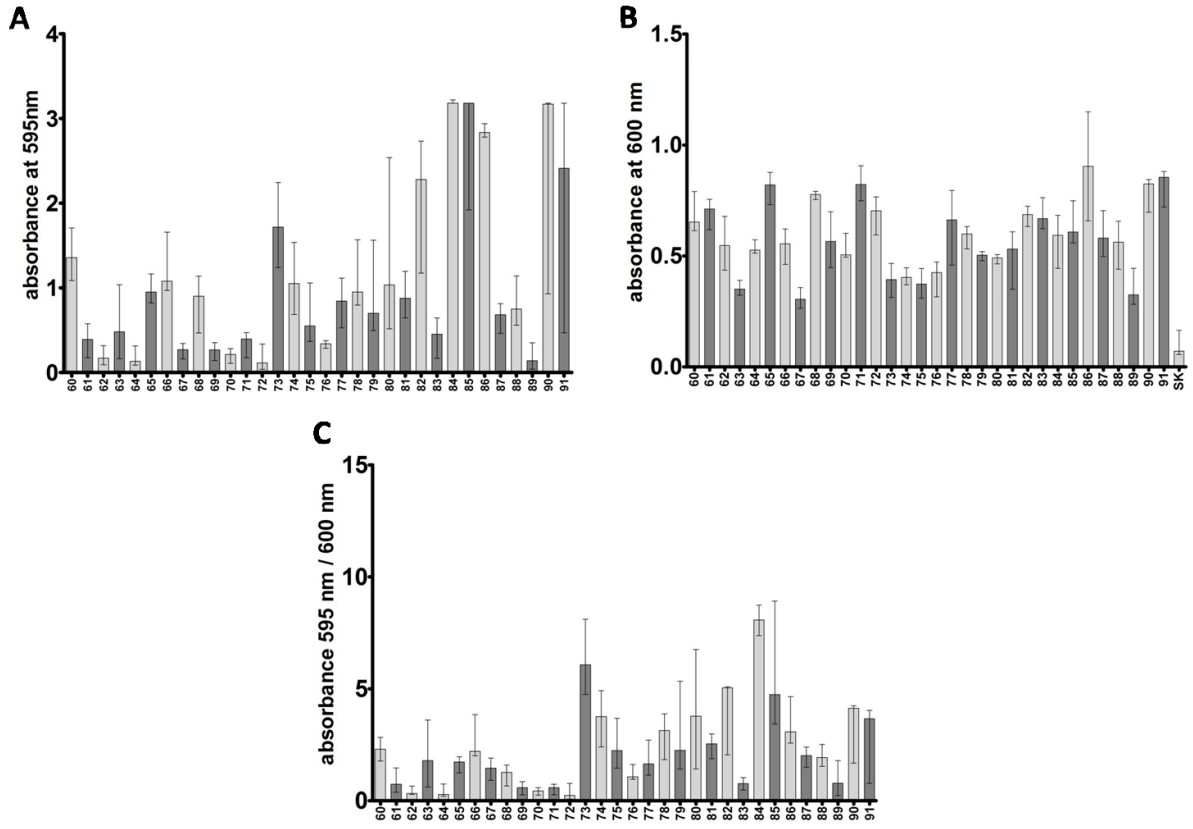

Figure 10: Static biofilm assay for BHI, 168h, skin isolates. The results of the static biofilm assay for 32 skin isolates (in BHI medium, 168h incubation) are summed up. Panel (A) shows biofilm quantity via absorbance of crystal violet at 595 nm. The blank was already subtracted. The bars peak at the median of at least 12 values with whiskers indicating the interquartile range of 25%. (B) depicts the growth (OD_{600}) of each strain at the respective time point. The ratio between the values of (A) and (B) led to the relative biofilm quantity standardized to OD_{600} = 1 (C).

The difference between 120h and 168h incubation appeared to be comparably slim (figure 9 and 10). The dynamic of biofilm growth seemed to have ended indicating a mature biofilm, which is why 7 days of incubation were taken as last time point.

4.1.3 BHG

The third media, BHI with the addition of glucose, was tested in parallel.

4.1.3.1 72h incubation in BHG

Figure 11 includes the biofilm production (panel A), the growth (B) and the biofilm per growth rate (C).

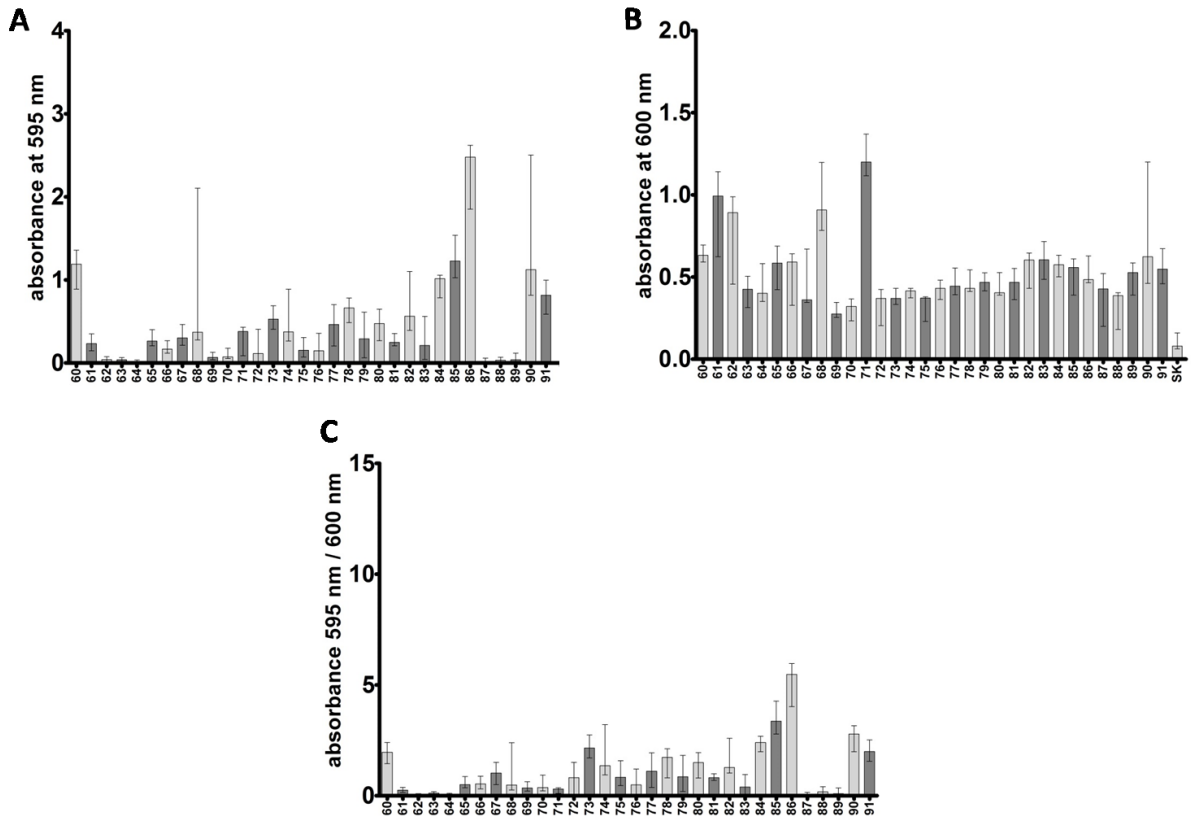

Figure 11: Static biofilm assay for BHG, 72h, skin isolates. The results of the static biofilm assay for 32 skin isolates (in BHG medium, 72h incubation) are summed up. Panel (A) shows biofilm quantity via absorbance of crystal violet at 595 nm. The blank was already subtracted. The bars peak at the median of at least 12 values with whiskers indicating the interquartile range of 25%. (B) depicts the growth (OD_{600}) of each strain at the respective time point. The ratio between the values of (A) and (B) led to the relative biofilm quantity standardized to OD_{600} = 1 (C).

When comparing the figure above to figure 8 (BHI/72h), the addition of glucose did not seem to improve the data other than enhancing the growth rate.

4.1.3.2 120h incubation in BHG

The following figure 12 contains growth in BHG medium after 5 days of incubation.

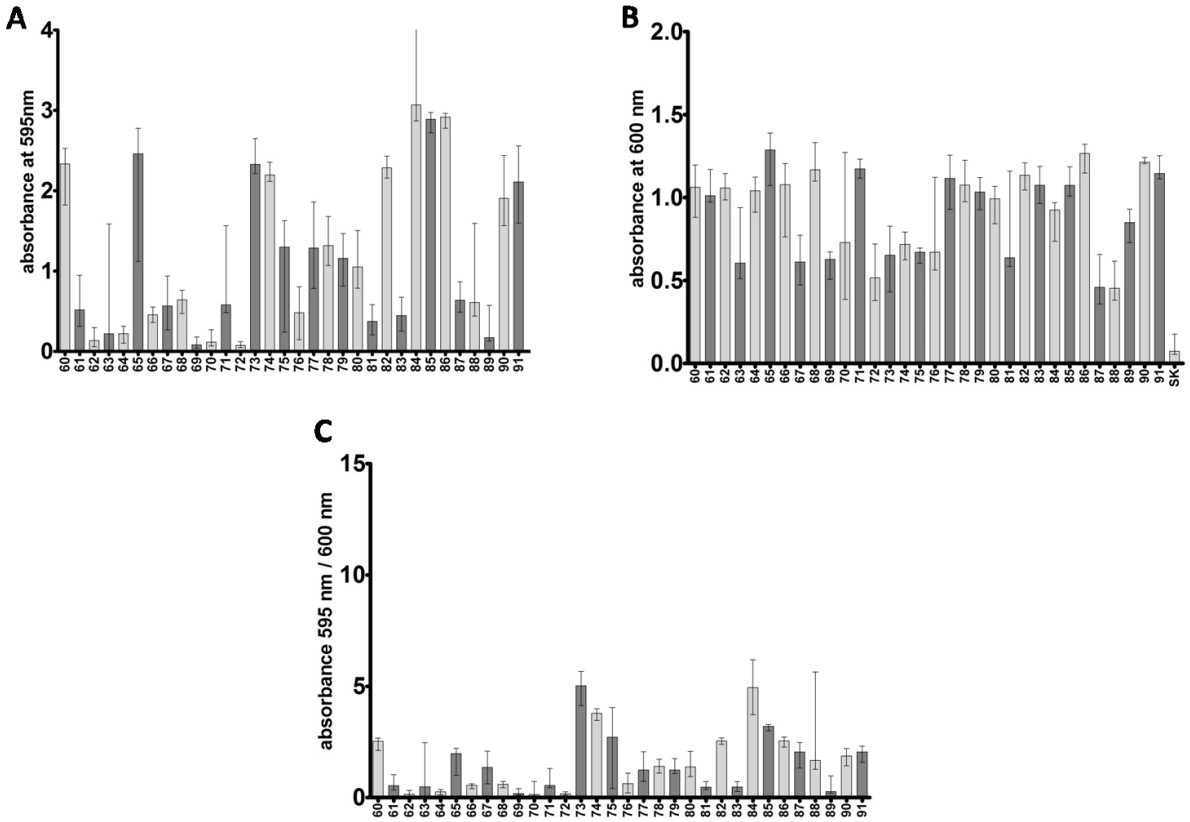

Figure 12: Static biofilm assay for BHG, 120h, skin isolates. The results of the static biofilm assay for 32 skin isolates (in BHG medium, 120h incubation) are summed up. Panel (A) shows biofilm quantity via absorbance of crystal violet at 595 nm. The blank was already subtracted. The bars peak at the median of at least 12 values with whiskers indicating the interquartile range of 25%. (B) depicts the growth (OD_{600}) of each strain at the respective time point. The ratio between the values of (A) and (B) led to the relative biofilm quantity standardized to OD_{600} = 1 (C).

After 5 days the growth rate (panel B) improved significantly, compared to BHI medium (from 0.4 – 1.0, to 0.5 – 1.4). No systemic change or improvement in biofilm dynamics could be detected.

4.1.3.3 168h incubation in BHG

The data of the last time point is shown in figure 13.

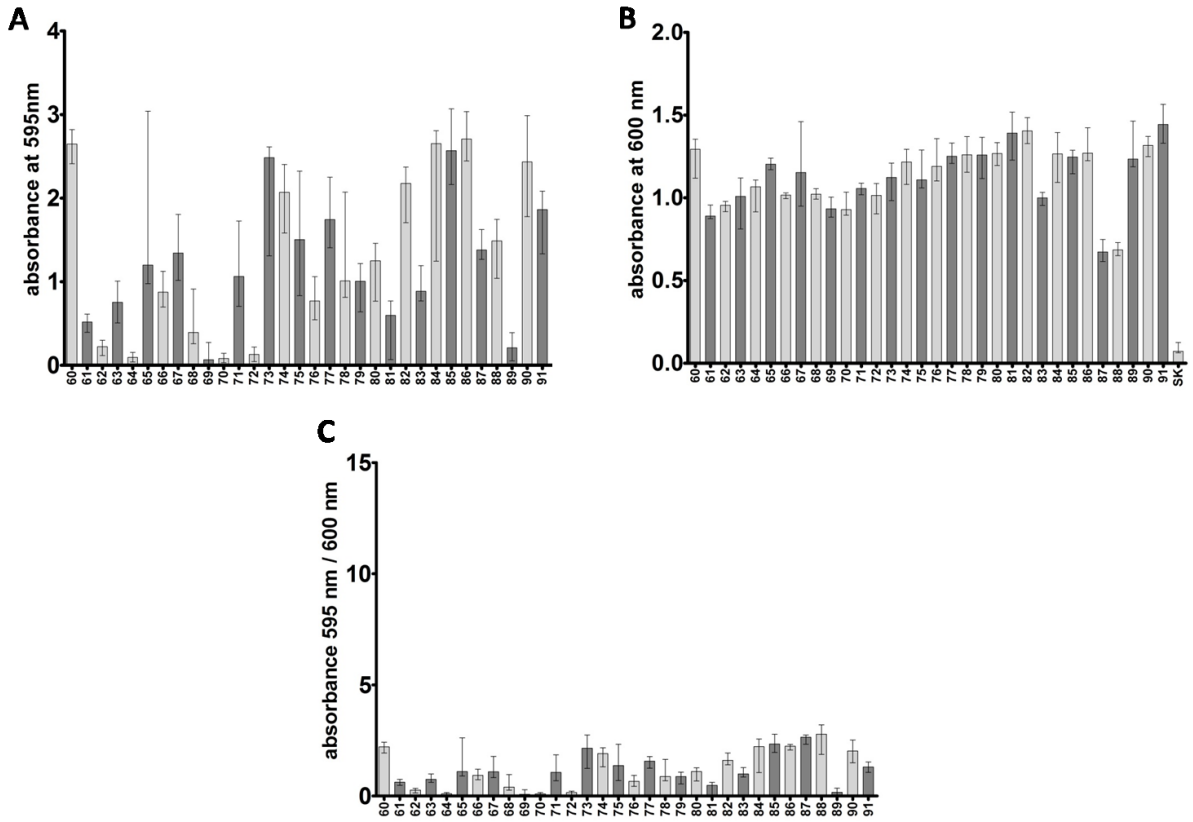

Figure 13: Static biofilm assay for BHG, 168h, skin isolates. The results of the static biofilm assay for 32 skin isolates (in BHG medium, 168h incubation) are summed up. Panel (A) shows biofilm quantity via absorbance of crystal violet at 595 nm. The blank was already subtracted. The bars peak at the median of at least 12 values with whiskers indicating the interquartile range of 25%. (B) depicts the growth (OD_{600}) of each strain at the respective time point. The ratio between the values of (A) and (B) led to the relative biofilm quantity standardized to OD_{600} = 1 (C).

The relative biofilm quantity of the different strains (when compared to BHI) stayed the same, with only a few strains showing an improved or reduced adherence to the surface.

The growth, however, improved greatly, changing from an average of around 0.5 (BHI 168h, figure 10/B) to 1.0 (BHG 168h, figure 13/B). The main effect of the addition of glucose thus seemed to be to simply increase growth, while maintaining equal biofilm production. Increased growth reduced the values of the biofilm / growth ratio though.

Thus BHI was chosen as medium for future static biofilm assays. The dynamic of a biofilm production and degradation was sufficiently represented by the time points 72h, 120h and 168h with 168h revealing the stagnation point for most strains. A test of 216h incubation led to lower biofilm values, indicating biofilm disintegration began between those time points (data not shown).

4.1.4 Correlation of Biofilm Formation and Serotypes

As mentioned in the BHI/120h chapter, strong biofilm production was seen particularly within the serotype group IA1. To find out about its significance, all biofilm / growth values from all IA1 strains grown in BHI were pooled, as well as all other serotype data. The results are shown in figure 12.

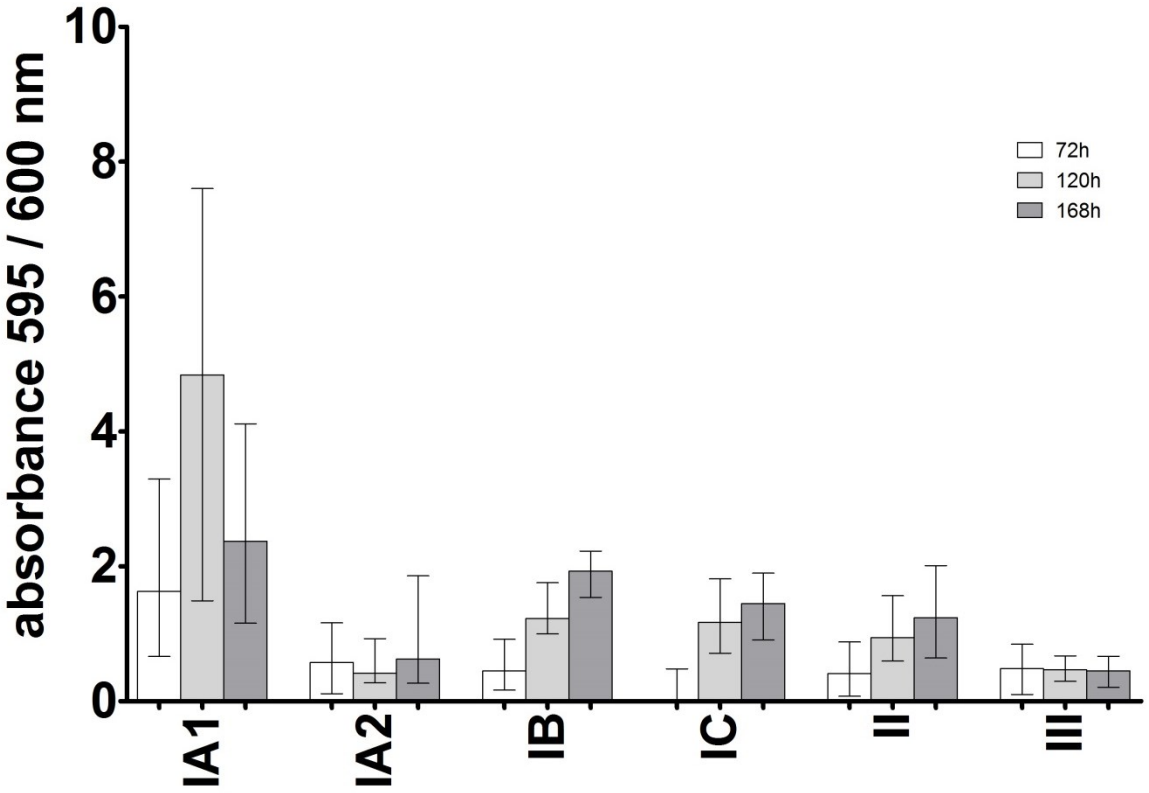

Figure 14: Static biofilm assay serotype summary (BHI). The values of all biofilm ratios (biofilm quantity / growth) in BHI (see figure 8 – 10) were summed up in serotype groups. The bars peak at the median of at least 12 values with whiskers indicating the interquartile range of 25%. The different time points were lined up to characterize the dynamic biofilm formation. The IA1 serotype group produced significantly more biofilm than the other groups.

The IA1 strains, especially after 5 days of incubation, showed significantly more biofilm than all other serotype groups. Type III strains had the lowest amount of biofilm.

4.2 Static Biofilm Assay – Implant Isolates

After establishing the static biofilm assay and investigating the quantity of the skin isolates, the question was whether there is a difference between skin and implant isolates.The setup of the final static biofilm assay establishment was chosen (3 time points at 72h/120h/168h, and BHI as medium). The 19 implant isolates (see methods/strain list) were serotyped a priory. To keep environmental parameters identical, implant isolates of certain serotypes were incubated on the same plate (in the same media of the same batch) as skin isolates of the same serotype. This way there was one plate with only IB strains (from skin and implant isolates), one plate with IA1 strains and one plate with the remaining plates. The static biofilm assay was done twice, resulting in at least 12 values per strain.

The data of each time point and each strain is shown in detail in the appendix. The following figures summarize the serotype outcomes.

4.2.1 BHI – Serotypes

The static biofilm assay data with the three time points (72h, 120h, 168h, in BHI) were merged to serotype groups in the following figures.

4.2.1.1 IA1

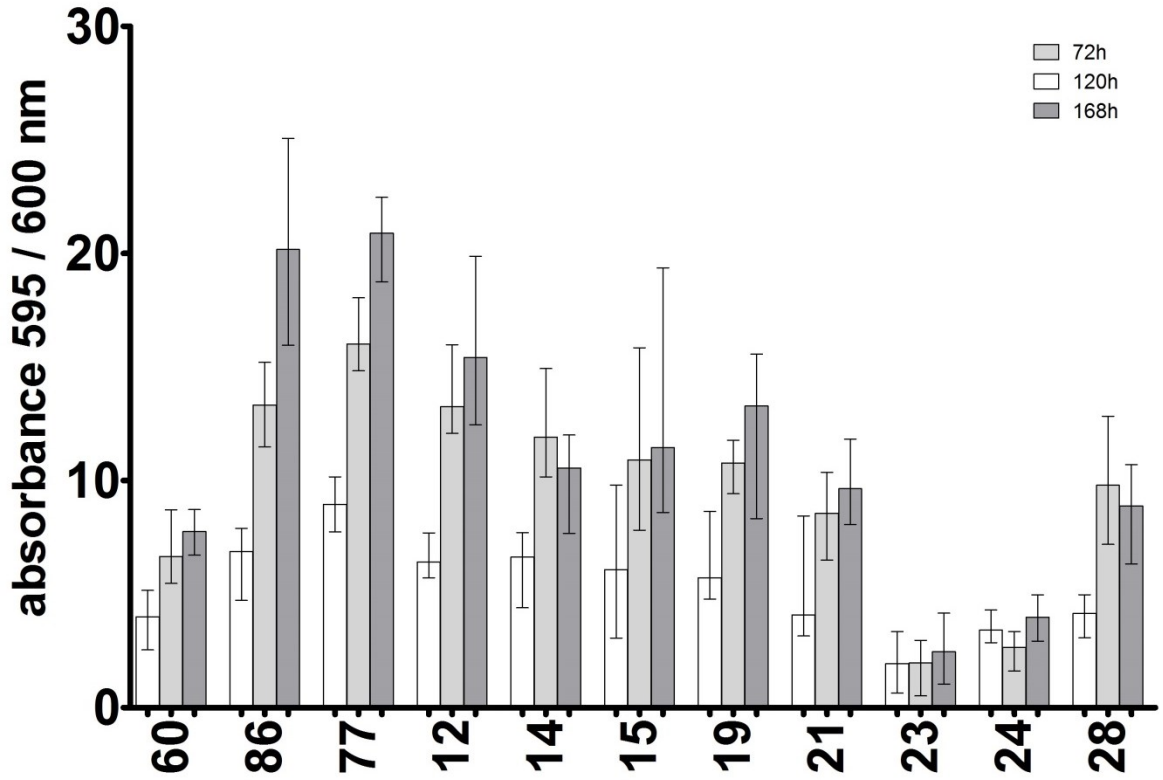

Figure 15: Static biofilm assay, IA1 summary (BHI). The biofilm ratio (biofilm quantity / growth) of skin and implant strains of the IAI group in BHI were summed up in one figure. The bars roof at the median of at least 12 values with whiskers indicating the interquartile range of 25%. The different time points were lined up to characterize the dynamic biofilm formation. 68 and 86 were skin isolates, the rest implant isolates. The quantity and dynamic of most IA1 strains had similar patterns.

The data of all IA1 strains is depicted in figure 15. The first three strains were skin isolates, the other 8 implant isolates. The dynamic of the strains was similar: a relative strong biofilm formation was observed with half of the total biomass being established already after 3 days. This was followed by a continued production towards day 5 and a slight stagnation in production till day 7. Strain #12, #15, #19 and #21 had similar dynamic.

4.2.1.2 IB

The results of the static biofilm assay of the IB strains are shown in the following figure:

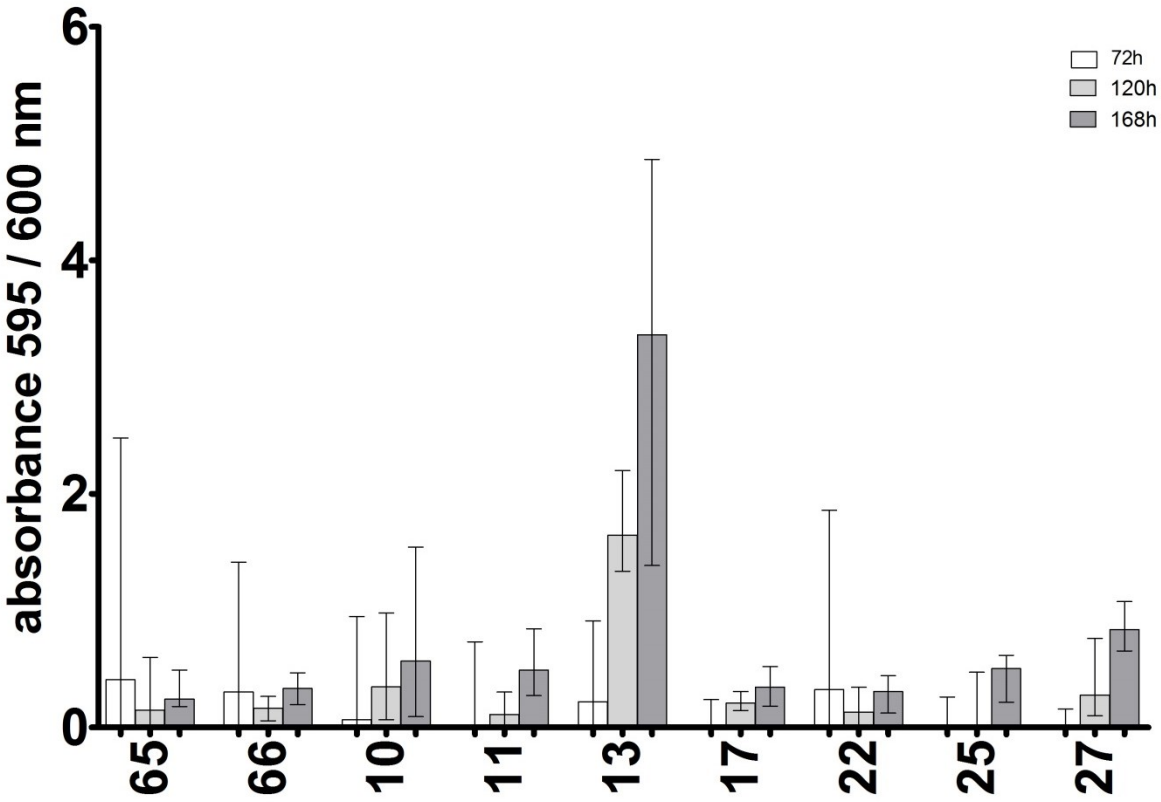

Figure 16: Static biofilm assay, IB summary (BHI). The biofilm ratio (biofilm quantity / growth) of skin and implant strains of the IB group in BHI were summed up in one figure. The bars roof at the median of at least 12 values with whiskers indicating the interquartile range of 25%. The different time points were lined up to characterize the dynamic biofilm formation. 65 and 66 were skin isolates, the rest implant isolates. The dynamics of IB seemed to have more heterogeneity, compared to the other serotypes the patterns were still somewhat unique.

The first two strains of figure 16 display the biofilm production per growth of skin isolates, the other ones are implant isolates. The general biofilm production median was mostly around 0.4, which appeared to be a lot lower than even the lowest IA1 strain (#23 with ~2 median).

4.2.1.3 IA2, IC, II and III

The other serotypes were compared in figure 17.

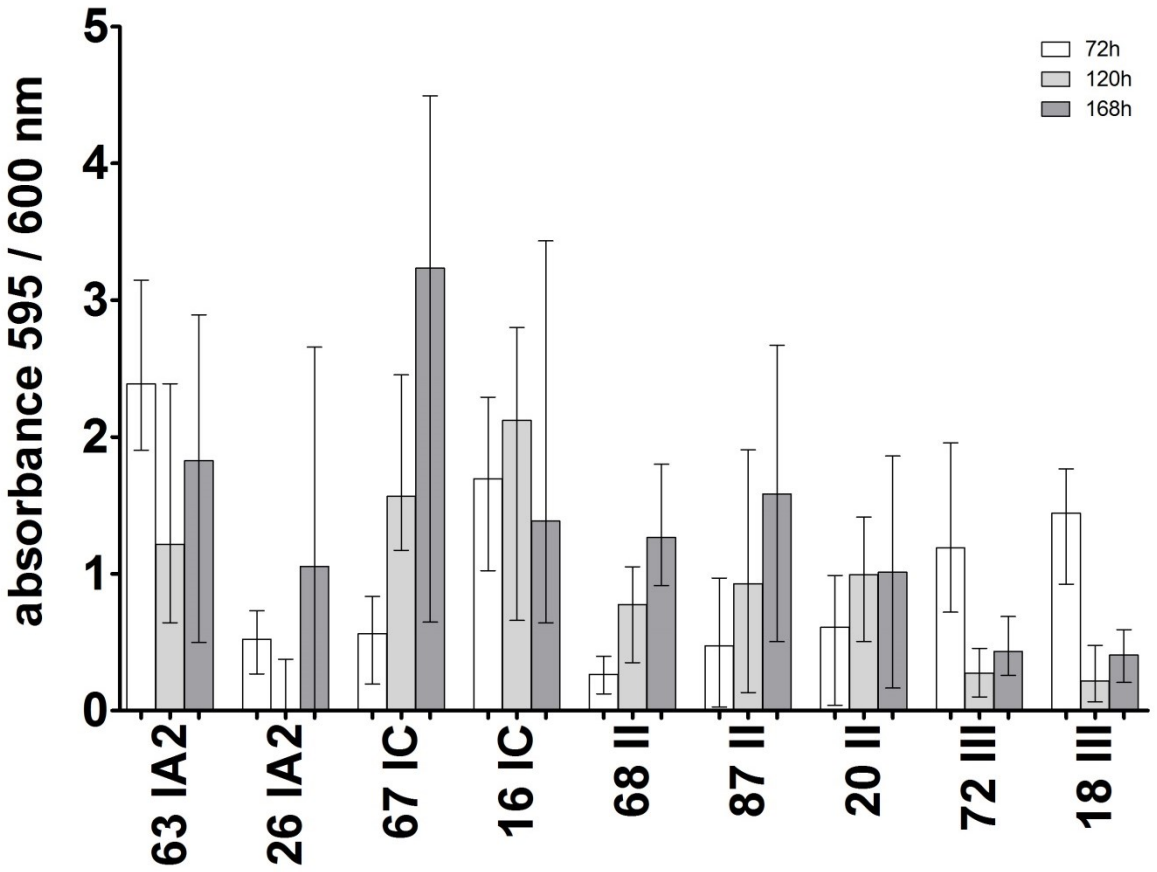

Figure 17: Static biofilm assay, IA2/IC/II/III summary (BHI). The biofilm ratio (biofilm quantity / growth) of skin and implant strains of the IA2/IC/II/III groups in BHI were summed up in one figure. The bars roof at the median of at least 12 values with whiskers indicating the interquartile range of 25%. The different time points were lined up to characterize the dynamic biofilm formation. Strains between #60 and #91 were skin isolates, strains between #10 and #28 implant isolates. The quantities and dynamics of the respective serotype groups showed similar patterns.

As the numbers of available strains for these groups were low, only 1 or 2 strains of each setup were compared. The dynamic production over time as well as relative quantity was surprisingly similar. Strain #68 and #87 (type II, from the skin) showed same growth dynamic as their implant counterpart #20. Same counted for serotype III: both grew a biofilm to a relative absorption unit of ~1.5, and then lost most of it within the next two days.

In summary it can be said that quantitative biofilm production, as well as dynamic production and degradation biofilm over time of *P. acnes* depends on the serotype, and not on the place of its isolation.

4.3 Macroscopic Evaluation

Images of the microtiterplates were taken in parallel to the static biofilm assay. They showed distinct macroscopic morphology which varied between serotypes and even within the serotype groups. These structures were characteristic for each strain in a reproducible way. Once these structures were known, they would allow for a quick analysis whether there was a change in phenotype (for example wildtype compared to gene knockout). Additionally, it would allow a verification of the expected strain and early detection of contaminations.

4.3.1 Skin Isolates

The images of skin isolates, grown in round-bottomed wells in BHI over 72h, 120h and 168h at 37°C, are shown in the following subchapters.

4.3.1.1 IA2, IB, IC, II and III

All skin isolates belonging to the serotype group of IA2, IB, IC, II and III were pictured in figure 18:

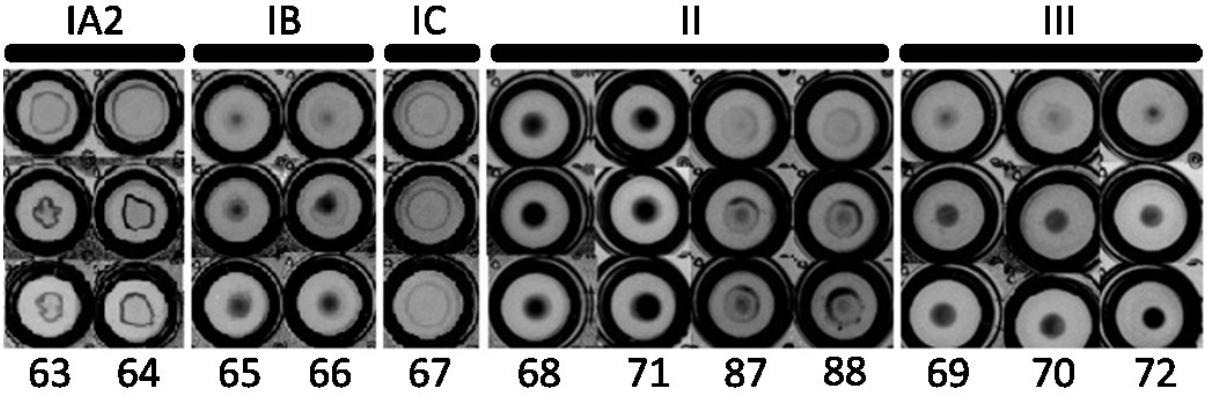

Figure 18: Macroscopic images IA2/IB/IC/II/III (BHI). Before applying the static biofilm assay, images were taken from microtiterplate. These images showed the characteristic macroscopic aggregates more or less adsorbed to the surface of the round-bottomed well. The dynamic change over time is shown by three time points (first row = 72h, followed by 120h and 168h). All available skin isolates were grouped into the respective serotype. Similar patterns can be recognized.

When looking at the first 2 columns of the wells of the IA2 strain, there were unevenly arranged circular lines. These represented the border of the *P. acnes* biofilm, which might have rolled in due to gravity from the round-bottomed well. The inner part was *P. acne* biofilm, the outer part was completely clear. The first row shows the biofilm

after 72h, the second row after 120h and the third after 168h. IB serotypes looked very different with cells sedimenting to the centre of the well, with only a few of them spreading against gravity. Most of II and III were merely consisting of a sedimented pellet at the lowest gravity point.

4.3.1.2 IA1

The following figures 19 and 20 show all IA1 strains of the skin isolates.

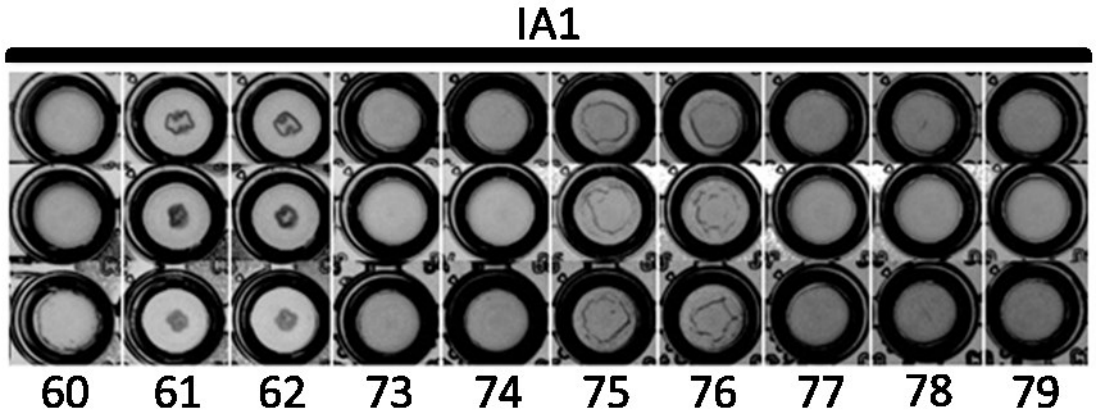

Figure 19: Macroscopic image of IA1 (#60-#79) skin isolates. Before applying the static biofilm assay, images were taken from microtiterplate. These images showed the characteristic macroscopic aggregates more or less adsorbed to the surface of the round-bottomed well. The dynamic change over time is shown by three time points (first row = 72h, followed by 120h and 168h). Skin isolates #60 – #79 of serotype group IA1 are shown in this figure. Similar patterns can be recognized. The seemingly empty wells consisted of a smooth layer of cell material adsorbed to the surface, actually growing against the gravity of the round-bottomed well to some degree.

Strain #61 and #62 display some sort of rolled in biofilm, sedimented to the centre of the round-bottomed well. Strain #75 and #76 featured some sort of partial biofilm detachment.

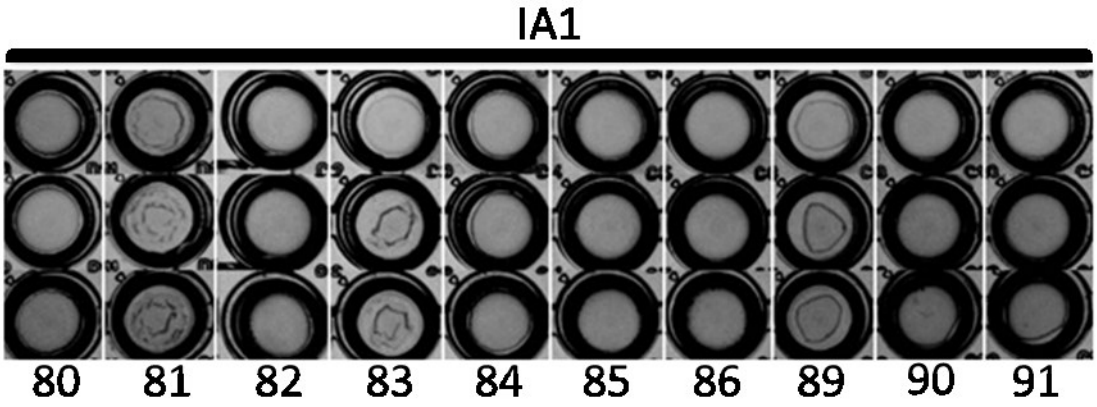

Figure 20: Macroscopic image of IA1 (#80-#91) skin isolates. Before applying the static biofilm assay, images were taken from microtiterplate. These images showed the characteristic macroscopic aggregates more or less adsorbed to the surface of the round-bottomed well. The dynamic change over time is shown by three time points (first row = 72h, followed by 120h and 168h). Skin isolates #80 – #91 of serotype group IA1 are shown in this figure. Similar patterns can be recognized. The seemingly empty wells consisted of a smooth layer of cell material adsorbed to the surface, actually growing against the gravity of the round-bottomed well to some degree.

The majority of the IA1 strains apparently had no macroscopic phenotype (like #60, #74 or #86). In reality those round-bottomed wells were completely covered with an evenly distributed layer of *P. acnes* biofilm. The medium above was completely clear. This layer of biofilm correlated with the biofilm quantity of the static biofilm assay.

4.3.2 Implant Isolates

The implant isolates were compared to the skin isolates in macroscopic appearance. To show the reproducibility of these macroscopic structures, the images within this chapter include images of two independently performed assays (called BA1 and BA2).

4.3.2.1 IA1

One IA1 skin isolate was compared to the IA1 implant isolates in figure 21.

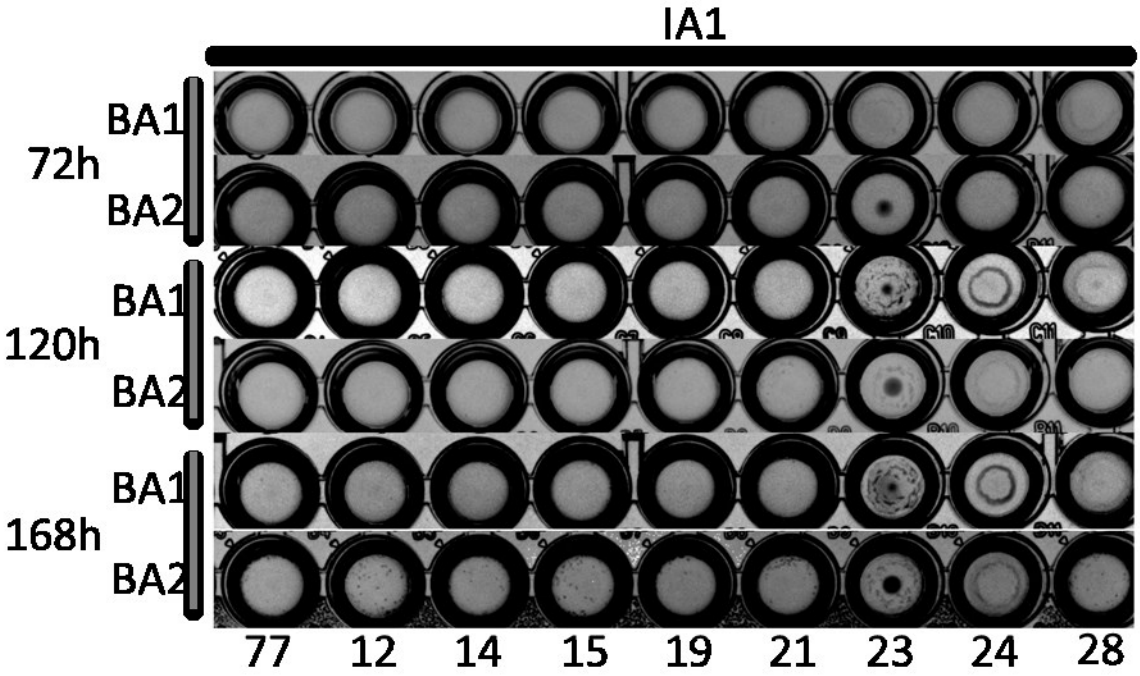

Figure 21: Macroscopic image of IAl skin vs implant isolates (BHI). Before applying the static biofilm assay, images were taken from the microtiterplates. These images showed the characteristic macroscopic aggregates more or less adsorbed to the surface of the round-bottomed well. The dynamic change over time is shown by three time points (first two rows = 72h, followed by 120h and 168h). Skin isolate #77 was compared to implant isolates #12 – #28, all of serotype group IA1. Similar patterns can be recognized. The seemingly empty wells consisted of a smooth layer of cell material adsorbed to the surface, actually growing against the gravity of the round-bottomed well to some degree. To show the reproducibility of these special characteristics, images of two independent assays (BA1 and BA2) were included.

The standard skin IA1 layer of biofilm was visible in the majority of implant isolates. Thus the IA1 structure of most IA1 skin isolates correlated with the structure of IA1 implant isolates. Only strain #23 and #24 showed some unique variations, which also reduced their biofilm adherence (see figure 15, #23 and 24 with lower biofilm quantity). Such deviations were seen also from skin isolates.

4.3.2.2 IB

The IB serotypes were summed up in figure 22.

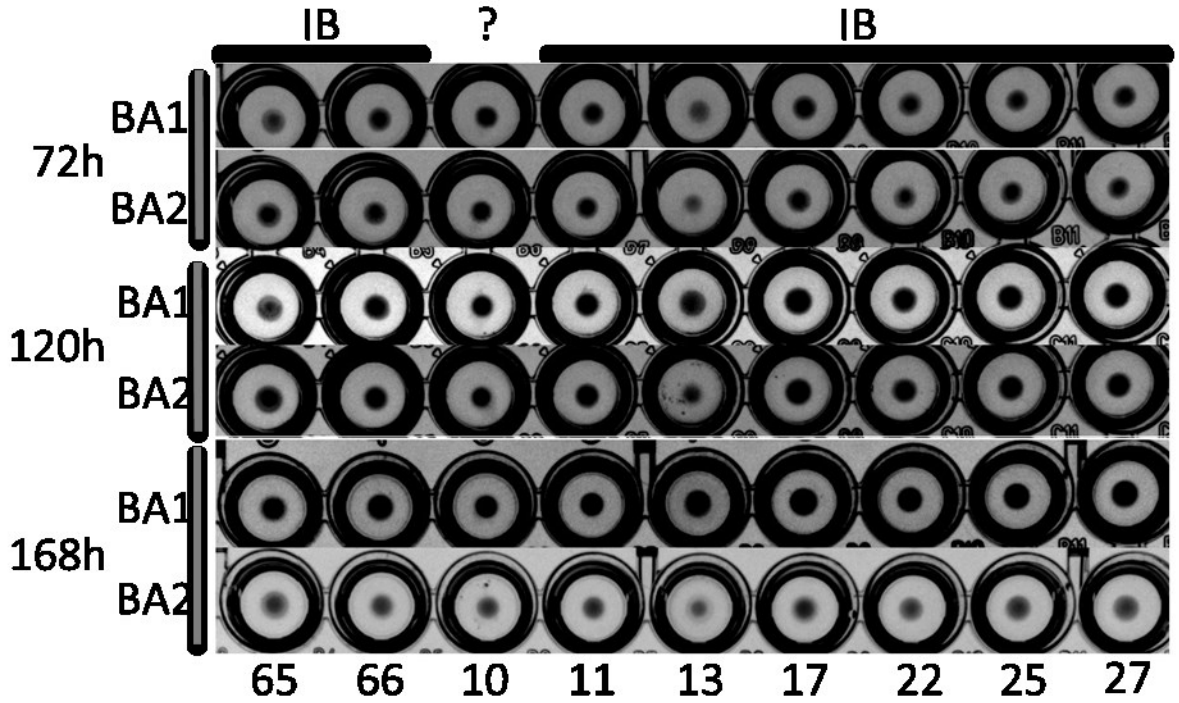

Figure 22: Macroscopic image of IB skin vs implant isolates. Before applying the static biofilm assay, images were taken from the microtiterplates. These images showed the characteristic macroscopic aggregates more or less adsorbed to the surface of the round-bottomed well. The dynamic change over time is shown by three time points (first two rows = 72h, followed by 120h and 168h). Skin isolates #65 and #66 were compared to implant isolates #10 – #27, all of serotype group IB (except #10). Equal patterns of the cells sedimenting to the centre of the round-bottomed wells can be recognized. To show the reproducibility of these special characteristics, images of two independent assays (BA1 and BA2) were included.

All of them (skin or implant isolate) had the same pellet-like phenotype. According to this macroscopic phenotype characterization it can be assumed that the strain #10, which was not serotyped yet, could be of IB type.

4.3.2.3 IA2, IC, II and III

The serotypes IA2, IC, II and III are shown in figure 23.

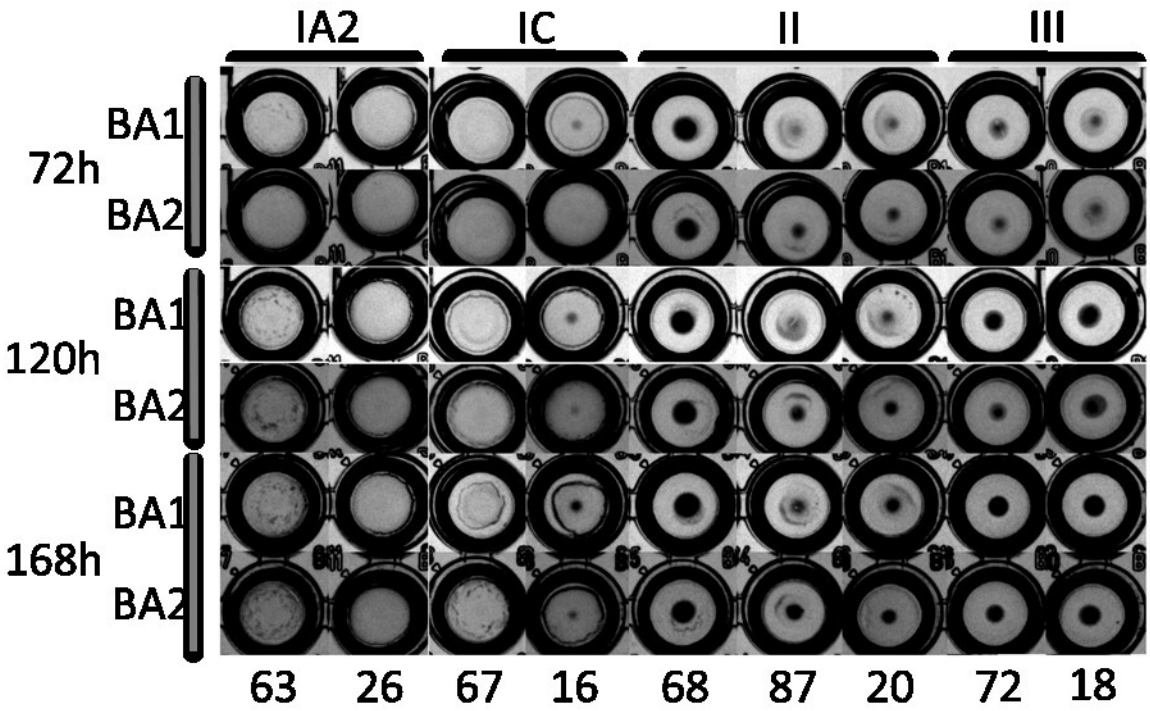

Figure 23: Macroscopic image of IA2/IC/II/III skin vs implant isolates. Before applying the static biofilm assay, images were taken from the microtiterplates. These images showed the characteristic macroscopic aggregates more or less adsorbed to the surface of the round-bottomed well. The dynamic change over time is shown by three time points (first two rows = 72h, followed by 120h and 168h). Skin isolates (with numbers between #62 and #87) were compared to implant isolates (numbered #16 – #26). Similar patterns within each serotype can be recognized. To show the reproducibility of these special characteristics, images of two independent assays (BA1 and BA2) were included.

IA2 (and to some degree also IC) correlated more with IA1. II and III looked more similar to IB. However, there was clear correlation of macroscopic appearance and serotype, independent of skin and implant isolates.

4.4 Fluorescence Microscopy

After investigation of the macroscopic aggregate formation and the biofilm adherence quantity, the third phenotypic characterization was about visualization of the biofilm morphology using fluorescence microscopy and analysing it bioinformatically.

4.4.1 Biofilm Morphology

Four representatives of three serotype groups (IA1, IA2 and IC) with comparable good biofilm adherence were visualized (figure 24). As the composition of the extracellular polymeric substance (the matrix of the biofilm) was unknown to this point, the cells themselves had to be stained with STYO9.

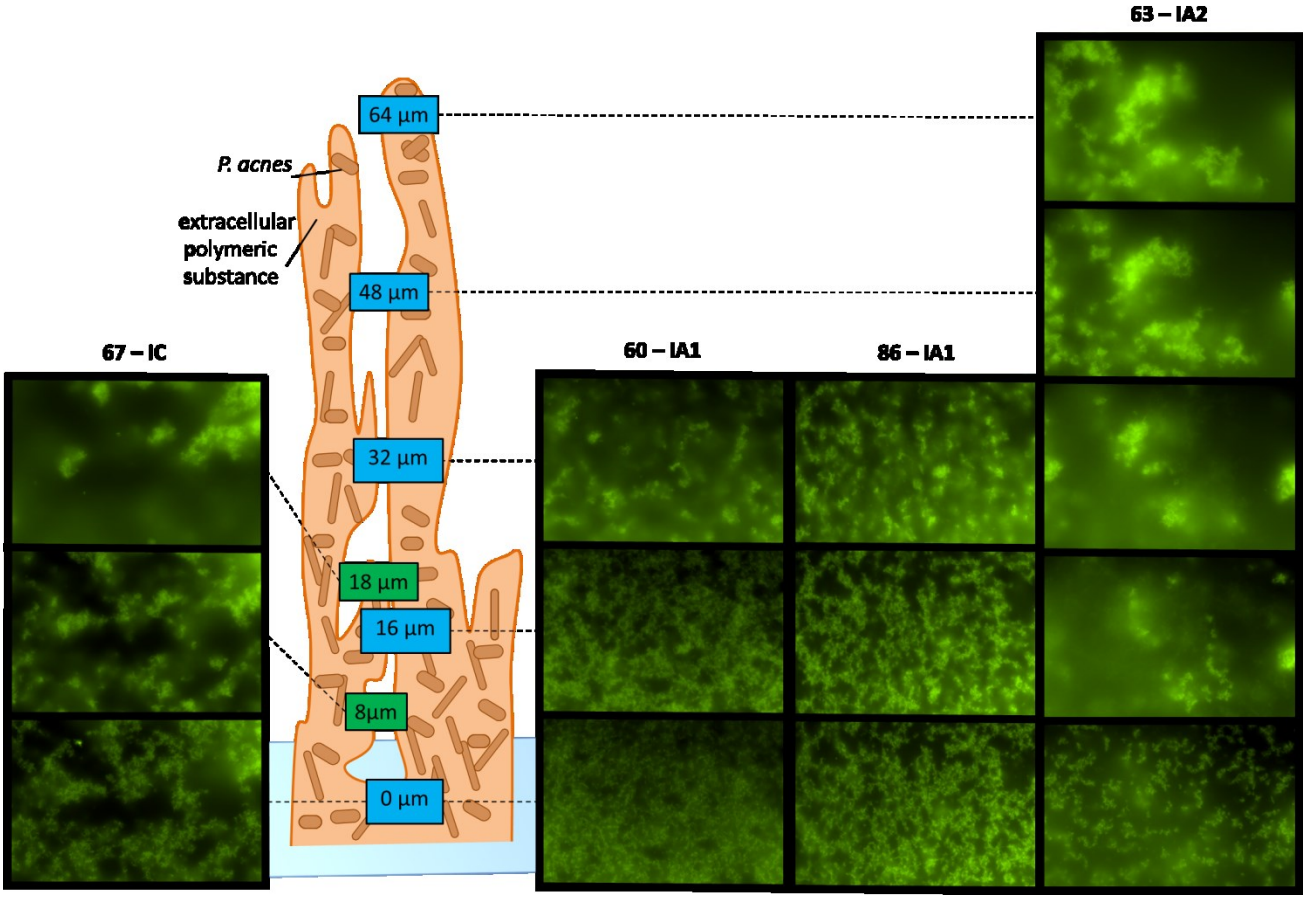

Figure 24: Fluorescence images, biofilm morphology. After 120h of incubation in BHI the cells of the different strains were stained with SYTO9 (targeting DNA) and photographed. “0 µm” shows *P. acnes* directly on the cover glass. They were aggregated in biofilm-typical morphology with cells being alternated by empty channels and caverns. “16 µm” shows images 16 µm above the cover class. The middle shows a schematic image of a biofilm, comprising *P. acnes* cells, eps (which was unknown to this point) and interspaces. Whereas the IA1 strains comprised of consistent, 32 µm high layers of biofilm cells, #63 had a more scattered phenotype with the layer of cells soon turning into high biofilm columns (up to 64 µm).

The reference strains #60 and #86 are shown in the middle panels of figure 24. The lowest part (0 µm) depicts the cell formation directly above the cover glass. Slides at 16 µm and 32 µm height (above the cover glass) follow. A dense, compact and evenly distributed biofilm with regular caverns and holes could be seen for the IA1 strains. Both biofilm formations (#60 and #86) looked similar in general morphology.

Figure 22 (left and right panels) includes a IA2 strain (#63) and a IC strain (#67). The density of the cells of #63/IA2 adsorbed to the cover glass was reduced compared to the IA1 strains. Still cells were evenly distributed in small fractions. The top of this covering layer ended before 16 µm height compared to IA1 strains ending at 32 µm. Additionally pillars of biofilm cells grew out of it high into the medium (more than 48 µm) and spreading similar to trees.

For strain #67 only a thin layer of 8 µm could be detected. Instead of consistently spread cells across the cover glass, the biofilm consisted of larger bulks of cells attached to the surface, divided by large holes and caverns. #67 also produced biofilm pillars, albeit just for a few µm.

4.4.2 Comstat Analysis

The images of figures of 24 were bioinformatically analysed using Comstat [25; 23; 24]. The results are shown in table 7.

Table 7: Comstat Analysis. Each image of a sequence (going for a 3D picture) of a certain strain was cropped into two equally sized square parts: left and right. Comstat analysis was performed with these cropped sequences to deliver two independent values.

	Biomass	Average thickness	Roughness coefficient	Maximum thickness	Maximum diffusion distance	Average diffusion distance
#60 (left)	15.7	20.7	1.30	74	88.2	1.89
#60 (right)	30.8	38.5	0.89	74	86.7	5.11
#63 (left)	143.9	154.5	0.23	176	n.d.	n.d.
#63 (right)	97.4	122.8	0.60	176	n.d.	n.d.
#67 (left)	15.5	25.6	0.23	29	92.2	7.09
#67 (right)	7.8	10.2	1.22	29	165.8	7.00
#86 (left)	50.5	67.5	0.69	108	69.8	5.21
#86 (right)	48.0	65.1	0.74	108	60.8	5.14

The units were nondimensional, as x and y values [µm] were replaced by relative ones “[1]”. But as the relative ratio stayed the same, the results from table 7 kept their comparability.

The sequence of images (many z layers forming a 3D image) was split into two equally sized squares (from a 2D point of view). As the format of the images was a rectangle, only the upper part of the image could be interpreted. These two squares were called #60 (left) and #60 (right).

“Average thickness” stands for the average thickness of the biofilm. The “roughness coefficient” stands for the average deviation from the average thickness. The “maximum thickness” shows the maximum thickness of the biofilm. The “maximum diffusion distance” is maximum distance from one side of the biofilm to the other. Finally, the “average diffusion distance” shows the average distance from beginning of the biofilm to the cells.

The data from table 7 correlates with the visual impression from figure 24.

4.5 Knockout Strategies

4.5.1 Bioinformatical Screening

As the newest research about *acne vulgaris* pathogenicity lists biofilm establishment as the first and main, strain-inherent virulence factor [16; 2], the target for genetic manipulation for a molecular biologist obviously is the biofilm involved genome. This is why several genes, which were predicted to be generally involved in biofilm formation, were chosen as targets [1] for a knockout. As IA1 strains have the highest frequency in *acne vulgaris* infections [11; 16], and as IA1 strain produce the most adhering, robust and compact biofilm of all serotypes (this work), genomic and transcriptomic differences between IA1 and other serotypes could possibly reveal genes connected to biofilm formations and its responsibility for pathogenicity [22]. 8 different genes were chosen to be cloned into a transformation vector for a knockout. See table 8 for a list including the gene shortcut used in this work (A-H), their KEGG numbers, origin of the sequence (“266” or “KPA”), presumed functions and authors to first identify them (to our knowledge).

Table 8: Gene Knockout Targets

Abr.	KEGG nr	Strain	Function	Reference	Gene bp	UP	DN
A	PAZ_c18730	266	TAG lipase	[22]	1014	818	818
B	PAZ_c21800	KPA/266	GehA lipase	[22]	1020	818	818
C	PAZ_c22060	KPA/266	Adhesin PA-25957	[22]	1275	638	638
D	PPA0230_ PPA0231	KPA	Twitching motility, pilus adherence		1167+ 771	818	818
E	PPA0146	KPA	O-AG-ligase	[1]	1260	818	818
F	PPA0148	KPA	UDP-N-acetylglucosamine 2-epimerase	[1]	1074	798	818
G	PPA0687	KPA	CAMP2	[21]	804	818	818
H	PPA1185	KPA	Poly-gamma-glutamate synthesis protein	[1]	1242	795	818
I	PPA2181	KPA	Polysaccharide biosynthesis protein	[1]	1368	818	818

Transformation vectors with these genes were constructed using a resistance cassette and a vector (table 9).

Table 9: *ermX* and pUC19 properties

Sequence	Database	Origin	Features	Bp uncut	Bp cut
ermC	20467026[a]	pIDN2	Erythromycin resistance	884	--
ermE	SACE_0733[a]	*S. erythraea*	Erythromycin resistance	1671	--
pUC19	M77789.2[b]	*E. coli* ML2061	AmpR	2686	2659

[a]… KEGG database

[b]… NCBI database

Gene **[A]** (KEGG: **PAZ_c18730**) translated for a triacylglycerol lipase in “266”. When compared to the homologous region of the IB strain “KPA” (**KEGG: PPA1797**), the lipase of “KPA” frameshifted into a shorter protein with unknown function. In order to test whether this frameshift between the serotypes had an influence on biofilm formation, the “266” TAG lipase was to be knocked out in the target IA1 strains (like #60 or #86). An example of comparative amino acid and DNA alignment between these two genes was added in the appendix.

Gene **[B]** (**PAZ_c21800**) in „266“, and **PPA_2105** in „KPA“, both encoded for a glycerol-ester hydrolase A, which was a secreted TAG lipase [22; 28]. The differences in homology were minimal (amino sequence comparison in appendix) but the mRNA was upregulated in “266” compared to “KPA” [22].

Gene **[C]** (**PAZ_c22060**) and **PPA2127** encoded for adhesion proteins, while having 94% homology. In “266” the gene was 6-fold upregulated compared to “KPA” [22].

The genes **[D]** (**PPA0230_PPA0231**) were located closely to each other in the genome of “KPA” (and identical in “266”), whereas PPA0230’s stop-codon simultaneously appeared to be PPA0231’s start-codon. Twitching motility is administered by extending and retracting pili with an adhesion protein at the top. This allows bacteria to slowly move along a surface. PPA0230 was identified by KEGG to be a “pilus assembly protein CpaF” and PPA0231 a “tight adherence protein B”.

Gene **[E]** (**PPA0146**), identical in „KPA“ and „266“, was predicted to be an O-antigen ligase and could possibly be involved in slime/capsular polysaccharide biosynthesis [1].

[F] (**PPA0148**), identical in “KPA” and “266”, encoded for a UDP-N-acetylglucosamine 2-epimerase, also possibly involved in slime/capsular polysaccharide biosynthesis.

Gene **[G]** (**PPA0687**) from KPA (and identical in “266”) translated for the CAMP2 factor, responsible for co-hemolytic activity. This gene was successfully knocked out according to published data [21]. It was included as a reference and positive control. If a knockout would not work with this gene, it was due to the transformation technique. If it worked for CAMP2 but did not work for the others, it was due to properties of the involved genes.

[H] (**PPA1185**) in „KPA“ (identical in „266“) was predicted to be a poly-gamma-glutamate synthesis protein involved in slime/capsular polysaccharide biosynthesis [1].

And finally, **[I]** (**PPA2181**) in “KPA” (identical in “266”) was said to be involved in possible slime/capsular polysaccharide biosynthesis, and predicted to be involved in the export of O-antigen and teichoic acid [1].

4.5.2 Construction

The construction of the transformation vectors is shown in this chapter.

4.5.2.1 Inserts, *ermX* Cassettes and pUC19

The upstream (UP) and downstream (DN) sequences of the genes were produced by Q5-PCR, digested (using restriction enzymes according to methods/figure 4) and analysed by agarose gel electrophoresis. Figure 25 shows the bands of these UP/DN fragments from A – D and the *ermC* cassette. The genes and their expected size are listed in table 8, which were A (UP: 818 bp and DN: 818), B (UP: 818 bp and DN: 818 bp), C (UP: 638 bp and DN: 638 bp), D (UP: 818 bp and DN: 818 bp) and *ermC* (884 bp)

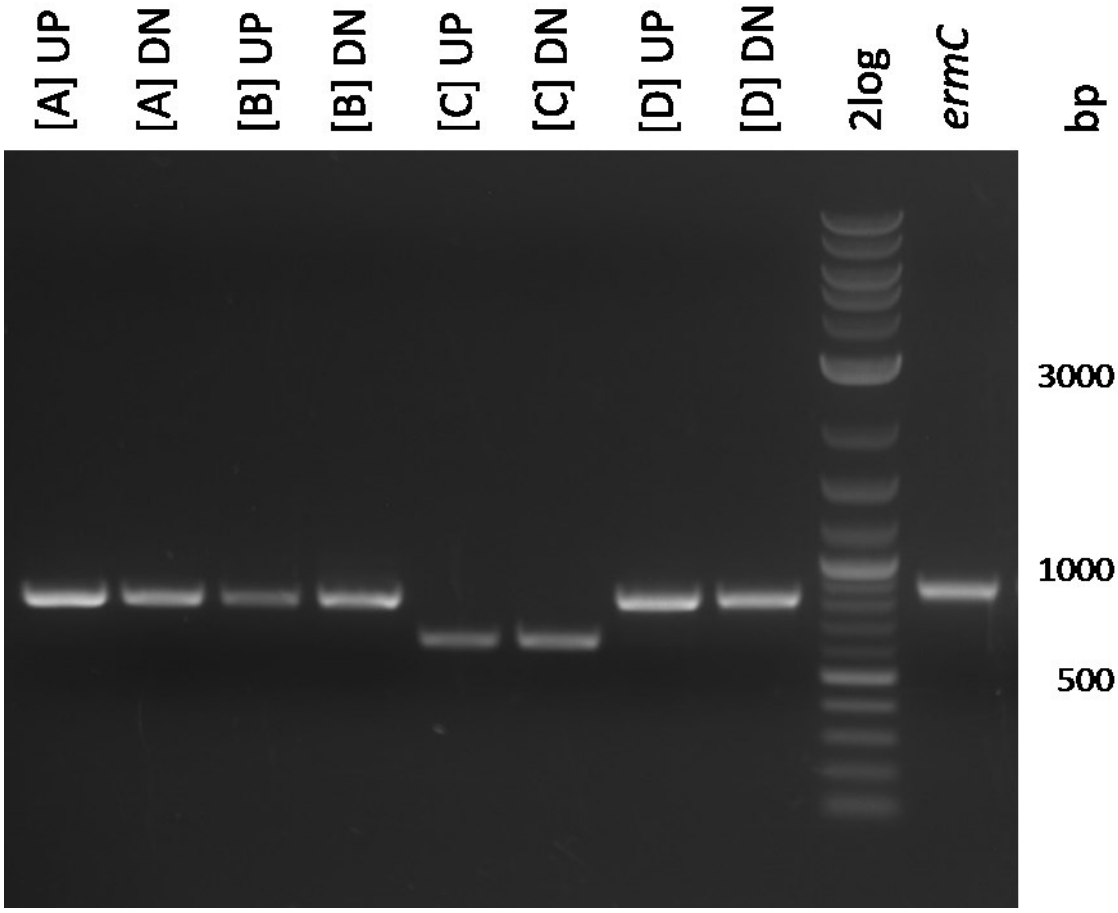

Figure 25: PCR constructs of gene A-D (UP and DN), and *ermC*. Agarose gel electrophoresis of the digested PCR constructed inserts. These were the upstream (UP) and downstream (DN) sequences of the genes [A] to [D], and the *ermC* cassette. The standard was 2log (methods/figure 3). The bands reached heights according to their *in silico* predicted size: fragments A, B and D with 818 bp, C with 638 bp and *ermC* with 884 bp (see table 8 and 9 for exact values).

The remaining sequences are shown in figure 26, which were E (UP: 818 bp and DN: 818 bp), F (UP: 798 bp and DN: 818 bp), G (UP: 818 bp and DN: 818 bp) and I (UP: 818 bp and DN: 818 bp).

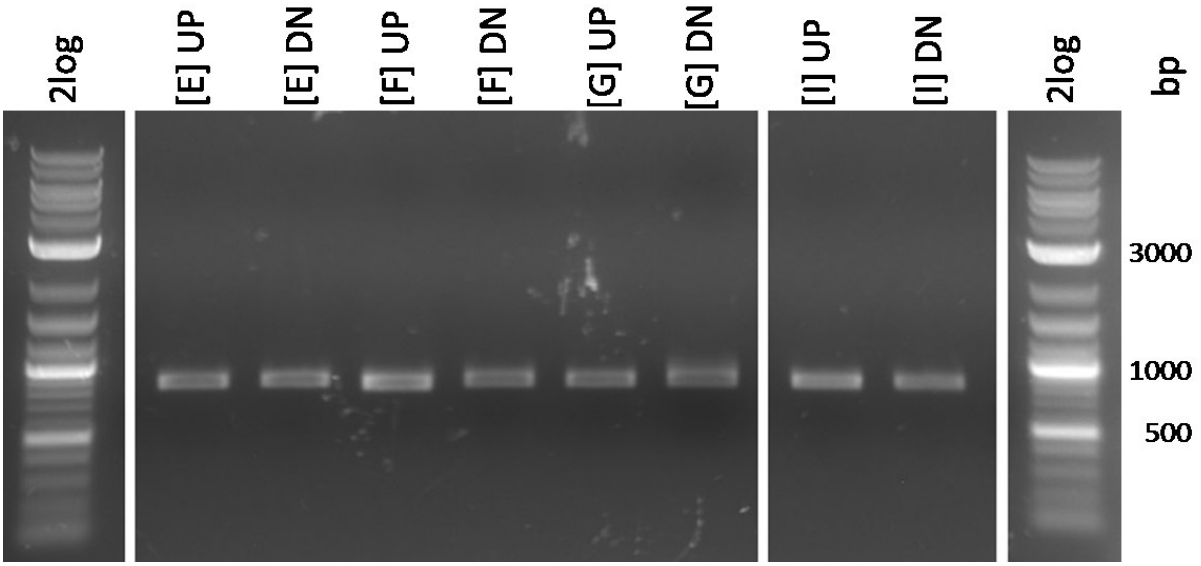

Figure 26: PCR constructs of gene E/F/G/I (UP and DN). Agarose gel electrophoresis of the digested PCR constructed inserts. These were the upstream (UP) and downstream (DN) sequences of the genes [E] to [G] and [I]. The standard was 2log (methods/figure 3). The bands reached heights according to their *in silico* predicted size between 795 and 818 bp (see table 8 and 9 for exact values).

The Q5 PCR product of the *ermE* gene is shown in figure 27/B with an expected size of 1671 bp.

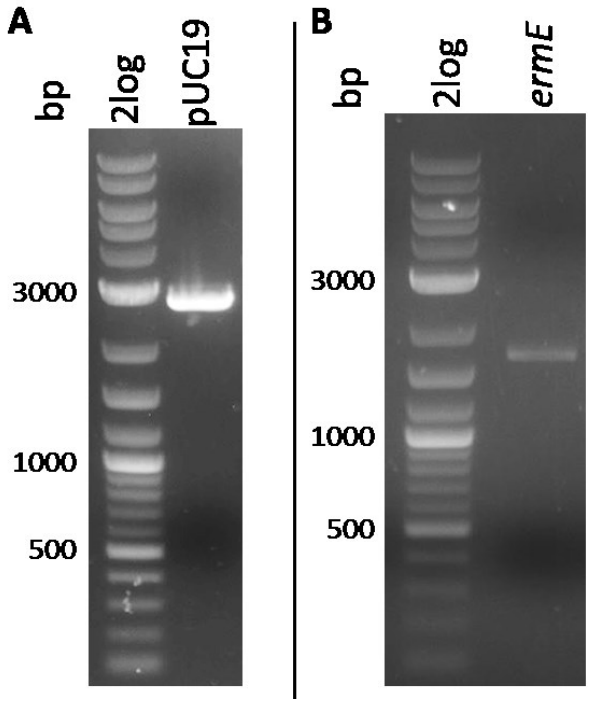

Figure 27: (A) pUC19*KpnI*SphI, (B) digested PCR construct of *ermE*. Agarose gel electrophoresis of the PCR constructed *ermE* cassette and the double cut pUC19. The standard was 2log (methods/figure 3). The bands reached heights according to their *in silico* predicted size: *ermE* with 1671 bp and pUC19 (double cut) at 2659 bp (see table 9 for exact values).

Finally, the digested (KpnI/SphI – see methods/figure 4) and dephosphorylated vector is shown in figure 27/A with an expected size of 2659 bp.These fragments were used for ligation, transformation and antibiotics selection.

4.5.2.2 Verification of Inserts in Transformants

Colony-PCR of the transformants and an agarose gel electrophoresis was done to screen for the correct construction of the vectors.The first trial contained vectors with the eight different UP and DN segments, pUC19 and the *ermC* cassette. The segments of the constructed vector: UP_*ermC*_DN, UP_*ermC* and *ermC*_DN (using the respective primers from materials/primer list) were screened in the following figure 28.

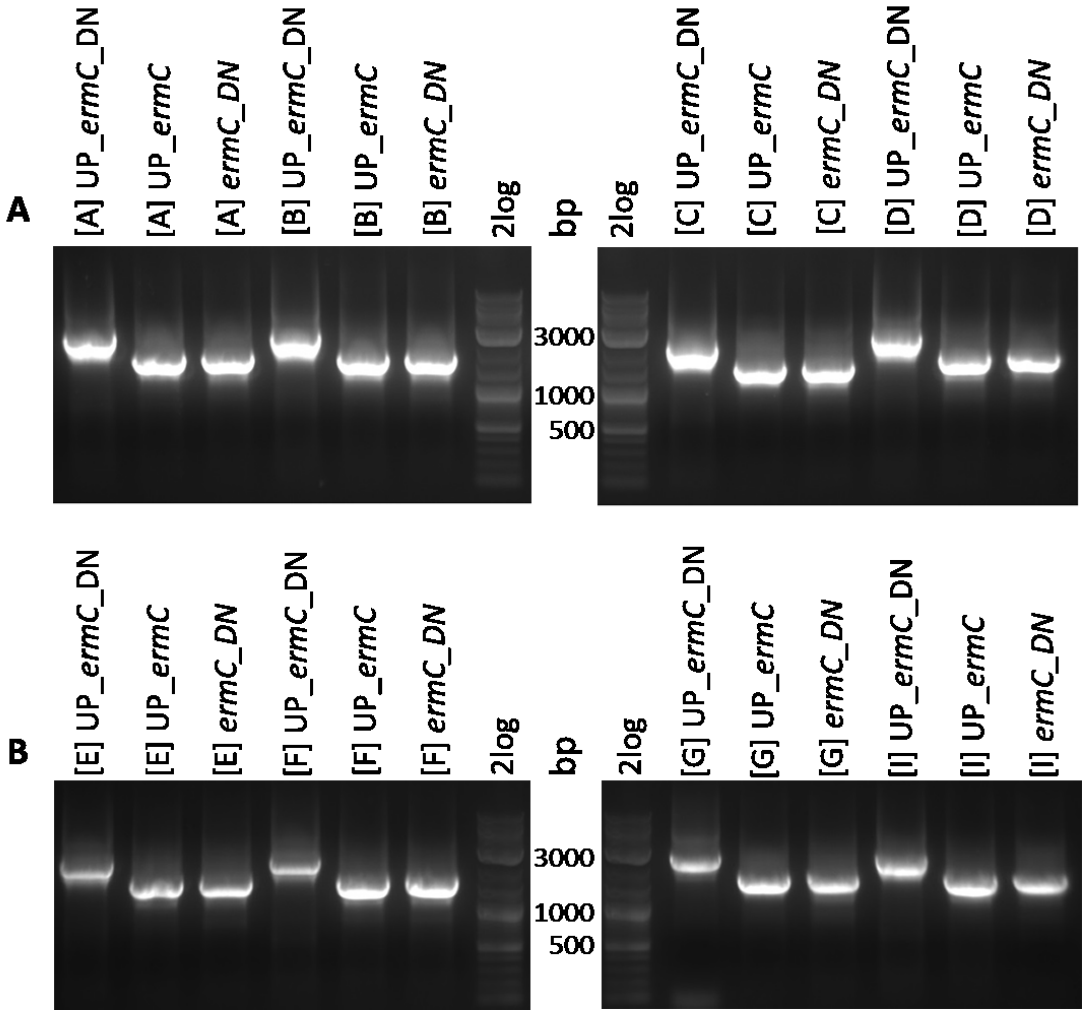

Figure 28: Verification of *ermC* cloning. The C-PCR batches of transformants were screened using agarose gel electrophoresis. Three primer pairs were used for the fragment UP_ermC_DN, UP_ermC or ermC_DN. Panel (A) shows genes A to D, panel (B) genes E to F. The standard was 2log (methods/figure 3). The bands reached heights according to their in silico prediction. A list of all fragment sizes is provided in table 10.

The expected *in silico* size of each fragment is shown in table 10. The comparison verified the correct construction of the vectors.

Table 10: Sequence length of UP/*ermC*/DN constructs.

	A	B	C	D	E	F	G	I
UP_*ermC*_DN	2520 - 24 by ligation = 2496	2496	2160	2496	2496	2476	2496	2496
UP_*ermC*	1702 - 12 by ligation = 1690	1690	1522	1690	1690	1670	1690	1690
***ermC*_DN**	1702 - 12 by ligation = 1690	1690	1522	1690	1690	1690	1690	1690

The second trial included the *ermE* instead of the *ermC* cassette. The pooled vector batches φ (containing 150 (E) to 400 (B/C/G) different transformants with a 71% *ermE* verification rate) were screened for the *ermE* cassette with a size of 1671 bp. All four batches showed a band at the expected height.

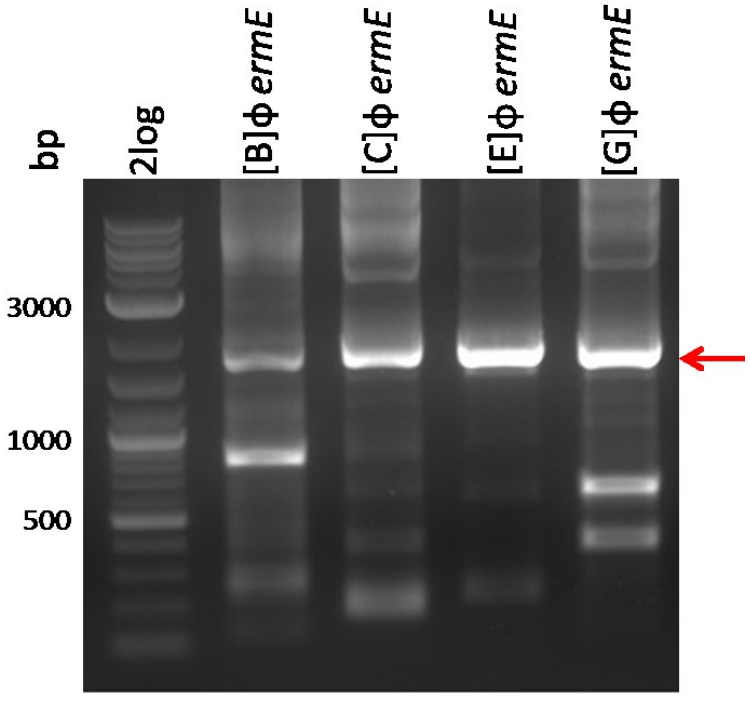

Figure 29: Verification of *ermE* in vector constructs. The C-PCR batches of transformants were screened using agarose gel electrophoresis. The primer pair for the *ermE* cassette was used. The standard was 2log (methods/figure 3 XXX). The bands reached heights according to their *in silico* prediction: 1671 bp.

The C-PCR batches of transformants were screened using agarose gel electrophoresis. The primers for the *ermE* cassette were used (see materials/primer list). Genes B, C, E and G were analysed. φ stands for a mixture of 150 – 400 transformants. The standard was 2log (methods/figure 3). The bands reached the expected height of 1671 bp.

The full segment of UP_*ermE*_DN was screened for in figure 30. The expected size was B with (818 bp UP + 818 bp DN + 1671 bp *ermE* – 24bp ligation =) 3283 bp, C with 2923 bp, E with 3283 bp and G with 3283 bp.

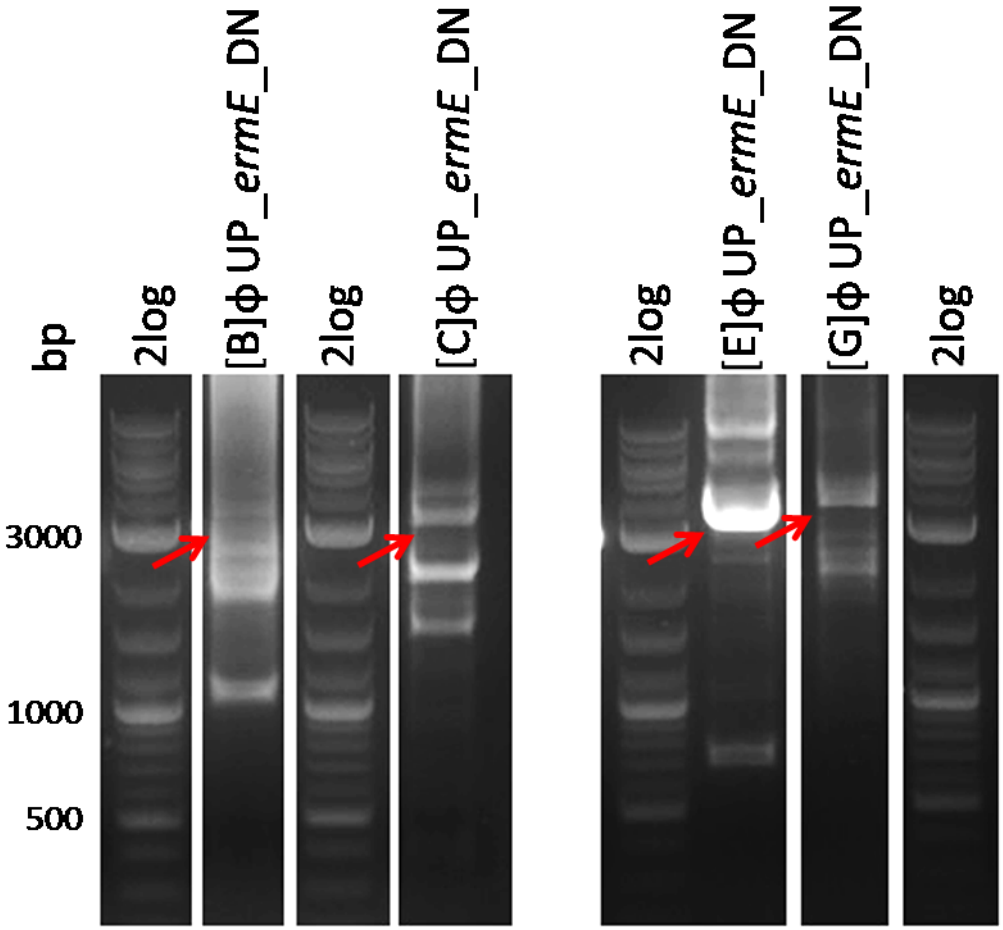

Figure 30: Verification of UP_ermE_DN in vector construction. The C-PCR batches of transformants were screened using agarose gel electrophoresis. The primers for the full cassette (UP_ermE_DN) were. The standard was 2log (methods/figure 3). Red arrows point at the target heights, B with 3283 bp, C with 2923 bp, E with 3283 bp and G with 3283 bp.. Images were taken from two separate gels. Small white stripes within the gels indicate graphical excisions.

The C-PCR batches of transformants were screened using agarose gel electrophoresis. The primers for the full recombination cassette UP_*ermE*_DN cassette of the respective genes were used (see materials/primer list). Genes B, C, E and G were analysed. φ stands for a mixture of 150 – 400 transformants. Expected size for B was 3283 bp, for C was 2923 bp, for E 3283 bp and for G 3283 bp. Whereas E delivered a clear expected band, all of them also included different increments of bands.

The combination of the last two figures shows that the *ermE* cassette was prominently existent in all batches. Correct assembly of the respective segments in the right direction was verified too (data not shown). The full segment had undergone some variations. The agarose gels (figure 30) show partially clear bands (like with the gene E) and partially increments of bands (B and G). However, at this stage of the study priority was no longer to knock out the target gene, but to get *P. acnes* to express the erythromycin resistance. Thus this variation was intended.

4.5.3 Transformation in *P. acnes*

After incubation on TG [Em10] plates for 7 to 14 days, single colonies were detectable. After streaking them on fresh TG [Em10] plates, these mutated strains were first screened for being *P. acnes* by using the primers of the B.UP segment.

NCBI blasting the B.UP sequence (including more dissimilar sequences – discontiguous megablast) displayed only *P. acnes* hits. The probability for giving a false positive signal on the exact same band height with the same primer sequence was considered to be negligible.

Figure 31/A, the upper gel image shows an example result of screening for B.UP segments. It revealed that all single colonies were *P. acnes* instead of contaminations. The last row included an untransformed wildtype of strain #60. The second gel image (B) shows the result of screening for the *ermC* cassette in the same strains with an expected size of 884 bp. A single-recombinant should contain the full plasmid integrated into the chromosome up- or downstream of the target gene. The strain “[E] #60” (standing for strain #60 which was transformed with the gene E vector) and the positive control (plasmid pUC_UP.B_*ermC*_DN.B as *ermC* template) gave a positive signal.

Thus, *ermC* segment was integrated into the chromosome. Unfortunately further screening for UP_*ermC* or *ermC*_DN showed no results, indicating a recombination at a random site.

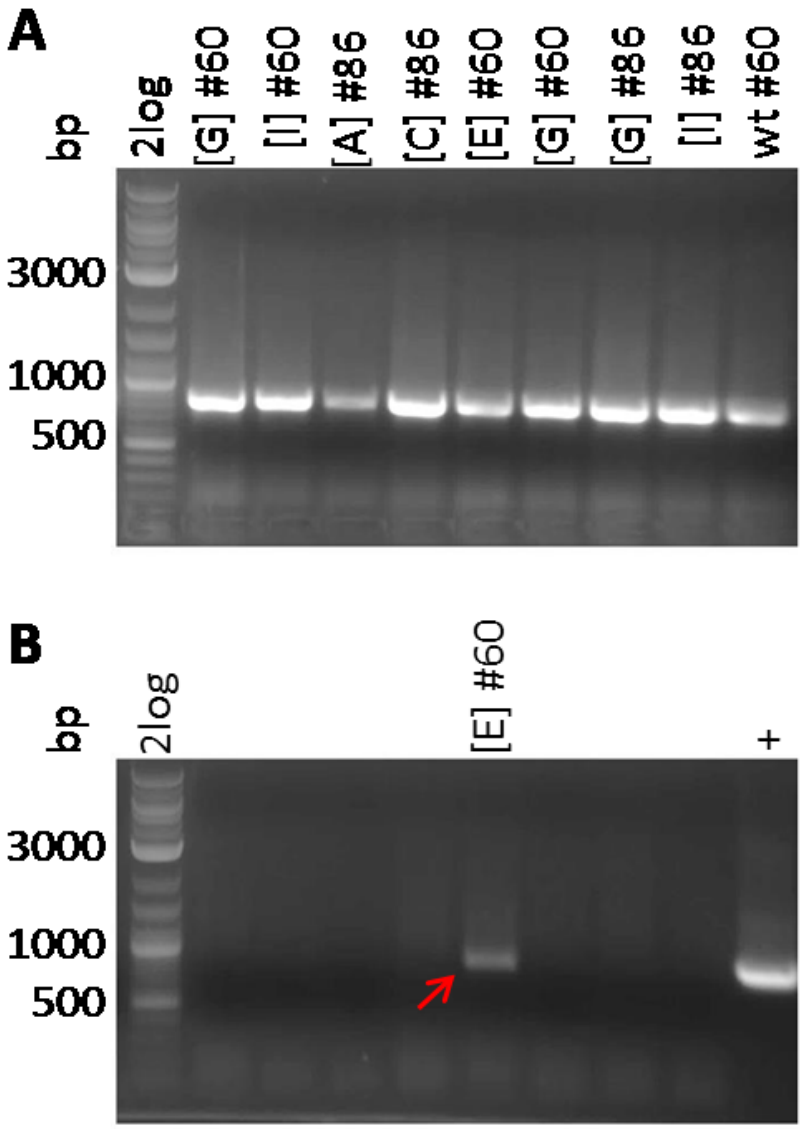

Figure 31: Screening of *P. acnes* transformants. The L-PCR batches of *P. acnes* transformants were screened using agarose gel electrophoresis. The primers of gene B.UP were used in panel (A) to see whether the respective mutant was *P. acnes* at all (expected size: 818 bp). In panel (B) it was searched for the *ermC* cassette (884 bp) as indication for a recombination. The standard was 2log (methods/figure 3). A positive signal for the *ermC* cassette was caught for recombinant "[E] #60" (vector containing gene E was transformed into #60). The template for the positive control "+" for the *ermC* cassette was pUC_UP.B_*ermC*_DN.B.

In the course of the study ~ 100 colonies were screened with the strain in figure 29/B being the only candidate with an incorporation of the DNA into its chromosome. As

untransformed wildtype #60/#86 strains incubated on TG[Em10] also showed a few colonies after 14 days (data not shown), it was likely that all the other colonies without an *ermX* signal gained erythromycin resistance due to spontaneous mutation.

4.5.3.1 Protocol Variation

The initial protocol (see methods) was slightly changed with each new run in hope to increase the transformation efficiency. The sums of all modifications are listed in table 11.

Table 11: Transformation strategies

Transformation step	Varied property	Transformation runs						
		1	2	3	4	5	6	7
Strains	#60	X	X	X	X	X	X	X
	#86			X	X	X	X	
	#66~[1]						X	X
Erythromycin resistance cassette	*ermC*	X	X	X	X	X		
	ermE [1] [2]						X	X
Electrocompetent cells incubation	10 days at 24°C[2]				X			
	3-5 days at 37°C[1]	X	X	X		X	X	X
	Including 160 rpm[1]							X
Electrocompetent cells incubation medium	In BHI	X	X	X	X	X	X	X
	In TG	X						
Electrocompetent cells washing buffer	H_2O	X	X				X	
	EPB (old) [1] [2]	X	X	X	X	X	X	
	EPB (new) [1] [2]							X
Electrocompetent cells washing temperature	on ice[1]	X	X			X	X	X
	at RT			X	X		X	
Transformation batches		16	16	16	20	30	32	15
Transformation plasmid quantity	≤ 1-20 µg/batch[1] [2]	X	X					
	20 – 40 µg/batch			X	X	X	X	X
Transformation temperature	on ice[1]	X	X		X	X	X	X
	at RT			X				
Transformation volt	7 kV/cm[1] [2]	X	X	X	X	X	X	X
	9 kV/cm[2]	X		X	X		X	X

	≥ 12.5 kV/cm[2]	X						X
Involved genes	A		X	X	X			
	B		X	X	X	X		
	C		X	X	X	X	X	X
	D		X	X	X	X		
	E	X		X	X		X	X
	F	X		X	X			
	G[1]	X		X	X		X	X
	I	X		X	X			
Recombination duration	≤ 12h[2]					X		X
	24h[1]	X	X	X	X		X	
Recombination medium	On TG plates	X	X	X	X	X	X	
	On BHI plates							X
Erythromycin selection duration	5-8 days[1] [2]	X	X	X		X		
	8-14 days			X	X		X	X
Erythromycin selection medium	On TG plates	X	X	X	X	X	X	
	On BHI plates							X
Erythromycin concentration	1 µg / ml selection					X		
	10 µg / ml selection[1] [2]	X	X	X	X	X	X	X

[1] … Successful knockout by Sörensen (2010)

[2]… Successful transformations by Cheong (2008)

X … "[E]60 *ermC*" detection

The conditions, which were used for a successful transformation of a *P. freudenreichii* plasmid into *P. acnes,* are marked by [2] in table 11 [27; 29]. The conditions for a successful knockout of the CAMP2 factor were tagged with [1] [21]. The protocol which allowed the recombination of the *ermC* cassette into the chromosome was marked with an X (black background and white font).

5 Discussion

5.1 Biofilm Assays

5.1.1 Medium

The biofilm assays allowed for a phenotypic analysis of *P. acnes* biofilm from three different angles. The static biofilm assay showed the quantity of biomass with a minimum adherence capability to surfaces. The macroscopic images revealed characteristic aggregations, and the fluorescence staining showed specific biofilm morphology on microscopic level.

Initially, the addition of glucose to BHI (to form BHG) was tested because published data suggested an improvement of biofilm production based on 5 isolates [14]. When comparing BHI and BHG biofilm quantity of 32 skin isolates, both assays resulted in robust and distinguishable biofilm values. BHG however had stronger growth, which in return reduced the biofilm / growth ratio. In the late phase (168h) BHG biofilm quantity increased over BHI, indicating an endured biofilm production. With less effort, similar biofilm production and a better biofilm / growth ratio BHI was thus chosen as main static biofilm medium.

The static biofilm values of TG were noticeably lower than those of the other two media. Even after 168h only a few of the strains could establish a relatively low biofilm. It is presumed that 0.5% agar kept the strain from adsorbing to the surface and building aggregates all through the broth. When incubating *P. acnes* in large volumes of TG broth, aggregates could be detected levitating through the media. Centrifuging for an hour was not enough to pelletize these into compact, flow-resisting sediments, in comparison to BHI where 20 minutes was enough. However, figures of TG presented high OD_{600} values. At the same time incubation of *P. acnes* on TG agar plates resulted in single colonies after 3 days, whereas BHI need 4 days. TG thus turned out to be unfavourable for the static biofilm assay and growing electrocompetent cells, but excellent for growth in liquid medium and on agar plates.

5.1.2 Time points

Preliminary data reported that the best time points for biofilm evaluation varied from total 28h in microtiterplates [9] to 144h on discs (silicone, steel or titanium) [13]. Holmberg et al tested 24h to 96h, whereas 24h didn’t result in any biofilm [14]. Their

assay was performed in BHG (0.5%) instead of BHI or BHG (0.2%), flat-bottomed instead of round-bottomed microtiterplates and their favourite turned out to be 72h.

Additionally, time points of 48h, 96h, 144h and 216h were tested (data not shown). When evaluating all biofilm data in this work, ranging from skin to implant isolates, across all serotype groups, from 24h to 9 days incubation, then the dynamic changes of biofilm quantity of several strains reached their peak of biofilm formation the earliest after 120h. Several strains reached their maximum only after 168h. Only after this point reduction in biofilm quantity was globally visible. In order to catch the full phenotypic spectrum of a strain's biofilm dynamic, these three time points (72h, 120h and 168h) turned out to be necessary.

Once these parameters were applied the static biofilm assay gave characteristic and significant statements about the biofilm production of each individual strain.

5.1.3 Serotypes and Point of Isolation

With research on *P. acnes* slowly emerging, more details about the strain got public. In 2005 a first discrimination was installed: differentiating between serotype I and II strain [19]. As described in the introduction, the genotypic diversity of *P. acnes* was further analysed and grouped into six serotypes: IA1, IA2, IB, IC, II and III. To see whether correlations between serotypes and biofilm dynamics could be seen, all biofilm / growth ratios of the respective skin serotypes were pooled and their averages compared. The IA1 average (especially at 120h) turned out to be noticeably higher than those of other serotypes. Following the definition of a biomass with regard to a minimum adsorption capability, IA1 strains could produce significantly higher amounts of biofilm than all other serotypes.

Another aspect became target of research: the point of isolation. Some strains lived directly on the human skin and were swabbed from it, some lived in the hair follicles from healthy or *acne vulgaris* patients, and some were isolated from the infected surfaces of implants.

When comparing the (mostly IA1) strains coming from healthy skin (#81, #85 – #91) versus strains coming from acne patients (#73 - #80, #82 - #84) over the different time points within the static biofilm assay, then similar patterns can be seen. Most of them showed high biofilm production. This means the capacity and quantity to

produce biofilm *in vitro* seemed not to be significantly altered in their presumed adaption to acne.

The static biofilm assay was also performed to compare biofilm quantity of implant isolates to skin isolates within the same assay. The IA1 strains of the skin (#60, #86, #77) show similar biofilm quantity and dynamic patterns to the implant isolates. The patterns from IB strains appear to have some heterogeneity, but they differ noticeably from the other serogroups. Although the remaining serotypes are represented only by a few strains, II and III show completely the same biofilm quantity and dynamic when comparing each skin and implant isolate. IC generally had a stronger biofilm production and IA2 had the same dynamic.

These results combined strongly indicate that the biofilm quantity and the dynamic production and degradation are determined by the serotype group. The location of isolation had no influence on the *in vitro* biofilm. This also highlights that generally received information on *P. acnes* biofilm of a certain serotype could be useful for all fields of pathogenicity.

5.1.4 Macroscopic Evaluation

The second phenotypic characterization was the macroscopic evaluation of *P. acnes* aggregates in the round-bottomed microtiterplate wells. Macroscopic appearance showed characteristics depending on the serotype. Most of the IA1 strains formed a cloudy layer of cells with similar height at all points directly above the surface. This layer could “crawl” up an eprouvette for the length of a cm against gravity. The impression of twitching mobility came up on that view and should be further investigated. The layer correlated with the quantity of the static biofilm assay. The medium directly above it was completely clear. A few strains grew into unique features with the layer sort of rolling in. #81 and #83 (IA1) produced the layer with fragmentations or partial detachments visible. IA2 strains displayed similar features. A slight variation could be detected with strain #63 (IA2) showing a rolled in characteristic, and a fragmented, partially detached characteristic in another assay. Seemingly the biofilm adherence capacity of this strain under these circumstances was just at the edge of staying attached to the surface or losing the grip. Under static biofilm conditions in BHI, #63 displayed an exceptionally high interquartile range with a median at almost zero and an interquartile range of 25 reaching up to over 2

relative absorbance units. When the strain rolled in the biofilm, the biofilm quantity would be low, when it stayed on the surface in the fragmented, partially detached phenotype, then the quantity would be higher. Serotype groups II, III and IB built none of these layers but instead sedimented to the ground building pellets in the centre of the well. No biofilm with minimum adherence capacities could be detected from these. Just a few exceptions like #87, #88 and #20 from serogroup II managed to spread a relatively short distance away from the central pellet. Group IC appeared to show some hybrid phenotype with a IA1 typical layer and a little sedimented pellet.

All in all, the macroscopic evaluation allowed for a quick and easy identification of contaminations, which was important when working with strains without any antibiotic resistance. More importantly, an instant general categorization was possible: pelletizing (II, III, IB), layer building (IA1), a mixture with unique structures like a layer with fragmentations, detachments or rolled in (IA2, IC).

5.1.5 Biofilm Morphology

The microscopic images of the 3D biofilm morphology revealed unique features even distinguishing between single strains. Recapitulating, strain #60 and #86 both showed a homogenous biofilm layer in macroscopic appearance. #60 had a relatively good biofilm production and #86 was among the best biofilm producer. Under the microscope #86 comprised slightly larger caverns between the cell aggregates and a somewhat higher biofilm layer. Apart from these slight variations, both strains were very similar.

IA2 strain #63 showed a fragmented or rolled in macroscopic characteristic leading to either a high or a low biofilm production. The first layer on the cover glass surface was lower and of more clearance than those of the IA1 strains. Instead of forming a compact biofilm layer of up to 32 µm, the layer was less than 16 µm high and turned into high towers of dense cell aggregates. The morphology of this biofilm strongly deviated from the other strains. IC strain #67 once again differed from the others with a small layer of cells turning into small towers. In all cases a biofilm typical change between cell aggregates and empty caverns could be detected on the surface of the glass cover. The nature of the flowcell technology and generally the nature of biofilm definition required discrimination between biofilm cells and planktonic cells. This could be achieved only by applying a minimum flow to the medium. In the process

examinations of representatives of other serotype groups could not be unequivocally identified as cells attached to the glass cover and thus had to be skipped. The attachment qualities of II, III and IB to plastic and glass surfaces were thus hardly detectable within this study, which either meant they did not form biofilm, or that they form aggregation structures (not defined as biofilm) which generally target no, or only very unique chemical surfaces like each other.

5.2 Deletion Mutagenesis

The idea of the mutagenesis was to perform a deletion of a specific gene presumed to be widely involved in biofilm formation. After the deletion, the triple phenotypic characterization was to be applied. If the gene influenced biofilm formation, then a change could be visible already in macroscopic evaluation. The clean #60 IA1 layer could be fragmented, rolled in or even fully pelletized. The static biofilm assay would show adherence and quantity differences. The microscopic fluorescence analysis, possibly with GFP tagged *P. acnes*, could reveal changes in microscopic characteristics like density, cavern sizes, aggregate sizes or tower production, and could be brought to numbers by Comstat.

As IA1 strains are predominantly associated to acne [12; 16], the DNA of strain #60 was taken as template for construction and for the knockout. #60 was isolated from acne initially and generally used as reference strain in published data. #86 was added because of its constantly high biofilm production, although initially isolated from a healthy patient. In the later trial #66 was added as IB strain, as this serotype group was also the target of the only described successful knockout by Sörensen et al [21].

The genes were described in detail in the results section and among others contained lipases, which were assumed to be involved in degradation of the sebum at the sebaceous gland. Lipases could also be involved in biofilm shaping in case the biofilm contains any sort of lipids, considering *P. acnes* hydrophobic environment by the sebum. The bioinformatical search based on published predictions on the genes' putative functions [1] and transcriptomic differences [22]. The process of knockout, as described in the introduction, based on double homologous recombination of a vector carrying a plasmid backbone with a first selection marker (ampicillin resistance), an

up- and downstream region of the target gene and a second selection marker (for erythromycin).

In order to find a way for a successful knockout, seven trials were carried out. The protocol based on three publications. The first one from Jore et al in 2000 described the construction of a transformation vector for *P. freudenreichii*, based on a rare plasmid they found in one of the subgroups [29]. One important finding was that *P. freudenreichii* had a strong restriction system for foreign DNA. The difference in transformation efficiency of taking *P. freudenreichii* amplified (and uniquely methylated) vectors instead of those from *E. coli* was 10^6 – 10^7. This led to the finding that plasmids had to be unmethylated. Cheong et al in 2008 requested this plasmid and used it for transformation in *P. acnes* [27]. In the end different strategies were carried out (varying transformation volt, electrocompetent cells growth properties, et cetera). Sörensen et al in 2010 also requested this plasmid from Cheong, but the transformation did not work [21]. They tried a knockout with their own vector nonetheless and described a successful deletion of the *camp2* gene, verified by band differences in PCR. It was noted that the transformation and recombination efficiency was very low with just a few recombinants growing after each transformation.

The expectations based on Cheong's data of 10^4 transformants per µg DNA. First to be noted is that these numbers referred to transformation only. Each transformant received the plasmid and was able to proliferate. One transformant thus represents one cell successfully receiving one plasmid of DNA without further negative impacts. These plasmids should also be available for a first recombination event. The plasmid could not replicate, as the necessary machinery was lacking. Beside transformation frequency the other bottleneck was recombination probability. If 1 µg of DNA led to 10^4 transformants, and a recombination probability in *P. acnes* was (theoretically) 1 to 10^5, then the chance would be 10% to get a single recombinant. If 10 µg of DNA were used, the probability would theoretically rise to 100%, respective 1 recombinant. This haggling and balancing was the basis for the introducing all sorts of variations – to rise the total sum of transformation efficiency and quantity above the unknown value of recombination probability. Sörensen et al transformed 6 - 8 µg of DNA and got a few recombinants. Rounding these values they had approximately 1

recombinant for 1 µg of DNA. This would result in a recombination probability of roughly 1 to 10^4.

The amount of DNA transformed in this work vastly exceeded 6 – 8 µg. Each transformation batch contained at least 20 µg. 145 transformations multiplied with approximately 20 µg resulted in 2900 µg of transformed plasmid DNA. Assuming the recombination probability of Sörensen et al was applicable also for this work, 400 transformants should have been received. This was an increase of quantitative recombination probability by $4 * 10^2$. Rephrased, a single successful transformant would have still been received if the recombination probability dropped down to one in 10^6. Unfortunately this was still not enough for a recombination at the correct position.

To increase the transformation efficiency, several variations were performed and shall be described shortly in the following.

Initially, *ermC* offered a well described erythromycin resistance to our instant avail while encoding for an enzyme catalysing the dimethylation of the 23S rRNA (EC 2.1.1.184). However, *P. acnes,* as part of the *Actinobacteria,* featured a high GC rate in the gnome. Upon further error analysis it was discovered that e*rmC* gene consisted of a GC rate of merely 27 %. The *ermE* cassette which was used in published knockout came from *S. erythraea* (also Gram positive *Actinobacteria*) and had a GC content of 72%. Although the function was the exact same with the same EC number, in order to avoid possible translational difficulties for *P. acnes S. erythraea* was ordered and used as template for further trials.

Although published knockout was performed with partial inclusion of Brucella agar, the ingredients of these complex mediums (BHI, TG) were of similar composition. The transformation volts were varied, however, according to Cheong et al all of these variations resulted in transformations within the same $\log_{10}$ region [27]. The regeneration time after transformation was varied between 8h and 24h, to see whether recombination needed more time. The erythromycin concentration was varied between 1 and 10, to reduce selective pressure, but also with no effect. The size of the up- and down segments were initially enlarged compared to Sörensen (800 instead of 600) to increase recombination homology.

In the end one strain did recombine the *ermC* cassette into the chromosome, but seemingly at the wrong position. Obviously, the rate and efficiency still has to be increased, but there are many other possibilities to try out for this difficult strain. These will be the target of future researches.

5.3 Conclusion

This work established a phenotypic *P. acnes* biofilm characterization protocol through three different assays. A first approach is the macroscopic evaluation. The second method relies on the static biofilm assay, allowing high throughput analysis of biofilm quantity. The third protocol – the microscopic biofilm morphology - offers a tool for analysis of features unique for each single strain.These protocols can henceforth be used to screen all kind of chemical, biochemical or biological substances on their influence in biofilm formation.

In the course of establishing these protocols, several results and indications were obtained. Skin isolated strains from healthy people and acne patients showed similar biofilm production. The same biofilm production and dynamic could also be seen for serotypes, irrespective of their point of isolation. This indicates that the respective serotype groups of *P. acnes* carry all available genetic tools for human colonization inherently, but as commensal require a dysfunctional host to act as pathogen (teenage hormonal transition, or unnatural introduction into the body). With biofilm being established *in vivo* in acne [11], biofilm being mostly produced by IA1 strains (this work), and IA1 strains being found predominantly in acne patients [12; 16], the hypothesis that biofilm production is the key virulence factor is supported by this work. Biofilm offers a scaffold for bacteria, leads to segregation from the environment with increased resistance to the immune system and antibiotics and an increased anaerobic environment. All aspects continually support the importance of biofilm establishment.

If the genetic regulation of biofilm is further investigated, for example by specific gene deletion and comparison of the phenotype, then future scientists can find more precise targets which go beyond the massive and lengthy hammer of broad-spectrum antibiotics with all its consequences. Notably acne is the most abundant dermal disease of all. Based on the limited progression of molecular biology analysis, continued research seems absolutely mandatory.

6 List of Figures

7 List of Tables

8 Abbreviations

2log	Standard DNA ladder (from NEB)
Amp	Ampicillin [concentration in µg / ml]
BA1	Static biofilm assay, run 1
BA2	Static biofilm assay, run 2
BHI	Brain Heart Infusion
BHG	Brain Heart Infusion + Glucose

bla	Gene for beta-lactamase = ampicillin resistance
DN	Downstream fragment of a target knockout gene
dNTP	Deoxy nucleaside triphosphate
dsDNA	Doublestranded DNA
Em[X]	Erythromycin [concentration in µg / ml]
EDTA	Ethylenediaminetetraacetic acid
eMLST	Expanaded multilocus sequence typing scheme
EPB	Electroporation buffer
eps	Extracellular polymeric substances
ermX	Gene for 23S rRNA methyltransferase = erythromycin resistance (X=C or E)
h	Hours
H-TEP	Hip total endoprosthesis
K-TEP	Knee total endoprosthesis
LB	Lysogen broth
Mb	Megabasepairs
NEB	New England BioLabs
ONC	Overnight culture
PCR	Polymerase chain reaction
rpm	Rounds per minute
sacB	Gene for levansucrase = sucrose suicide
SDS	Sodium dodecyl sulfate
SEM	Scanning electron microscopy
SS	Strain collection
TAG	Triacylglycerol
TEM	Transmission electron microscopy
Tris	Tris(hydroxymethyl)aminomethane
TE	Tris EDTA
TG	Thioglycollate (sic)
TNE	Tris NaCl EDTA
TNEX	Tris NaCl EDTA triton-X
TAE	Tris Acetate EDTA
UP	Upstream fragment of a target knockout gene

9 References

1. Brüggemann, H., Henne, A., Hoster, F., Liesegang, H., Wiezer, A., Strittmatter, A., Hujer, S., …Gottschalk, G. (2004). The complete genome sequence of Propionibacterium acnes, a commensal of human skin. *Science (New York, N.Y.)*, *305*(5684), 671–673
2. Metiko, B., Brooks, K., Burkhart, C. G., Burkhart, C. N., & Morrell, D. (2015). Is the current model for acne pathogenesis backwards? *Journal of the American Academy of Dermatology*, *72*(6), e167
3. Vorkapic, D., Pressler, K., & Schild, S. (2016). Multifaceted roles of extracellular DNA in bacterial physiology. *Current genetics*, *62*(1), 71–79
4. Abee, T., Kovács, A. T., Kuipers, O. P., & van der Veen, S. (2011). Biofilm formation and dispersal in Gram-positive bacteria. *Current opinion in biotechnology*, *22*(2), 172–179
5. Flemming, H.-C., & Wingender, J. (2010). The biofilm matrix. *Nature reviews. Microbiology*, *8*(9), 623–633
6. Donlan, R. M. (2002). Biofilms: microbial life on surfaces. *Emerging infectious diseases*, *8*(9), 881–890
7. Hammer, B. K., & Bassler, B. L. (2003). Quorum sensing controls biofilm formation in Vibrio cholerae. *Molecular microbiology*, *50*(1), 101–104
8. Ramage, G., Tunney, M. M., Patrick, S., Gorman, S. P., & Nixon, J. R. (2003). Formation of Propionibacterium acnes biofilms on orthopaedic biomaterials and their susceptibility to antimicrobials. *Biomaterials*, *24*(19), 3221–3227
9. Coenye, T., Peeters, E., & Nelis, H. J. (2007). Biofilm formation by Propionibacterium acnes is associated with increased resistance to antimicrobial agents and increased production of putative virulence factors. *Research in microbiology*, *158*(4), 386–392
10. Alexeyev, O. A., & Jahns, A. C. (2012). Sampling and detection of skin Propionibacterium acnes: current status. *Anaerobe*, *18*(5), 479–483
11. Jahns, A. C., Lundskog, B., Ganceviciene, R., Palmer, R. H., Golovleva, I., Zouboulis, C. C., McDowell, A., …Alexeyev, O. A. (2012). An increased incidence of Propionibacterium acnes biofilms in acne vulgaris: a case-control study. *The British journal of dermatology*, *167*(1), 50–58
12. Lomholt, H. B., & Kilian, M. (2010). Population genetic analysis of Propionibacterium acnes identifies a subpopulation and epidemic clones associated with acne. *PloS one*, *5*(8), e12277

13. Bayston, R., Ashraf, W., Barker-Davies, R., Tucker, E., Clement, R., Clayton, J., Freeman, B. J. C., …Nuradeen, B. (2007). Biofilm formation by Propionibacterium acnes on biomaterials in vitro and in vivo: impact on diagnosis and treatment. *Journal of biomedical materials research. Part A*, *81*(3), 705–709

14. Holmberg, A., Lood, R., Mörgelin, M., Söderquist, B., Holst, E., Collin, M., Christensson, B., …Rasmussen, M. (2009). Biofilm formation by Propionibacterium acnes is a characteristic of invasive isolates. *Clinical microbiology and infection : the official publication of the European Society of Clinical Microbiology and Infectious Diseases*, *15*(8), 787–795

15. Stepanović, S., Vuković, D., Dakić, I., Savić, B., & Švabić-Vlahović, M. (2000). A modified microtiter-plate test for quantification of staphylococcal biofilm formation. *Journal of microbiological methods*, *40*(2), 175–179

16. McDowell, A., Barnard, E., Nagy, I., Gao, A., Tomida, S., Li, H., Eady, A., …Patrick, S. (2012). An expanded multilocus sequence typing scheme for propionibacterium acnes: investigation of 'pathogenic', 'commensal' and antibiotic resistant strains. *PloS one*, *7*(7), e41480

17. McDowell, A., Gao, A., Barnard, E., Fink, C., Murray, P. I., Dowson, C. G., Nagy, I., …Patrick, S. (2011). A novel multilocus sequence typing scheme for the opportunistic pathogen Propionibacterium acnes and characterization of type I cell surface-associated antigens. *Microbiology (Reading, England)*, *157*(Pt 7), 1990–2003

18. McDowell, A., Perry, A. L., Lambert, P. A., & Patrick, S. (2008). A new phylogenetic group of Propionibacterium acnes. *Journal of medical microbiology*, *57*(Pt 2), 218–224

19. McDowell, A., Valanne, S., Ramage, G., Tunney, M. M., Glenn, J. V., McLorinan, G. C., Bhatia, A., …Patrick, S. (2005). Propionibacterium acnes types I and II represent phylogenetically distinct groups. *Journal of clinical microbiology*, *43*(1), 326–334

20. Barnard, E., Nagy, I., Hunyadkürti, J., Patrick, S., & McDowell, A. (2015). Multiplex touchdown PCR for rapid typing of the opportunistic pathogen Propionibacterium acnes. *Journal of clinical microbiology*, *53*(4), 1149–1155

21. Sörensen, M., Mak, T. N., Hurwitz, R., Ogilvie, L. A., Mollenkopf, H. J., Meyer, T. F., & Brüggemann, H. (2010). Mutagenesis of Propionibacterium acnes and analysis of two CAMP factor knock-out mutants. *Journal of microbiological methods*, *83*(2), 211–216

22. Brzuszkiewicz, E., Weiner, J., Wollherr, A., Thürmer, A., Hüpeden, J., Lomholt, H. B., Kilian, M., …Brüggemann, H. (2011). Comparative genomics and transcriptomics of Propionibacterium acnes. *PloS one*, *6*(6), e21581

23. Heydorn, A., Nielsen, A. T., Hentzer, M., Sternberg, C., Givskov, M., Ersbøll, B. K., & Molin, S. (2000). Quantification of biofilm structures by the novel computer program COMSTAT. *Microbiology (Reading, England)*, *146 (Pt 10)*, 2395–2407

24. Vorregaard, M. (2008). Comstat2 - a modern 3D image analysis environment for biofilms, in Informatics and Mathematical Modelling. *Technical University of Denmark: Kongens Lyngby, Denmark*,

25. www.comstat.dk.

26. Hamilton, H. L., Schwartz, K. J., & Dillard, J. P. (2001). Insertion-duplication mutagenesis of neisseria: use in characterization of DNA transfer genes in the gonococcal genetic island. *Journal of bacteriology*, *183*(16), 4718–4726

27. Cheong, D.-E., Lee, H.-I., & So, J.-S. (2008). Optimization of electrotransformation conditions for Propionibacterium acnes. *Journal of microbiological methods*, *72*(1), 38–41

28. Miskin, J. E., Farrell, A. M., Cunliffe, W. J., & Holland, K. T. (1997). Propionibacterium acnes, a resident of lipid- rich human skin, produces a 33 kDa extracellular lipase encoded by gehA. *Microbiology*, *143*, 1745–1755.

29. Jore, J. P., van Luijk, N., Luiten, R. G., van der Werf, M J, & Pouwels, P. H. (2001). Efficient transformation system for Propionibacterium freudenreichii based on a novel vector. *Applied and environmental microbiology*, *67*(2), 499–503

30. web.expasy.org/translate/.

31. ncbi.nlm.nih.gov/.

32. serialbasics.free.fr/Serial_Cloner.html.

33. genome.jp/kegg/.

10 Appendix

10.1 Comparing Biofilm Genes A, and B

Gene **[A]** (KEGG: **PAZ_c18730**) translated for a triacylglycerol lipase in “266”. The amino acid sequence was the following:

Met K K N W L L T T L L A T V T I A **Met** G T T T T A F A S P P T D I T P E H P G G V T A P H S P D G I P S N I E G P S T P S W T S A I R F A **Met** K N P G A K V P G T N D F A C K P R K G T H P V V L I P G T S E D A F I T W S Y Y G P H L K A A G F C A Y T F N Y N P E T H P L V E A A E T S G N I Y S T A A F **Met** A H F I D R V L K T T G A Q K V D L I G H S Q G G G P L P R A Y I K Y Y G G A K K V H H L V G L V P S N K G T S **Met** L G L E K F L N A S G N P L N T I F N A V A Q F H N L G S L P Q Q L Q D S T F L R E L N A D G **Met** T V P G I T Y T V I A T R F D N R V F P W T N T F I N E P G V K N I V I Q D V C P L D H S A H T N I P Y D P **Met** T F Q I V I N A L D P E R A A P V I C T I R P F R P R **Stop**

[30]

When compared to the homologous region of “KPA” (KEGG: PPA1797), the lipase frameshifted into a shorter protein with unknown function.

Met P S W T S A I R F A **Met** K N P G T K V P G T N D F T C K P R K G T H P V V L I P G T S E D A F I T W S Y Y G P R L K A A G F C A Y T F N Y N P E T H P L V E A A E T S G N I Y S T A A F **Met** A H F V D R V L K A T G A Q K V N L V G H S Q G G G P L P R A Y I K Y Y G A P R K S S S R R F G S F Q Q G N T H A R P G E V P Q C Q R K P A Q H Y L Q C C S T V S K A G I P A P T V A R L H I S Q G T Q R G W N D R P R H H I H R H R H P V R Q P S I S V D **Stop** Y L H Q **Stop** A R G Q E H R H P R R L S L G P Q R P H G Y P **Stop** D P **Met**

[30]

The alignment of the DNA sequences resulted in a homology of 94%:

```
„266“  174  GCCCAGCTGGACCTCTGCAATCAGGTTCGCAATGAAGAATCCCGGCGCGAAGGTCCCGGG  233
           ||||||||||||||||||||||||||||||||||||||||| |||||| |||| ||||||||
„KPA“  3    GCCCAGCTGGACCTCTGCAATCAGGTTCGCAATGAAGAACCCCGGCACGAAAGTCCCGGG  62

„266“  234  CACCAACGACTTCGCCTGCAAACCGAGGAAAGGCACCCATCCCGTCGTGCTCATCCCGGG  293
           |||||||||||||  ||||||||||||||||||||||||||||||||||||||||||||||
„KPA“  63   CACCAACGACTTCACCTGCAAACCGAGGAAAGGCACCCATCCCGTCGTGCTCATCCCGGG  122

„266“  294  CACATCCGAGGACGCCTTCATCACGTGGTCGTACTACGGCCCCCACCTCAAGGCAGCAGG  353
           |||||||||||||||||||||||||||||||||||||||| |||| ||||||||||||||
„KPA“  123  CACATCCGAGGACGCCTTCATCACGTGGTCGTACTACGGTCCCCGCCTCAAGGCAGCAGG  182

„266“  354  ATTCTGCGCCTACACGTTCAACTACAACCCGGAAACACATCCGCTTGTGGAAGCTGCTGA  413
           |||||||||||||||||||||||||||||||||||||||||||||||||||||||| |||||
„KPA“  183  ATTCTGCGCCTACACGTTCAACTACAACCCGGAAACACATCCGCTTGTGGAAGCCGCTGA  242

„266“  414  GACCAGCGGCAACATCTACTCCACGGCAGCCTTCATGGCCCACTTCATTGACAGGGTGCT  473
           |||||||||||||||||||||||||||||| ||||||||||||||| ||||||| |||||
„KPA“  243  GACCAGCGGCAACATCTACTCCACGGCAGCTTTCATGGCCCACTTCGTTGACAGAGTGCT  302

„266“  474  CAAGACAACCGGTGCTCAGAAGGTCGATCTCATCGGCCATTCGCAGGGTGGCGGTCCCCT  533
           |||| |||||||||||||||||| | ||| |||||||||| ||||| ||||| |||||
„KPA“  303  CAAGGCAACCGGTGCTCAGAAGGTCAACCTCGTCGGCCATTCTCAGGGCGGCGGCCCCCT  362
```

```
„266"  534  GCCGCGCGCGTACATCAAATATTACGGAGGCGCCAAGAAGGTCCATCATCTCGTCGGTTT  593
           ||||||||||||||||||||||||||| |||||||||| |||| ||||||||||||||||
„KPA"  363  GCCGCGCGCGTACATCAAATATTACGG-GGCGCCAAGAAAGTCC-TCATCTCGTCGGTTT  420

„266"  594  AGTTCCTTCCAACAAAGGAACAAGCATGCTCGGCCTGGAGAAGTTCCTCAATGCCAGTGG  653
            ||||||||||||  |||||| ||||||||||||||||||||||||||||||||||| ||
„KPA"  421  GGTTCCTTCCAACAGGGGAACACGCATGCTCGGCCTGGAGAAGTTCCTCAATGCCAGCGG  480

„266"  654  AAATCCGCTCAACACTATTTTCAATGCCGTAGCGCAGTTTCACAATCTGGGATCCCTGCC  713
           ||| ||||||| |||||| |||||||| | ||| |||||||  || |||| |||||||||
„KPA"  481  AAACCCGCTCAGCACTATCTTCAATGCTGCAGCACAGTTTCGAAAGCTGGAATCCCTGCC  540

„266"  714  CCAACAGTTGCAAGACTCCACATTTCTCAGGGAACTCAACGCGGATGGAATGACCGTCCC  773
           ||||||||||||||||||||||||||||||||||||||||||||||||||||||||||||
„KPA"  541  CCAACAGTTGCAAGACTCCACATTTCTCAGGGAACTCAACGCGGATGGAATGACCGTCCC  600

„266"  774  CGGCATCACATACACCGTCATCGCCACCCGGTTCGACAACCGAGTATTTCCGTGGACGAA  833
           |||||||||||||||||||||||||||||||||||||||||||||||||||||||||| ||
„KPA"  601  CGGCATCACATACACCGTCATCGCCACCCGGTTCGACAACCGAGTATTTCCGTGGACTAA  660

„266"  834  TACCTTCATCAATGAGCCCGGAGTCAAGAACATCGTCATCCAAGATGTCTGCCCCTTAGA  893
           |||||||||||||||||||| ||||||||||||||||||||||| ||||| ||||| ||
„KPA"  661  TACCTTCATCAATGAGCCCGGGGTCAAGAACATCGTCATCCAAGACGTCTGTCCCTTGGA  720

„266"  894  CCACAGCGCCCACACGAATATCCCCTATGACCCGATGA  931
           |||||||||||||||| |||| ||||| ||||||||||
„KPA"  721  CCACAGCGCCCACACGGATAT-CCCTAGGACCCGATGA  757
```

[31]

Gene **[B]** (**PAZ_c21800**) in „266“, and **PPA_2105** in „KPA“, both encoded for a glycerol-ester hydrolase A, which was a secreted TAG lipase [22; 28]. The differences in homology were minimal, as we can see from the amino acid sequences.

KPA:

Met K I N A R F A V **Met** A A S V A V L **Met** A A A P I A Q A A T S P G D I H P L V Q A A H S P D G
I P G N G V G P E F H T S S **Met** A R S Y S E K H L G V A P R G V N D F S C K V K P G D R P V I L
I P G T G G N A F A T W S F Y G P H L A H E G Y C V Y T F T T N V P V G I L D E G W G F T G D
V R A S A Q A L G A F V D R V R K A T G S E K V D F V G H S Q G G G I L P N A Y I K **Met** Y G G
A S K V D K L I G L V A A N H G T T A V G L D K L V D G L P E A V K D F L S T W S Y D H N **Met** E
A Y G Q Q L K G S A L **Met** Q Q V Y R D G D T V P G I A Y T V I S T R L D **Met** T V T P Y T Q A F L
K G A K N **Met** T V Q D A C P L D A Y G H G R L P Y D P V A Y Q **Met** V L N A L D P N H P R E I S
C T W R P R V L P V S T T D A A **Stop**

[30]

266:

Met K I N A R F A V **Met** A A S V A V L **Met** A A A P T A Q A V T S P G D I H P L V Q A A H S P D G
I P G N G V G P E F H T S S **Met** A R S Y S E K H L G V A P R G V N D F S C K V K P G D R P V I L
I P G T G G N A F A T W S F Y G P H L A H E G Y C V Y T F T T N V P V G I L D E G W G F T G D
V R A S A Q A L G A F V D R V R K A T G S E K V D V V G H S Q G G G I L P N A Y I K **Met** Y G G
A S K V D K L I G L V A A N H G T T A V G L Y K L V D G L P E A V K D F L S T W S Y D H N **Met** E
A Y G Q Q L K G S A L **Met** Q Q V Y R D G D T V P G I A Y T V I S T R L D T T V T P Y T Q A F L K
G A K N **Met** T V Q D A C P L D A Y G H G R L P Y D P V A Y Q **Met** V L N A L D P K H P R E I S C
T W R P R V L P V S T T D A A **Stop**

[30]

However, the mRNA was upregulated in “266” compared to “KPA” [22].

10.2 *ermC* from pIDN2

Construction of *ermC* from pIDN2 with the primers XXX and XXX.

AATtctagaCTCATGTTTGACAGCTTATCATCGCGTGCTATAATTATACTAATTTTATAAGGAGGAAAAAATAAAGAGGG
TTATAATGAACGAGAAAAATATAAAACACAGTCAAAACTTTATTACTTCAAAACATAATATAGATAAAATAATGACAAAT
ATAAGATTAAATGAACATGATAATATCTTTGAAATCGGCTCAGGAAAAGGGCATTTTACCCTTGAATTAGTACAGAGGTG
TAATTTCGTAACTGCCATTGAAATAGACCATAAATTATGCAAAACTACAGAAAATAAACTTGTTGATCACGATAATTTCC
AAGTTTTAAACAAGGATATATTGCAGTTTAAATTTCCTAAAAACCAATCCTATAAAATATTTGGTAATATACCTTATAAC
ATAAGTACGGATATAATACGCAAAATTGTTTTTGATAGTATAGCTGATGAGATTTATTTAATCGTGGAATACGGGTTTGC
TAAAAGATTATTAAATACAAAACGCTCATTGGCATTATTTTTAATGGCAGAAGTTGATATTTCTATATTAAGTATGGTTC
CAAGAGAATATTTTCATCCTAAACCTAAAGTGAATAGCTCACTTATCAGATTAAATAGAAAAAAATCAAGAATATCACAC
AAAGATAAACAGAAGTATAATTATTTCGTTATGAAATGGGTTAACAAAGAATACAAGAAAATATTTACAAAAAATCAATT
TAACAATTCCTTAAAACATGCAGGAATTGACGATTTAAACAATATTAGCTTTGAACAATTCTTATCTCTTTTCAATAGCT
ATAAATTATTTAATAAGTAAGTTAACGCATGCATAAACTGCATCCCTTAACTTGTTTTTCGTGTACCTATTTTTTctgca
gTTA

[31; 32]

-35 -10 region, RBS, ORF, Terminator, Poly-T tail, ORF of *ermC*, XbaI cutting site, PstI cutting site,

10.3 *ermE* from *Saccharopolyspora erythraea*

Construction of *ermE* from *S. erythraea* with the primers ermE_XbaI.fw and ermE_PstI.rv. Position of the primers were equal to the published successful knockout [21].

AAAtctagaAGCCCGACCCGAGCACGCGCCGGCACGCCTGGTCGATGTCGGACCGGAGTTCGAGGTACGCGGCTTGCAGG
TCCAGGAAGGGGACGTCCATGCGAGTGTCCGTTCGAGTGGCGGCTTGCGCCCGATGCTAGTCGCGGTTGATCGGCGATCG
CAGGTGCACGCGGTCGATCTTGACGGCTGGCGAGAGGTGCGGGGAGGATCTGACCGACGCGGTCCACACGTGGCACCGCG
ATGCTGTTGTGGGCTGGACAATCGTGCCGGTTGGTAGGATCCAGCGGTGAGCAGTTCGGACGAGCAGCCGCGCCCGCGTC
GCCGCAACCAGGATCGGCAGCACCCCAACCAGAACCGGCCGGTGCTGGGCCGTACCGAGCGGGACCGCAACCGGCGCCAG
TTCGGGCAGAACTTCCTCCGCGACCGCAAGACCATCGCGCGCATCGCCGAGACAGCCGAGCTGCGGCCCGATCTGCCGGT
GCTGGAAGCCGGCCCCGGCGAAGGGCTGCTCACCAGGGAACTCGCCGACCGCGCGCGTCAGGTGACGTCGTACGAGATCG
ACCCCCGGCTGGCGAAGTCGTTGCGGGAGAAGCTTTCCGGCCACCCGAACATCGAAGTCGTCAACGCCGACTTCCTCACC
GCCGAACCGCCGCCCGAGCCGTTCGCCTTCGTCGGCGCGATCCCCTACGGCATCACCTCGGCGATCGTGGACTGGTGCCT
GGAGGCGCCGACGATCGAGACGGCGACGATGGTCACGCAGCTGGAGTTCGCCCGGAAGCGGACCGGCGATTACGGCCGCT
GGAGCCGCCTCACGGTGATGACCTGGCCGCTGTTCGAGTGGGAGTTCGTCGAGAAGGTCGACCGCCGGCTGTTCAAGCCG
GTGCCCAAGGTCGACTCGGCGATCATGCGGCTGCGCAGGCGCGCCGAACCGCTGCTGGAAGGCGCGGCGCTCGAACGCTA
CGAGTCGATGGTCGAGCTGTGCTTCACCGGCGTCGGCGGCAACATCCAGGCGTCGCTTCTGCGCAAGTACCCGAGGCGCC
GCGTCGAGGCGGCGCTCGACCACGCGGGGGTCGGGGGCGGCGCCGTGGTCGCCTACGTCCGGCCGGAGCAGTGGCTCCGG
CTGTTCGAGCGGCTGGATCAGAAGAACGAACCGAGGGGTGGGCAGCCCCAGCGGGGCAGGCGAACCGGCGGACGGGACCA
CGGGGACCGGCGAACCGGCGGGCAGGATCGCGGCGATCGGCGAACCGGCGGCCGCGACCACAGGGACCGGCAAGCCAGCG
GCCACGGCGATCGTCGCAGCAGCGGACGCAATCGCGACGACGGACGAACCGGCGAGCGCGAGCAGGGGGACCAAGGCGGG
CGGCGGGGGCCGTCCGGGGGTGGACGGACCGGCGGACGTCCAGGGCGACGCGGCGGACCCGGGCAGCGGTAGTCCCCGGC
ACGCGGAACGGGGCAGGCCGTCGAGCGGCCTGTTGGTCGAGAGGAATCAGAGGTTGATGTCGGCCCGGAGGTCGATGTCG
CGCGACGACGAGCCGATCTCCACCGCTCGCTTGCCGCCCCCGAGCTTCCAGCCGCCCGCGGCTTCGTCCCAGTGCTGGAG
GGCCCGCTCCGCGACGTGCACCCGGACGCGCTTGGTCTCGCCCGGTGCGAGTTCGACCTTCTctgcagTTT

[33; 32]

ORF of *ermE*, XbaI cutting site, PstI cutting site

10.4 pUC19

The vector pUC19 was used as backbone for the construction of the knockout vector.

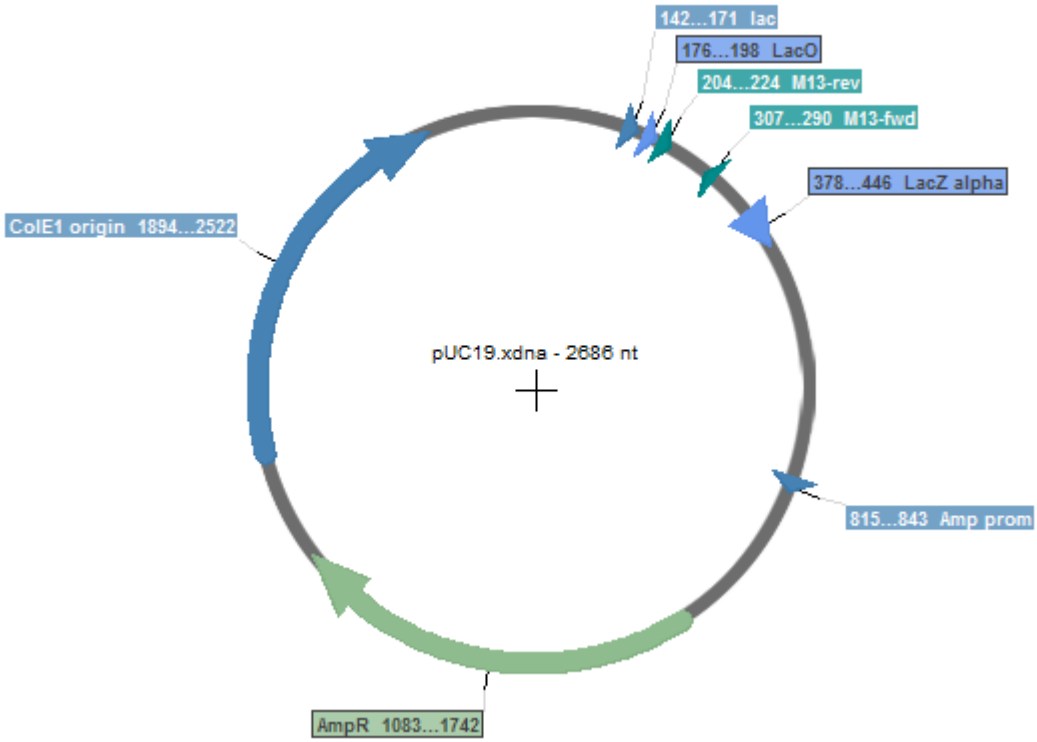

[32]

Figure 32: pUC19 Sequence Map.

```
>gi|6691170|gb|M77789.2|SYNPUC19V Cloning vector pUC19, complete sequence
GCGCCCAATACGCAAACCGCCTCTCCCCGCGCGTTGGCCGATTCATTAATGCAGCTGGCACGACAGGTTT
CCCGACTGGAAAGCGGGCAGTGAGCGCAACGCAATTAATGTGAGTTAGCTCACTCATTAGGCACCCCAGG
CTTTACACTTTATGCTTCCGGCTCGTATGTTGTGTGGAATTGTGAGCGGATAACAATTTCACACAGGAAA
CAGCTATGACCATGATTACGCCAAGCTTGCATGCCTGCAGGTCGACTCTAGAGGATCCCCGGGTACCGAG
CTCGAATTCACTGGCCGTCGTTTTACAACGTCGTGACTGGGAAAACCCTGGCGTTACCCAACTTAATCGC
CTTGCAGCACATCCCCCTTTCGCCAGCTGGCGTAATAGCGAAGAGGCCCGCACCGATCGCCCTTCCCAAC
AGTTGCGCAGCCTGAATGGCGAATGGCGCCTGATGCGGTATTTTCTCCTTACGCATCTGTGCGGTATTTC
ACACCGCATATGGTGCACTCTCAGTACAATCTGCTCTGATGCCGCATAGTTAAGCCAGCCCCGACACCCG
CCAACACCCGCTGACGCGCCCTGACGGGCTTGTCTGCTCCCGGCATCCGCTTACAGACAAGCTGTGACCG
TCTCCGGGAGCTGCATGTGTCAGAGGTTTTCACCGTCATCACCGAAACGCGCGAGACGAAAGGGCCTCGT
GATACGCCTATTTTTATAGGTTAATGTCATGATAATAATGGTTTCTTAGACGTCAGGTGGCACTTTTCGG
GGAAATGTGCGCGGAACCCCTATTTGTTTATTTTTCTAAATACATTCAAATATGTATCCGCTCATGAGAC
AATAACCCTGATAAATGCTTCAATAATATTGAAAAAGGAAGAGTATGAGTATTCAACATTTCCGTGTCGC
CCTTATTCCCTTTTTTGCGGCATTTTGCCTTCCTGTTTTTGCTCACCCAGAAACGCTGGTGAAAGTAAAA
GATGCTGAAGATCAGTTGGGTGCACGAGTGGGTTACATCGAACTGGATCTCAACAGCGGTAAGATCCTTG
AGAGTTTTCGCCCCGAAGAACGTTTTCCAATGATGAGCACTTTTAAAGTTCTGCTATGTGGCGCGGTATT
ATCCCGTATTGACGCCGGGCAAGAGCAACTCGGTCGCCGCATACACTATTCTCAGAATGACTTGGTTGAG
TACTCACCAGTCACAGAAAAGCATCTTACGGATGGCATGACAGTAAGAGAATTATGCAGTGCTGCCATAA
CCATGAGTGATAACACTGCGGCCAACTTACTTCTGACAACGATCGGAGGACCGAAGGAGCTAACCGCTTT
TTTGCACAACATGGGGGATCATGTAACTCGCCTTGATCGTTGGGAACCGGAGCTGAATGAAGCCATACCA
AACGACGAGCGTGACACCACGATGCCTGTAGCAATGGCAACAACGTTGCGCAAACTATTAACTGGCGAAC
TACTTACTCTAGCTTCCCGGCAACAATTAATAGACTGGATGGAGGCGGATAAAGTTGCAGGACCACTTCT
GCGCTCGGCCCTTCCGGCTGGCTGGTTTATTGCTGATAAATCTGGAGCCGGTGAGCGTGGGTCTCGCGGT
ATCATTGCAGCACTGGGGCCAGATGGTAAGCCCTCCCGTATCGTAGTTATCTACACGACGGGGAGTCAGG
CAACTATGGATGAACGAAATAGACAGATCGCTGAGATAGGTGCCTCACTGATTAAGCATTGGTAACTGTC
AGACCAAGTTTACTCATATATACTTTAGATTGATTTAAAACTTCATTTTTAATTTAAAAGGATCTAGGTG
AAGATCCTTTTTGATAATCTCATGACCAAAATCCCTTAACGTGAGTTTTCGTTCCACTGAGCGTCAGACC
```

```
CCGTAGAAAAGATCAAAGGATCTTCTTGAGATCCTTTTTTTCTGCGCGTAATCTGCTGCTTGCAAACAAA
AAAACCACCGCTACCAGCGGTGGTTTGTTTGCCGGATCAAGAGCTACCAACTCTTTTTCCGAAGGTAACT
GGCTTCAGCAGAGCGCAGATACCAAATACTGTTCTTCTAGTGTAGCCGTAGTTAGGCCACCACTTCAAGA
ACTCTGTAGCACCGCCTACATACCTCGCTCTGCTAATCCTGTTACCAGTGGCTGCTGCCAGTGGCGATAA
GTCGTGTCTTACCGGGTTGGACTCAAGACGATAGTTACCGGATAAGGCGCAGCGGTCGGGCTGAACGGGG
GGTTCGTGCACACAGCCCAGCTTGGAGCGAACGACCTACACCGAACTGAGATACCTACAGCGTGAGCTAT
GAGAAAGCGCCACGCTTCCCGAAGGGAGAAAGGCGGACAGGTATCCGGTAAGCGGCAGGGTCGGAACAGG
AGAGCGCACGAGGGAGCTTCCAGGGGGAAACGCCTGGTATCTTTATAGTCCTGTCGGGTTTCGCCACCTC
TGACTTGAGCGTCGATTTTTGTGATGCTCGTCAGGGGGGCGGAGCCTATGGAAAAACGCCAGCAACGCGG
CCTTTTTACGGTTCCTGGCCTTTTGCTGGCCTTTTGCTCACATGTTCTTTCCTGCGTTATCCCCTGATTC
TGTGGATAACCGTATTACCGCCTTTGAGTGAGCTGATACCGCTCGCCGCAGCCGAACGACCGAGCGCAGC
GAGTCAGTGAGCGAGGAAGCGGAAGA
```

[31]

10.5 Skin vs Implant Isolate Static Biofilm Assay

10.5.1.1 72h Incubation in BHI

The results of the static biofilm assay after 72h incubation in BHI are shown in figure 33.

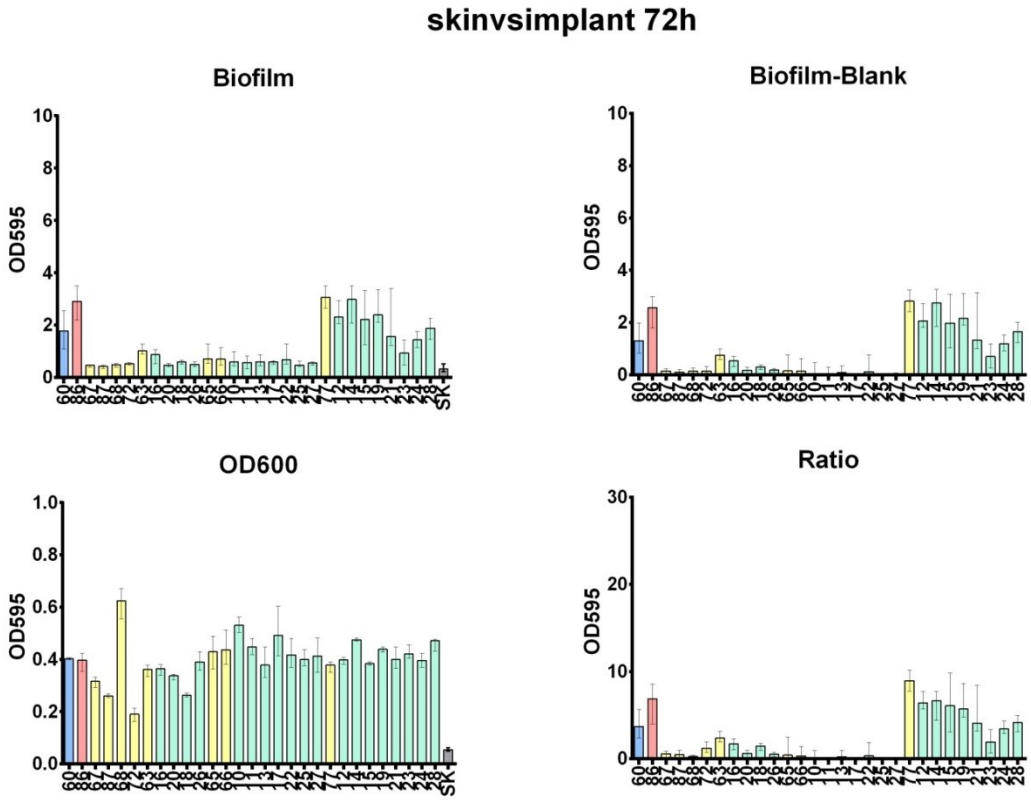

Figure 33: Static biofilm assay of skin vs implant isolates, 72h, BHI. The results of the static biofilm assay for a few skin isolates (in BHI medium, 72h incubation) versus 19 implant isolates are summed up. The top left panel shows the original biofilm absorbance with sterile control (SK) via absorbance of crystal violet at 595 nm. The top right panel shows the biofilm minus sterile control. The bars peak at the median of at least 12 values with whiskers indicating the interquartile range of 25%. Down left panel depicts the growth (OD_{600}) of each strain at the respective time point. The ratio between biofilm-blank and OD_{600} led to the relative biofilm quantity standardized to OD_{600} = 1 (C).

10.5.1.2 120h Incubation in BHI

The results of the static biofilm assay after 120h incubation in BHI are shown in figure 34.

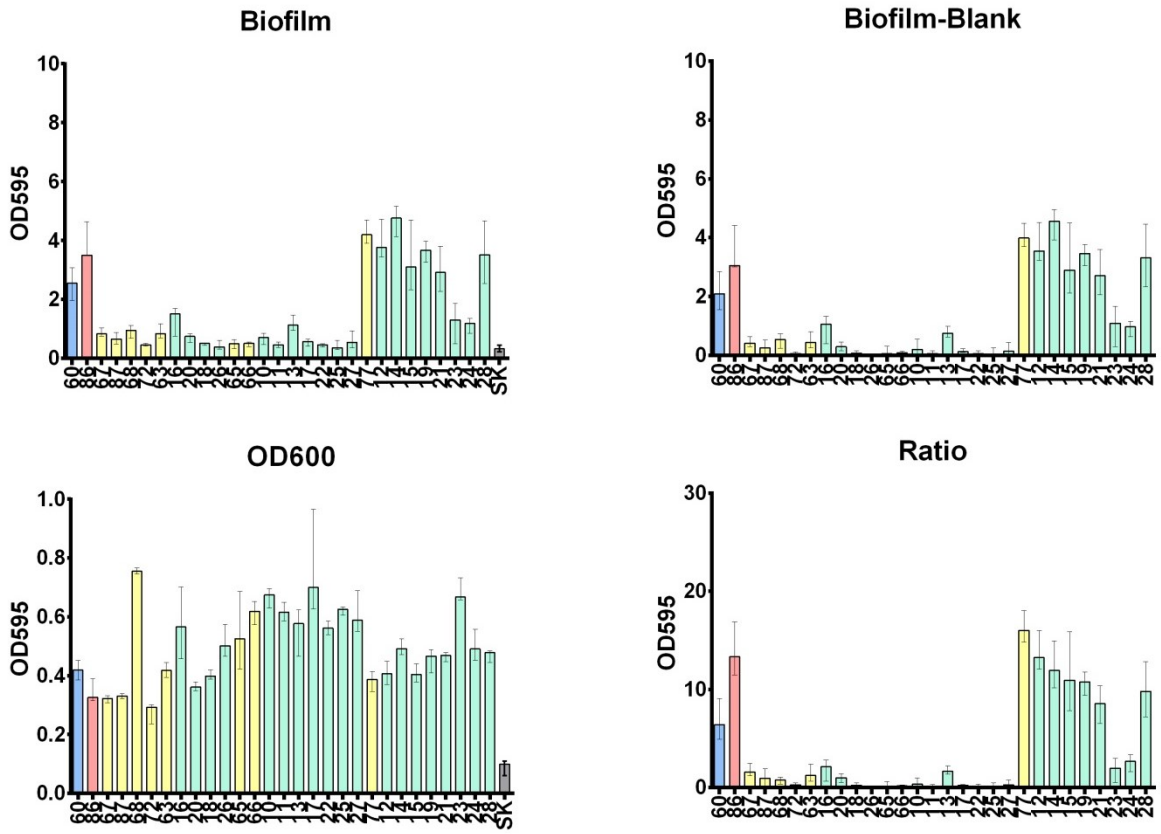

Figure 34: Static biofilm assay of skin vs implant isolates, 120h, BHI. The results of the static biofilm assay for a few skin isolates (in BHI medium, 120h incubation) versus 19 implant isolates are summed up. The top left panel shows the original biofilm absorbance with sterile control (SK) via absorbance of crystal violet at 595 nm. The top right panel shows the biofilm minus sterile control. The bars peak at the median of at least 12 values with whiskers indicating the interquartile range of 25%. Down left panel depicts the growth (OD_{600}) of each strain at the respective time point. The ratio between biofilm-blank and OD_{600} led to the relative biofilm quantity standardized to OD_{600} = 1 (C).

10.5.1.3 168h Incubation in BHI

The results of the static biofilm assay after 168h incubation in BHI are shown in figure 35.

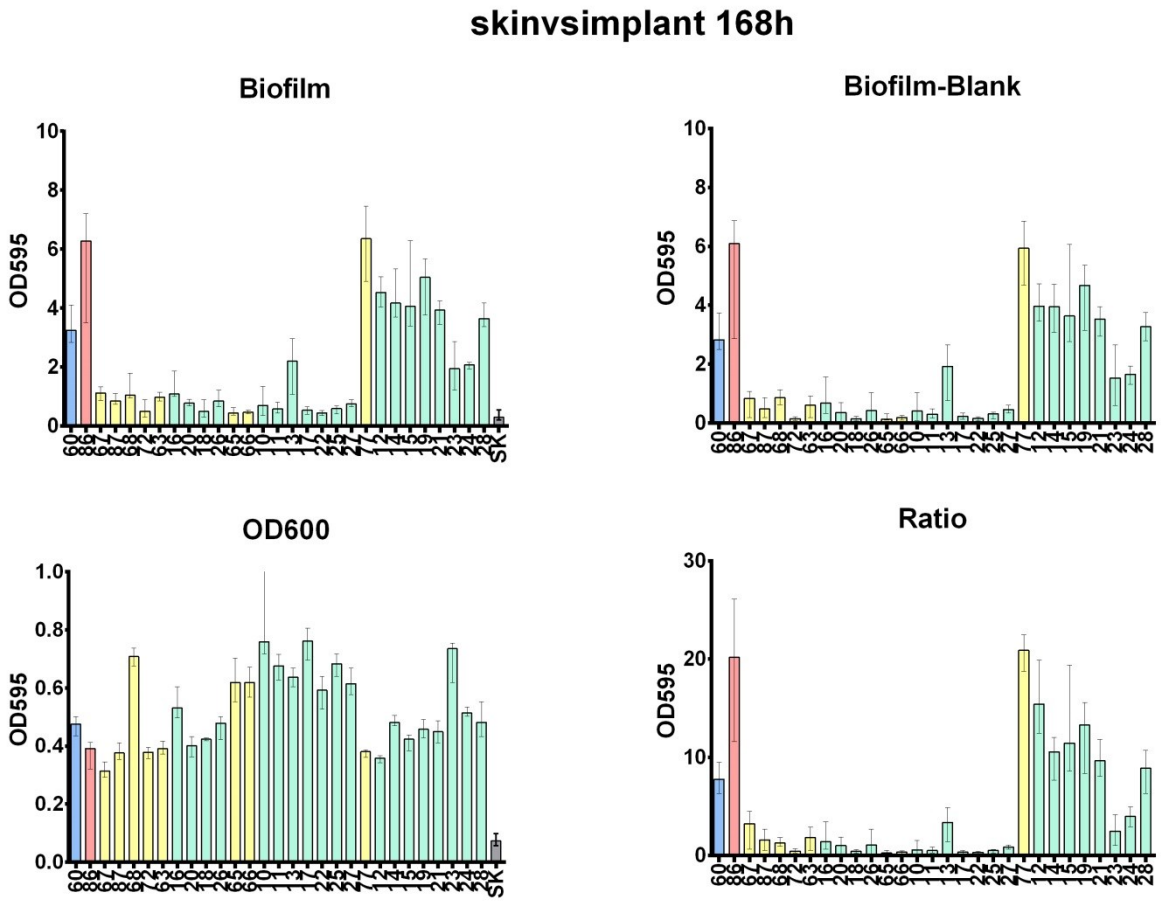

Figure 35: Static biofilm assay of skin vs implant isolates, 168h, BHI. The results of the static biofilm assay for a few skin isolates (in BHI medium, 168h incubation) versus 19 implant isolates are summed up. The top left panel shows the original biofilm absorbance with sterile control (SK) via absorbance of crystal violet at 595 nm. The top right panel shows the biofilm minus sterile control. The bars peak at the median of at least 12 values with whiskers indicating the interquartile range of 25%. Down left panel depicts the growth (OD_{600}) of each strain at the respective time point. The ratio between biofilm-blank and OD_{600} led to the relative biofilm quantity standardized to OD_{600} = 1 (C).

10.6 Macroscopic Phenotype – Mixture of strains

A mixture of strain #60, #62, #64, #70, #71, #72, #77, #78, #80, #83, #90, #91 was also included in one of the assays, resulting in a phenotypic mixture of IA1 strains

Figure 36: Macroscopic image of strain mixture. The strains were grown in BHI for 72h (upper well), 120h (middle well) and 168h. The mixture consisted of #60, #62, #64, #70, #71, #72, #77, #78, #80, #83, #90 and #91.